Real-time simulation based analysis of Fast Active Power Regulation strategies to enhance frequency support from PE interfaced Multi-Energy system.

Nidarshan Kumar V

Technische Universiteit Delft

TU Delft Delft University of Technology

Challenge the future

Real-time simulation based analysis of Fast Active Power Regulation strategies to enhance frequency support from PE interfaced Multi-Energy system.

by

Nidarshan Kumar V

in partial fulfillment of the requirements for the degree of

Master of Science
in Power Engineering

at the Delft University of Technology,
to be defended publicly on August 30, 2019 at 12:00 PM.

Supervisor:	Dr. ir. J.L. (Jose) Rueda Torres	
Thesis committee:	Prof. ir. M.A.M.M. (Mart) van der Meijden,	IEPG
	Dr. ir. J.L. (Jose) Rueda Torres,	IEPG
	Dr. T. (Thiago) Batista Soeiro	DCES
	Dr. Zameer Ahmad,	IEPG
	Dr. Elyas Rakhshani,	IEPG

This thesis is confidential and cannot be made public until December 31, 2021.

TU Delft Delft University of Technology

Acknowledgement

ಅಕ್ಕಯ್ಯ ತಾಯಿನಾಡು,
ಈ ಸುಂದರವಾದ ಪತ್ರದಲ್ಲಿ ನನ್ನ ಸಂತೋಷ ಅಗು ಭಾವನೆಗಳನ್ನು ವ್ಯಕ್ತಪಡಿಸಲಾಗಿದೆ. ನನ್ನ ದೇಶ ಅಗು ಭಾಷೆ, ನನಗೆ ಸರ್ವತ್ರಿಕ ಸ್ವೀಕಾರ, ಅಗು ವೇಗವಾಗಿ ಮುಂದುವರೆಯುವುದನ್ನು ಕಲಿಸಿದೆ. ಬುದ್ಧಿವಂತಿಕೆಯಿಂದ ಮೂಲದ ಕುಲವ ವ್ಯಯಿಸುವುದನ್ನು ಹುಡುಕಿಯುವ ಮಾರ್ಗವನ್ನು ತೋರಿಸಿದೆ. ಕೊನೆಯದಾಗಿ, ಎಂದಿಗೂ, ಯಾವ ಕಂದಭ್ರಮದಲ್ಲು, ನನ್ನ ಸ್ವಾಭಿಮಾನವನ್ನ, ನನ್ನ ತಾಯಿನಾಡನ್ನು ಅವಿಸುವುದಿಲ್ಲ ಅಗು ಕಡೆಗಣಿಸುವುದಿಲ್ಲ ಎಂದು, ಪ್ರತಿಜ್ಞೆ ಮಾಡುತ್ತೇನೆ

The Last 8 months of my life has been a defining moments of my education carrer. Hence it is necessary to express my gratitude to individuals who supported me in completing it sucessfully.

Firstly I would like to thank PROF. Jose Ruede TORRes for being the backbone of my work. His proficiency in strategy making, Risk managment, marvelous writing skills and attitude towards work have been an inspiring lesson throughout the journey. His organised work culture, yet down to earth attitude are some of the few skills that i would like to adopt in my life.

Next i would like to thank PROF. Mart Van der Meijden for being a guardian angel of our work. I also thank him for having trust in me and provide a bigger platform to present at international projects. Next i would like to thank my daily supervisor Dr. Elyas Rakhmani for supporting me with clarifications regarding concepts and providing timely feedbacks. His valuble advise when it was absolutely in need was one of the fundamental reasons for sucessful completion of this thesis.

Lastly, on my Supervisor list, I would like to thank my daily supervisor Dr. Zameer Ahmed for his consistent support, brilliance in HIL and creating peaceful environment amidst critical deadlines. No amount of thanks will be less for his support.

It would be an omission if i don't thank my friends &/ greek gods stelios and christos. Also Lastly i would extend my gratitude to miss. Medha for proof reading my thesis in a timely fashion.

Furthur, I need to send my gratitude to friends at Domino's for supporting me during critical deadlines. Nevertheless, I feel the need to thank PORSHE for dropping me of their thesis program and teaching me critical life lessons.

Lastly, I would like to thank my family for having faith in me and teaching me things to focus in life.

Abstract

Until recent times, electrical power grids have been dominated by conventional power plants run by fossil or nuclear fuels in order to cater to the electrical load demand. These power plants employ large generators that operate in synchronous with each other to maintain a stable frequency and voltage across the power grid. The frequency and voltage stability, which are respectively linked to active and reactive power serves as a backbone for a secure operation of the power system. Furthermore, since these classical generation sources promised support of ancillary services during unstable conditions, along with power generation, they were characterized as a reliable solution for maintaining the security of the power system.

But, due to the high emission of carbon by-products from these fossil-fuelled generators, challenges of global warming and climate change have made it inevitable to decommission them. And more emphasis has been embarked on the adaptation of renewable energy sources (RES) which offer minimum carbon footprint. Geothermal heat, wind, sunlight, and tides constitute some of the Renewable energy sources since their availability are unlimited and involve the least emission of greenhouse gasses, hence Renewable Energy Sources have a minimal impact on the environment compared to traditional energy sources and can effectively tackle the problems which arise with fossil fuel usage. For all these reasons, during the last decades, there is fierce research on finding ways to produce the needed energy in a sustainable fashion.

Synchronous Generators, which are dominant in the existing power grid, have the inherent characteristics to relate system's frequency with load balance. This considerable advantage is found missing from Power Electronic interfaced renewable energy resources due to the following reasons. Firstly, since active power support was earlier the main purpose of using these devices, they were operated at Maximum power point tracking (MPPT). Secondly, in wind energy technology, isolation between electrical and mechanical circuits had to be introduced due to their variable behavior of energy production, and this has led to no inertia backing from the synthetically produced frequency.

So with high penetration of RES in the future grids, the aforementioned problems pose huge risks for grid stability and reliability. The current research mainly focuses on the development, implementation, testing, and validation of frequency regulation strategies under the umbrella of Fast Active Power Regulation controllers specifically to support during large load frequency variation in low inertia power system grid. These controllers developed are very generic and can be implemented with slight modifications in all the renewable energy devices with ease.

In order to simulate more real-time behavioral conditions, dynamic simulation studies are performed in RSCAD software interfaced with a Real-Time Digital Simulator (RTDS). Two Test benches have been considered in this thesis, one being an IEEE 9 bus system modified with 52% wind share and another is the North of Netherlands Network.

In the first stage of the project, FAPR controller's proof of concept has been tested on a Type-4 Wind generator setup connected to the modified IEEE 9 bus system. Here wind penetration is scaled up to 52% and a low inertia grid have been simulated. Later, the results obtained here were validated by Hardware in Loop setup utilizing a mock-up grid side converter.

The next stage of the project aims at making FAPR controllers more generic. For this the North of Netherlands network was modified by adding FAPR integrated 300MW solar farm, FAPR integrated 82MW full converter based Type-4 Wind Turbine and lastly, a responsive load (Electrolyser) was modified to accommodate FAPR controllers. All together formed a Multi-Energy Hub and simulations were performed to check the practical feasibility and boundaries of operation of FAPR controllers in the future power grid.

The results prove that the proposed topology and control strategies can effectively provide frequency ancillary services to the grid by providing support during dynamic load frequency variations.

Nidarshan Kumar V
Delft, August 2019

Contents

List of Figures

List of Tables

List of Abbreviations

BESS Battery Energy Storage System.

BPMS Battery Power Management System.

CHIL Control Hardware In Loop.

CIPC circular inter-process communication.

DUT Device Under Test.

FAPR Fast Active Power Regulation.

GSC Grid Side Converter.

H Inertia Constant.

HIL Hardware In Loop.

MPPT Maximum Power Point Tracking.

MSC Machine Side Converter.

PEIG Power Electronic Interfaced Generation.

PHIL Power Hardware In Loop.

PWM Pulse Width Modulation.

RES Renewable Energy Sources.

RMS Root Mean Square.

RoCoF Rate of Change of Frequency.

RTDS Real Time Digital Simulator.

RTT Real Time Target.

SGs Synchronous Generators.

VSC Voltage Source Converter.

VSP Virtual Synchronous Power.

WT Wind Turbine.

1

Introduction

This chapter presents an overview of the selected topic under studies and the content of the presented thesis.

To start with, the necessary background about the share of renewable energy devices in the future grid, fundamental meaning of frequency stability is discussed. Subsequently, the motivation for the research is presented, and the problems that this thesis is trying to solve are defined through a research objective. Later, through a literature review, various control strategies built over the years related to frequency stability studies have been discussed.

With this understanding, the research questions are formulated and the objectives of the present thesis are outlined. Finally, the approach chosen in order to answer the research questions and fulfill the objectives is demonstrated through a flowchart, and a summary of each following chapter is presented.

1.1. Background and Motivation

Until recent times, electrical power grids have been dominated by conventional power plants run by fossil or nuclear fuels in order to cater to the electrical load demand. These power plants employ large generators that operate in synchronous with each other to maintain a stable frequency and voltage across the power grid. The frequency and voltage stability, which are respectively linked to active and reactive power serves as a backbone for a secure operation of the power system. Furthermore, since these classical generation sources promised support of ancillary services during unstable conditions, along with power generation, they were characterized as a reliable solution for maintaining the security of the power system.

But, due to the high emission of carbon by-products from these fossil-fuelled generators, challenges of global warming and climate change have made it inevitable to decommission them. And more emphasis has been embarked on the adaptation of renewable energy sources (RES) which offer minimum carbon footprint. Geothermal heat, wind, sunlight, and tides constitute some of the Renewable energy sources since their availability are unlimited and involve the least emission of greenhouse gasses, hence RES is considered as a feasible solution to mitigate the aforementioned climate change and global warming problems.

So far the integration of RES has provided positive feedback in terms of energy management since the grid stability and security of supply was still being guaranteed by large synchronous generators in power plants. But with higher penetrations of RES and decommissioning of synchronous generators the spinning reserve out of operating reserves available in the grid reduces, thereby also reducing the provision of major ancillary support. Also, since most of the RES operate on Maximum Power Point Tracking (MPPT), they fundamentally cannot provide ancillary support without control modifications [2]. These issues pose a threat to grid stability and reliability.

A stable power system grid is quantified in terms of a steady frequency and voltage value which is respectively governed by active and reactive power in the grid. Power systems are maintained stable by balancing production and consumption. In other words, the active power balance in the grid results in a steady frequency and reactive power balance in the grid results in a steady voltage. Since this thesis focuses on grid frequency regulation, keeping active power balance at all times, under all circumstances

will be the main focus. In traditional power systems, as in any mechanical systems, any imbalance in power yields an acceleration/deceleration of spinning of rotor mass, covering the power deficit by releasing/absorbing kinetic energy. This support in electrical terms is quantified as the inertia and is defined as a property of large synchronous generators, which contain large rotating masses, and which acts to overcome the immediate imbalance between the power supply and demand for electric power systems, typically the electrical grid. Hence, when a power grids active power balance is disturbed, the frequency changes, but inertia will slow down this change and provides more reaction time for corrective measures.

The problems with low inertia are very prominent in isolated power grids, where the system inertia constant(H) is low since there are less spinning reserves operating to maintain active power balance. With the increasing share of power electronic interfaced renewables, the proportion of non-synchronous based generation increases. This results in lower H/MVA and further reduces inertia making the system even more vulnerable and prone to system failures and blackouts. One such incident that occurred recently is illustrated below.

On August 9th, 2019, Friday afternoon at soon after 16:52, two sources of power were lost within less than a minute of each other[1]:
The first source was a 790 MW from Hornsea 1 offshore wind farm and the second was 660 MW from Little Barford gas-fired power station. The combined total loss of 1430 MW was significantly greater than what appears to have been the largest single infeed loss risk in a less interconnected grid. This created a large generation-load imbalance event and the frequency trace measured at Strathclyde showed a rapid fall in system frequency. From figure 1.1 the first outage result was arrested by the combination of responses on the system but dropped to below 49.2 Hz. However, the second loss of 660MW further dropped in frequency about a minute after the first one. But now, with much of the frequency ancillary services from primary frequency reserves being already depleted and had no time for recovery, system frequency subsequently fell to less to 48.8 Hz at which point the first stage of 'Low-Frequency Demand Disconnection' ((LFDD) operated where demand-side loads disconnected automatically causing a major blackout.

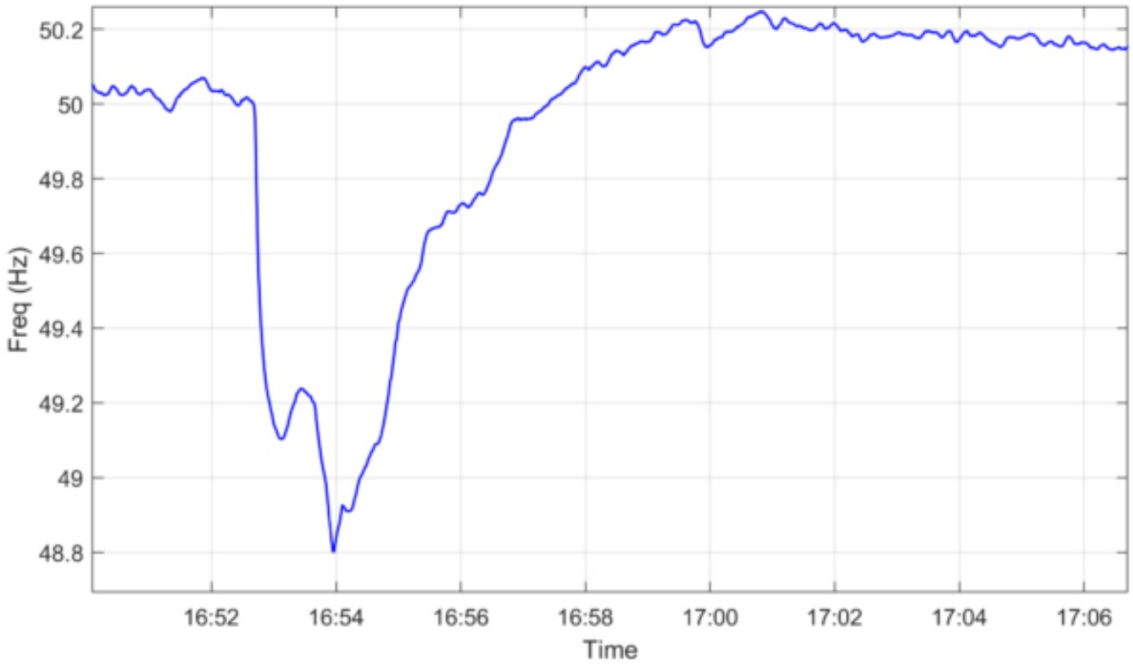

Figure 1.1: Great Britain system frequency during a generation outage on August 9th 2019[1]

The whole incident could have been avoided if there was a fast active power support within few seconds after the generation outage. This would have minimized the generation load imbalance and frequency would not have reached 49.2 Hz in the first place. This incident mapped the importance of

frequency regulation and fast active power balance in a future low inertia grid.

It is estimated by 2030, 300GW of wind share is expected in North-West Europe alone and this demands for progressive phase-out of high inertial synchronous generators even in mainland Europe [3], leading to a low inertia grid. If proper measures are not taken, a sudden load increase or generation outage of 2% to 4% could lead to load shedding, damage of the grid-connected machine, system instability and sometimes even a blackout thereby threatening the security of grid power supply. Hence higher penetration of RES is possible only if they can promise grid stability through frequency and voltage ancillary support along with steady supply of power.

Since frequency control through synchronous generators is not a reliable option in the future power system grid, the burden of providing frequency control under ancillary support falls onto the RES. Based on this, RES can be broadly classified as sources that can and cannot provide ancillary support, precisely inertial response. This classification is based on the presence of spinning reserves. For example hydro and wind energy involves rotational mass that offers inertial response, also tidal energy involves a reciprocating motion that will be converted into rotational energy thereby providing inertial support. On the other hand, solar energy does not involve any moving parts and hence no stored energy in any other form is available to support inertia. Out of the collective RES, solar and wind energy being the predominant source, a major part of frequency support is expected. But the question of whether they can provide inertial support of frequency as in the case of/better than synchronous generators have to be explored. If yes, automatic frequency control strategies should be developed in RES so that they can behave as fast frequency reserves. Also, since frequency and active power are related, it is necessary to see how the active power from the RES should behave during frequency containment period[4], [5], so that frequency deviation is the least from nominal. For instance, if the loads or sources can vary their active responses to mitigate the power imbalance caused in the grid, frequency regulation is possible.

In summary, the overall motivation of this thesis will be to develop fast active power regulation controllers in RES which act in favor of mitigating frequency deviation from the nominal 50Hz.

1.2. Problem Definition

It is comprehensible from the previous section 1.1 that the main focus of this thesis shall be frequency regulation during large power imbalance events. This can be either an under-frequency event (caused by a sudden increase in load /generation outage) or over-frequency event (caused by large load outage/connection of large power source). But from literature, it is seen that under-frequency event pose a major threat to the power system and is a immediate question to resolve.

Figure 1.2 presents the response of frequency for a large under-frequency event. As observed, after the event, frequency drops at a faster rate and reaches a minimum value called Nadir and recovers to a stable lower value based on the difference in active power.

Except for frequency, rate of change of frequency (RoCoF) is another important index that needs to be taken into consideration. In a conventional power grid, since generation was from SGs with inherent inertial property, RoCoF had a minor significance.

But in a future power system with a high share of RES, due to decreased system's inertia, RoCoF values will increase, leading to a large dynamic change in frequency curve that endangers grid stability. Also higher RoCoF, due to mechanical limitations may lead to activation of protection devices, thereby tripping SGs further worsening the problem.

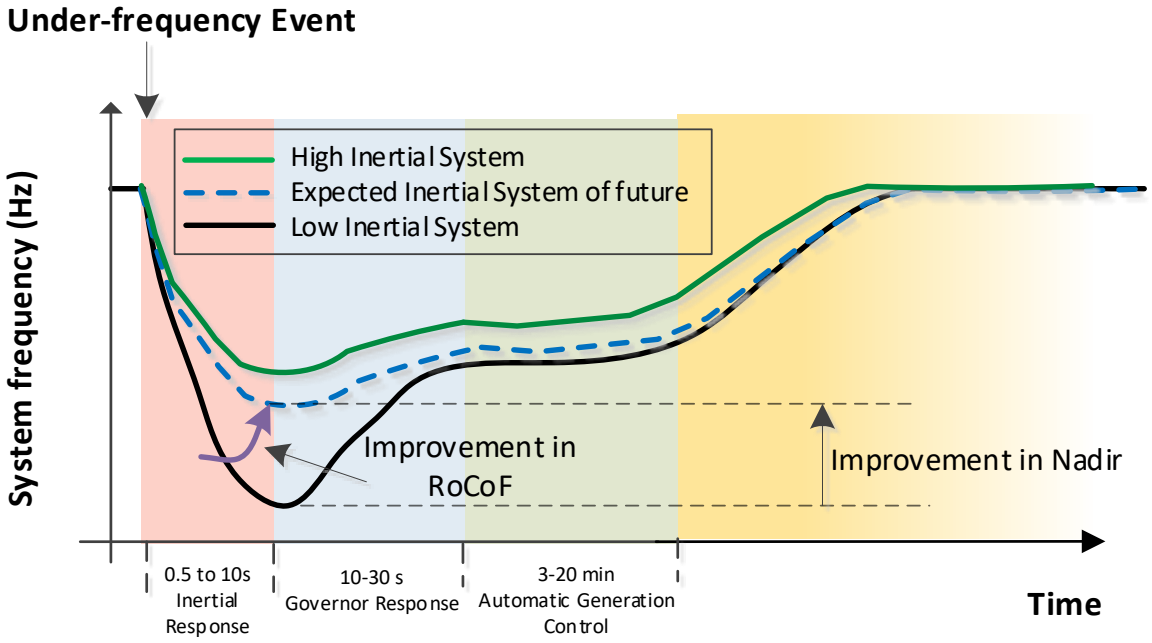

Figure 1.2: Comparison of Frequency response to a large under-freqeuncy event observed in system which possess different inertia

1.3. Literature Review

The focus of literature review was to firstly search for next-generation control strategies that can be implemented without major modifications in any Power Electronic interfaced RES which can assist the grid during the inertial response period. Secondly to check for present and future grid code requirements with respect to frequency regulation and grid stability.

Most of the review papers which intend to define frequency regulation strategies through RES have used the terms synthetic inertia, virtual inertia, and fast frequency response. These alternative names have raised due to different areas of application like micro-grids, grid-forming wind energy technologies and ancillary services support through a battery energy storage system (BESS) respectively. The common factor that can be noticed from all these different terms is that they serve a unanimous goal of supporting the grid during the period of frequency containment period. The concepts presented in these literature are very application-specific and are not generic to be applied to all the renewable resources. Hence there is a need to define a generic term and definition which can be applied across RES.

State of the art related to controllers supporting frequency regulation, mainly focuses on inertial support through wind energy since they possess spinning reserve similar to that of synchronous generator. Hence, more research has been guided towards this sector. The most common approach out of the group was that of curtailed load operation of wind turbines that enables reserve power dispatch during the perturbation period [6], [7], [8]. The drawback of curtailed load operation is that they operate the WT at a lower point than their rated MPPT value so that they have extra reserve during inertial support period; as a result, power generation is not optimal. This is not advantageous for neither the Wind Farm (WF) operators, who are rewarded by the active power injected to the grid nor the TSO's, since during steady-state there is a percentage of "clean" renewable energy that is being wasted.

Another approach suggested in literature is the Virtual Synchronous Machine (VSM) concept[9], VSM method involves emulation of dynamic behaviour of a conventional synchronous machine (by using third or higher-order model), this results in synthesizing more state variables during simulations. Due to this complex non-linear method, simulation time increases resulting in delayed behavior which are not favourable for fast frequency regulation controllers.

State of the art, which make use of full converters like Type-4 wind generators, solar plants focused on developing control strategies for utilizing chopper circuit to actuate during over frequency period. The chopper circuit is fundamentally designed for protection of dc-link from higher voltages during

fault periods. However, it can support over-frequency events by controlled actuation. But this method cannot be applied to under-frequency event. Hence this method was disregarded. Some literature has also suggested making DC capacitors which maintains a constant voltage across DC-link larger so that it can support the under-frequency event[10], but these studies were performed in RMS studies which used an average model of Type-4 wind generator. Hence the limitation that arises due to direct variation of DC-link reference voltage was not examined. This is important because DC link voltage is a reference-based on which consistency of active power dispatch from the inverter is derived. Meddling with this parameter will affect many operations on both GSC and MSC, hence this method was not valid for the present scenario.

Further researching on energy storage systems (ESS) and super-capacitors paved a path to understanding how ESS could be used for a sudden active power boost[11],[12],[13]. But since super-capacitors are still an emerging technology, detailed models were still not available but this research scope was selected for implementation, where by using approximate models of BESS, proof of concept can be investigated. A more concrete study that utilizes the mechanical inertia of a Wind turbine to mitigate short term frequency discrepancies by tracking available mechanical torque, wind speed, drive-train rotor speed for stable operation has been performed by [14], here the kinetic energy of the rotating masses and the surplus power normally discarded through pitch control are being used intelligently to provide necessary positive reserves. A control strategy developed in order to enable this extraction follows the measurement of grid frequency droop values and measurement of RoCoF. Hence the droop and derivative-based controllers were selected for analysis and modifications, if needed.

A more thorough comparison of the different heuristic methods available [15], [16],[17],[18] was outside the scope of this project since it was more complex and less evolved to suggest to industries.

After examining more literature on this front, it was found that droop and derivative-based controllers [14], are feasible only in systems which have rotational inertia reserves, precisely big wind turbines. Also, the models of WT or other renewable energy sources on which these controllers were mostly implemented was built on RMS based simulations. Some analysis has been done on offline EMT based PSCAD software but the wind turbine models used were average models. The drawbacks of RMS based simulations were that they work on mathematical models which consider only electro-mechanical transients but neglect electromagnetic transients (which is a basis on which all power system components operate). Also, average models do not provide complete information about physical limitations on the interaction of multiple controllers. As a result, EMT based real-time studies with full-scale models were given importance. The models considered here were of full-scale, which simply means it includes all the controls and power system components present in an actual real system. By this, it could be ensured that the behavior of all controllers along with their performance limitations will be considered. RSCAD was chosen which was EMT based real-time simulation software satisfying all the requirements and also integration with hardware in Loop (HIL) setup was feasible for validation purposes.

As introduced before, another aspect of the literature study was to discuss with experts from industries regarding the selected controllers and request for feedback regarding compliance strategies developed for testing of the controllers. But before this, there was a need to set a common ground since most of the review papers which intend to define Synthetic Inertia[19], Virtual Inertia[20], Fast Frequency Response[21], [20], and Fast Active Power Regulation fails to underpin the reader to clearly understand the conceptual difference between them. Also, it was found that the grid codes and other TSO related documents also lacked concrete information regarding frequency regulation strategies. Hence it was important to provide a plausible generic definition of Fast Active Power Regulation (FAPR) which encompasses all the definitions put forward in literature and can be applied to any RES which affirms to support frequency regulation. Based on this proposed definition, the FAPR controller strategies have to be built. To this end, feedback from industrial experts will be taken care to fine-tune definition, controller strategies and criteria for compliance testing.

1.4. Research Questions

Since the thesis objectives were defined, it is possible to define the research questions, that this thesis is called to answer. Those questions are summarized below:

Q1: What is the added value of using Real Time Digital Simulation (RTDS) instead of offline RMS simulations to model and evaluate the performance of FAPR?

From the literature review, it was found that on one front, most of the frequency regulation strategies built have been tested through an RMS based simulation software like PowerFactory where the frequency curve analyzed for generation-load imbalance condition was very defined and smooth deviation from normal 50/60Hz. But on another front, reports submitted by TSO's mention that the national grid frequency when subjected to similar load-frequency imbalance was distorted, dynamically varying and non-smooth frequency variation. Also, some literature points out that this effect increases with a higher share of renewable resources. This was due to 2 reasons, one being a decrease in inertia in the grid and the second due to less efficient filters of switching signal at the output of RES. All these issues pointed out towards the importance of Electro-Magnetic Transient (EMT) studies and hence the question arose: is it possible to create a test bench which facilitated a qualitative assessment of real-time frequency including but not limited to the projected above 50% share renewable of 2030/2040 grid?

Q2: Is it possible to propose a generic definition of FAPR, considering the existing propositions in the current state of the art? Going through the national grid codes and other TSO operations of grid-related details, it was clear that there is a lack of understanding regarding the concept of RoCoF, solutions related to frequency regulation strategies in the future RES shared grids and there is also a lack of clear guidelines related to the measurement of frequency. All these concerns pointed towards lack of understanding of the existing controller propositions in the current literature review. This problem existed since the literature lacked a unified converging definition which could be applied to any renewable generation, storage, and responsive demands that could support frequency regulation in a multi-energy system. This search resulted in a question stating, is it possible to propose a generic definition of FAPR which can be collectively applied to any RES that could regulate instantaneous active power dispatch to achieve a common goal of mitigating the frequency deviation caused by an imbalance?

Q3: Is it necessary to modify the existing compliance requirements on FAPR?

The national grid codes on which TSO's operate defines a set of compliance requirements during the inertial response period. But these requirements were defined basically for power plants which operate synchronous generators. But since these traditional fossil-fuel generators are gradually being decommissioned, and are being replaced by Renewable Energy Sources (RES), there is a need for these sources to provide ancillary services, specifically frequency regulation support through FAPR strategies. With this coming into existence, there will be a need to modify existing compliance requirements such that it is more suitable for FAPR controllers. Discussion with experts from industries regarding this will provide a better insight to shape the future grid codes.

Q4: What are the most effective FAPR strategies that can help to elevate frequency Nadir and decrease RoCoF when applied to different sources of Fast Frequency Reserve?

To achieve FAPR, there are different proposed control strategies in the literature. All these controllers operate with a common aim to improve frequency nadir and decrease RoCoF, but will have a different principle of operation. However, support from one of these FAPR controllers will be predominant. Hence, it will be interesting to check which FAPR controller strategy gives the best response.

Q5: Does HIL testing provides similar findings as observed with only RSCAD based analysis?

As a part of the validation, the aim is to test the controller strategies by applying signals on a real system. By performing this validation, it can be made sure that the FAPR controllers will not abruptly interact with other controller limits leading to a trip of the inverter. Since the HIL setup has the inverter operating very similar to that developed in RSCAD. It will be interesting to observe if different dynamic response of frequency and output active power curve are noticed.

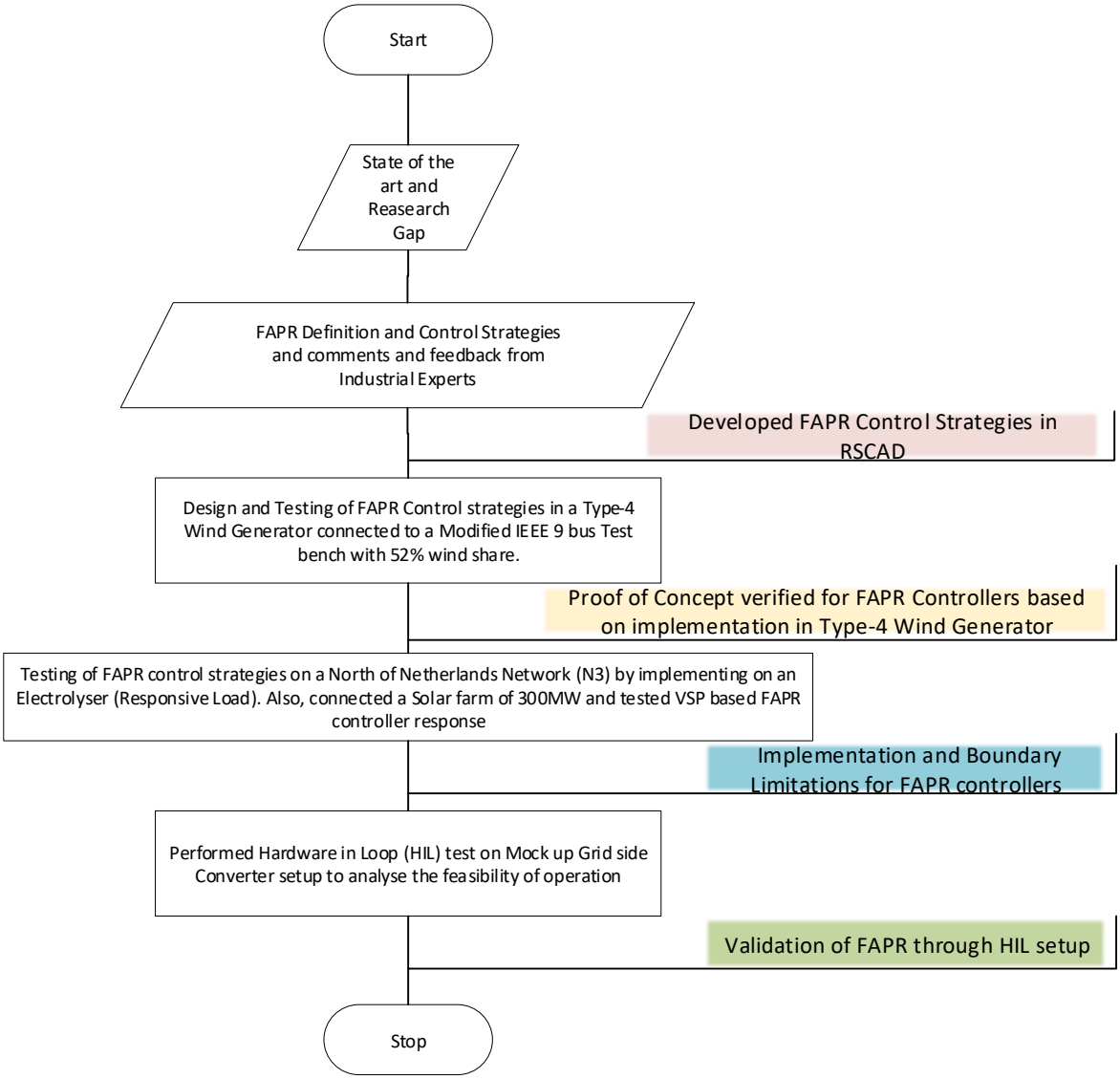

Figure 1.3: Overall Thesis Flowchart

1.5. Thesis Outline

In this section, a brief description of the chapters of this report is provided.

Chapter 1: Introduction First of all, an introduction to the project is provided, where the research theme, the urgency for such a project and the societal impact are discussed. Moreover, state-of-the-art is presented and the scientific gaps are identified. Also, the scope of the project and the main research questions are presented. A more thorough description of the project follows, while the most important contributions of this project are highlighted and the boundaries are set for the priorities of the study to become clear and the outline of the report is given.

Chapter 2: Theoretical Background In this chapter, a qualitative comparison of the past, present and future AC grids are presented. A detailed study of frequency and its relation with inertia and grid stability during steady-state operation is discussed. The conventional frequency control mechanisms and problems arising due to the loss of these controls are presented. Also, state of the art controllers developed and the fundamental basis of operation of these controllers are examined.

Chapter 3: Fast Active Power Regulation Definition and Control Strategies In this chapter, a generic definition of FAPR on which the developed controllers are operating is stated. The development of FAPR on a Real-Time Digital Simulation (RTDS) platform is explained.

Chapter 4: Application of FAPR controllers to Type-4 Wind Power Generation This chapter starts with a brief description of the development of a Modified IEEE 9 bus system with a share of 52% wind share. Next, modification of Type-4 wind generation system in order to accommodate FAPR control strategies is explained. Later, simulations are performed and system behavior under various load frequency variations, gain and dead-band sensitivities, other impacting system-dependent parametric sensitivities are explained. A comparative assessment between various controller strategies is also illustrated. To this end, a generic tuning methodology for FAPR controllers and interconnected systems are described in detail.

Chapter 5: Application of FAPR controllers to a Multi-Energy System This chapter starts with a brief description about North of Netherlands Network, Renewable systems connected and feasibility of connecting FAPR controllers to them. Next, modifications done in electrolyzer and Solar Farm to provide frequency support is described. To this end, simulations are performed and system behavior under load-frequency variations with different controllers are discussed.

Chapter 6: Hardware-in-the-Loop Validation and Testing In this chapter, a brief description of Hardware in Loop set up has been discussed. Implications and importance of this study have been briefed. Later, a comparative assessment between results obtained from RSCAD and HIL setup has been performed.

Chapter 7: Conclusions and Future Work The most important conclusions obtained through this study are summarized in this chapter. The research questions of the project are answered, with references to the corresponding chapters that contain more analytical information related to each research question. In this chapter, the most important topics to be further studied are highlighted and briefly explained, and this serves as a guide for the continuation of this thesis project.

2

Theoretical Background

This chapter depicts the fundamentals of the subject study. The fundamentals include system frequency, inertia, kinetic energy of the rotor mass in a synchronous generator, inertia constant, supporting ancillary services to keep the frequency stable, necessity to have a stable frequency, and lastly new age frequency regulators like fast frequency controllers being developed in the literature.

So the chapter starts with a brief introduction regarding motivation of this chapter, then the emergence of the concept frequency' is stated, furthermore the concept frequency has been explained in detail with a wheel speed analogy and later what is the impact on the power system components if frequency deviates from the fixed steady-state is briefed. Further, a conglomerate summary of frequency-related grid code limits and regulations has been presented in the table. Besides this, inertia and its relation with frequency is explained in terms of the equations. In addition to this, new age concepts of inertial sources under different titles and definition available in the literature has been again explained in brief. And lastly, this chapter ends with, what is the need for a new definition of frequency regulation strategies and how controllers have to be developed in conjecture with the proposed definition.

2.1. Introduction

In any cyclical process, frequency is defined as the measure of the number of cycles per unit time. Cyclical processes can be rotation, oscillation or wave motions. The SI unit of frequency is Hertz (Hz). Hertz is the number of repetitions of a cyclical process that happens in a second[22]. In Electrical Power Engineering, frequency is usually measured for 3 ϕ AC voltage wave and in Europe, as a standard, it is agreed to maintain the grid frequency steady at 50Hz. The process involved in achieving this is like "a great balancing act", where an equal balance between generation and loads must be maintained in order to achieve the respective frequency value. With power generating sources ranging from gas and coal to solar and wind, there are a vast number of power plant control strategies and possibilities, but based on their feasibility and efficiency, they all share grid operation responsibilities to one degree or another. Steam-based turbo-generators was traditionally regarded as a great contributor in frequency stabilization around the steady steady-state condition, due to the heaviness of their rotational mass. But due to gradual phasing out has led to a concern, which will be discussed further. Never-the-less, t he following section aims to highlight the importance of system frequency. It will also provide the influential factors responsible for keeping frequency stable.

2.2. Emergence of the concept frequency

The conventional power grid was made up of synchronous machines spinning in near-exact synchronization to each other such that frequency remains close to 50 Hz across the network, which means all the generator's rotor which are spinning at different speeds, are still governed by frequency through a formula:

$$N_s = \frac{120f}{P} \tag{2.1}$$

N_s = Rated synchronous speed of a generator

f = System Nominal Frequency
P = Number of Poles
Table 2.1 represents the number of poles, synchronous speed relation along with area of application. It can be seen that synchronous speed, number of poles have a direct relation with each other while inertia constant H is inversely related. This is related again to the diameter to weight ratio of the drive-train. For simplicity, lets consider wheel diameter, speed analogy.

Number of Poles	Synchronous Speed	Applications	Features	Approx. Inertia Constant
2	3000 RPM	Steam, Thermal, Nuclear, Co-Generation Plants	High Inertia Constant	8 - 10 s
4	1500 RPM	Steam, Thermal, Diesel, Gas and small Co-Generation Plants	Higher MW rating, higher the inertia constant	6 - 8 s
8/6	750 RPM/1000 RPM	Diesel Engine, Gas Turbines, Hydro Turbines(Pelton)	Low Inertial support but has black start capability	4 - 6 s
10/12 more	600 RPM/ 500 RPM/..	Hydro (Keplan and Francis) depending on water head and site conditions	Least inertial support, and best for black start capability	2 - 3 s

Table 2.1: Number of Poles, Synchronous speed and inertia constant comparison between generators used in different applications

2.3. Wheel Speed Analogy

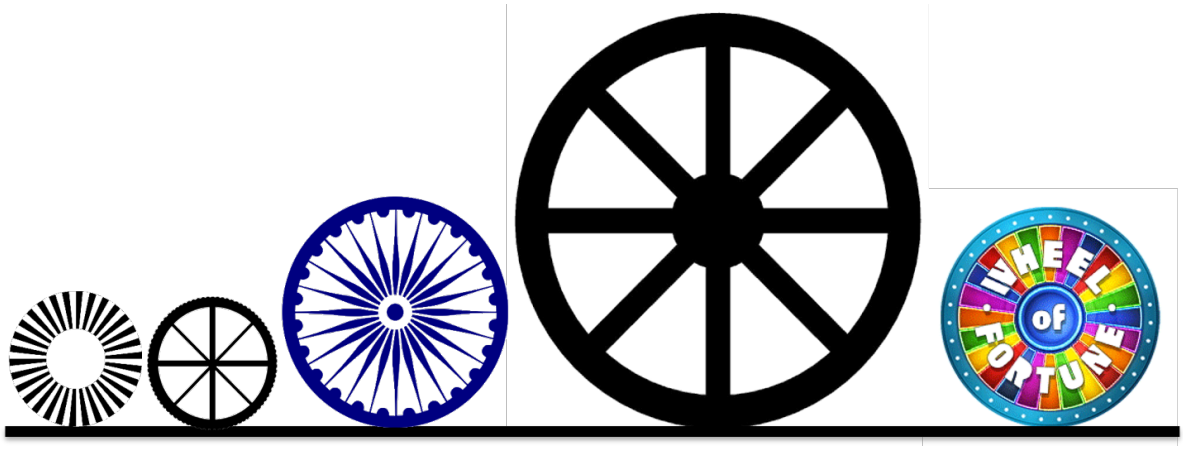

Figure 2.1: Wheel Speed vs diameter Anology

Figure 2.1 represents an analogy of how rotor speed, frequency and synchronized operation is interlinked. Here, say, the distance covered by all the wheels revolving at different speeds are same, and this is in resemblance with system frequency 50Hz. Wheel diameter represents the diameter of synchronous generators. So, all the wheels have to cover the same distance in same time, but the rotation speed of the wheel is inversely proportional to the diameter. This shows how, though turbo-rotors have higher speeds, due to lower number of poles, they operate at 50Hz while water-wheel rotors which

rotate slower but due to larger number poles they again operate at 50Hz. But here the challenge is that each vehicle like each vehicle have their own cruise control, each rotor has their own governor setup regulating rotational speed and ensuring equal power. Now if, vehicles that set the cruise speed slightly higher would be doing more work, while vehicles with the speed set slightly lower would be applying no power, similarly, synchronous generators which rotate at higher speed than their respective rated speed will have to bear more load. But, if the generators are operated at a slightly lower speed, then due to sluggish behavior they act as a burden to the grid, in contrast, if they are operated at a slightly higher speed then they share a higher burden of the grid. The synchronous speed for a particular application will be designed as per table 2.1. This simple but challenging problem used to be a daunting engineering problem. However, with the introduction of system frequency as a common reference, the problem of over and under-powered systems was resolved. For example, say that the generator power of 90% corresponds to the target frequency of 50Hz, but if generator power reduces to 85% then frequency gets lowered to 49Hz. Conversely, if the power ramps up to 95% then this corresponds to a frequency of 51Hz. This regulation of active power in real-time based on frequency value is termed as 'Primary Frequency Response'. The time period of this operation will be around 10 – 30 secs and it's called rebound period. 'Secondary Frequency Response' can be provided by spinning reserves and other generators over several minutes commonly called recovery period (3 to 20 minutes). In summary, from this analogy is could be understood that though there are different types of synchronous generators contributing in terms of generation to the power systems, all are governed by a single global law called frequency which serves as a benchmark for sharing of electrical load connected to the power systems.

2.4. Meaning of Frequency Variation

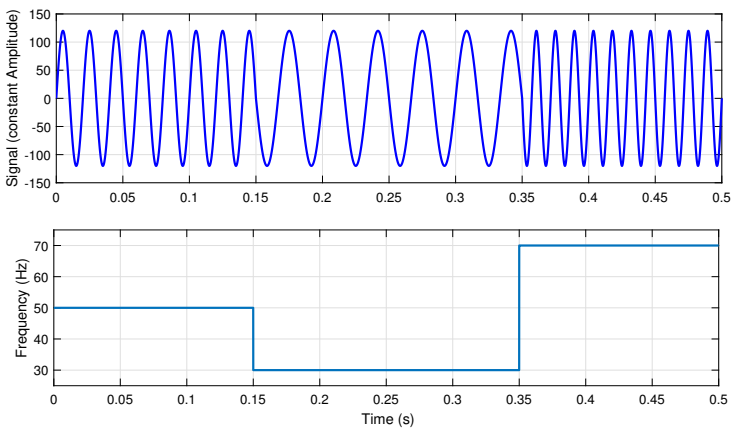

Figure 2.2: Signal representing a constant amplitude with varying frequency scenario

In figure 2.2 shows the relation between instantaneous voltage wave with constant amplitude and varying frequency. Here 3 frequency plots are considered for demonstration, Initially, frequency of a signal with 50Hz is shown and later when the frequency is 30Hz, it is observed that the signal is expanded and at last when the frequency is raised to 70Hz, the signal looks compressed. This is exactly what happens in a power system frequency, but the bandwidth of variation is not so extreme as shown in fig 2.2, but rather between 47 to 51.5 Hz under extreme conditions. This depiction clarified the exact wave behaviour of voltage and currents during generation load mismatch conditions.

2.5. Problems of unsteady frequency in future grids.

With measurement and regulation of frequency through power plant governors being explained in the previous section, this section discusses the need to maintain stable frequency at 50Hz and the issues that will arise due to unstable power frequency in the grid. Frequency is a global parameter which means it is assumed to be constant at all voltage levels, generations and distribution levels. But when the grid is subjected to contingencies like loss of transmission, increase in load, forced generation

outages or other load-generation imbalance events, the frequency becomes unstable. So this instability affects various components starting from generators, transformers, and loads.

Since the generation sources decide the system frequency, as explained in the above section, at generation level, there may be issues with load sharing, and due to multiple feedback loops operating at different time constants, issues of low-frequency harmonics, uncontrolled oscillations may lead to instability. Further, if the disturbance is sudden, torsional dynamics may cause rotor pole slip which can lead to large changes in currents which may activate the trip command.

At the distribution level, electronic equipment like audio amplifiers, when subjected to uncontrolled oscillations can destroy power stages and speakers.

More importantly, in transformers, frequency is directly related to voltage and flux density. Hence with constant system voltage and with an increase in frequency, the flux in the core increases and the transformer goes into saturation. This also increases eddy current and hysteresis losses and may cause concentrated heating issues.

2.6. Inertia and its role in keeping the frequency constant

Until now, the discussion was revolving around the relationship between steady-state frequency and its corresponding rotational speed of rotors. Now in this section, the discussion is extended towards kinetic energy of the rotating mass and its reflection on inertia and inertia constant along with frequency. During steady-state operation, in a power grid, there exists always a balance between generation and demand including losses. Now when a generation-load imbalance event occurs, the grid restoration to normalcy will be crucial and various generator auxiliary controllers enact, but since these controllers involve valve operation, they consume more time to enact. However, since synchronous generators within oil, coal, gas and nuclear plants run by large heavy rotating turbo-generators usually at 3000 RPM or 3600 RPM. The rotational kinetic energy involved will be huge which replicates to be the inertia of these generators in electrical terms. This forms the main backbone for immediate frequency regulation of 50Hz/60Hz under disturbance. Inertia is defined as a physical property of synchronous units which provides an inherent response to slow the Rate of Change of Frequency.

Figure 2.3 depicts the case of an under frequency event due to the loss of generator/increase in load. It can be observed that frequency drops from normal 50Hz at a particular rate called RoCoF reaches the lowest point called Nadir and recovers to a stable value and then later brought back to the normal position. This well-established process is termed as system frequency regulation. As noticed there are 4 control strategies responsible for this operation, namely

- Inertial Control
- Primary Frequency Control
- Secondary Frequency Control
- Tertiary Frequency Control

In this thesis, since the focus is about inertial response, inertial and primary frequency controllers will be explained in the following sections.

2.7. Inertial System Control

Inertia is an inherent property that synchronous generators possess that behaves as a "first line of defense" against frequency change. Like any physical load, when the electrical load in the system increases, the burden on the generation sources increase and they try to cater to the increase in load by decreasing their rotational speed (or in other words loss of kinetic energy). This response will be immediate, and its support depends on the product of mass and speed of the rotational mass. This can also be translated as mechanical power (P_m). Swing Equation 2.2 provides a clear relational explanation regarding the inertial response that can be expected from any synchronous generator.

$$\frac{d\omega}{dt} = \frac{\omega_o}{2HS_b\omega}(P_g - P_L) \tag{2.2}$$

As noticed, the term P_g–P_l represents the generation load imbalance condition, ω_s, synchronous speed being fixed for a particular pole as per equation 2.3, H and $\frac{d\omega}{dt}$ (Rate of Change of Angular

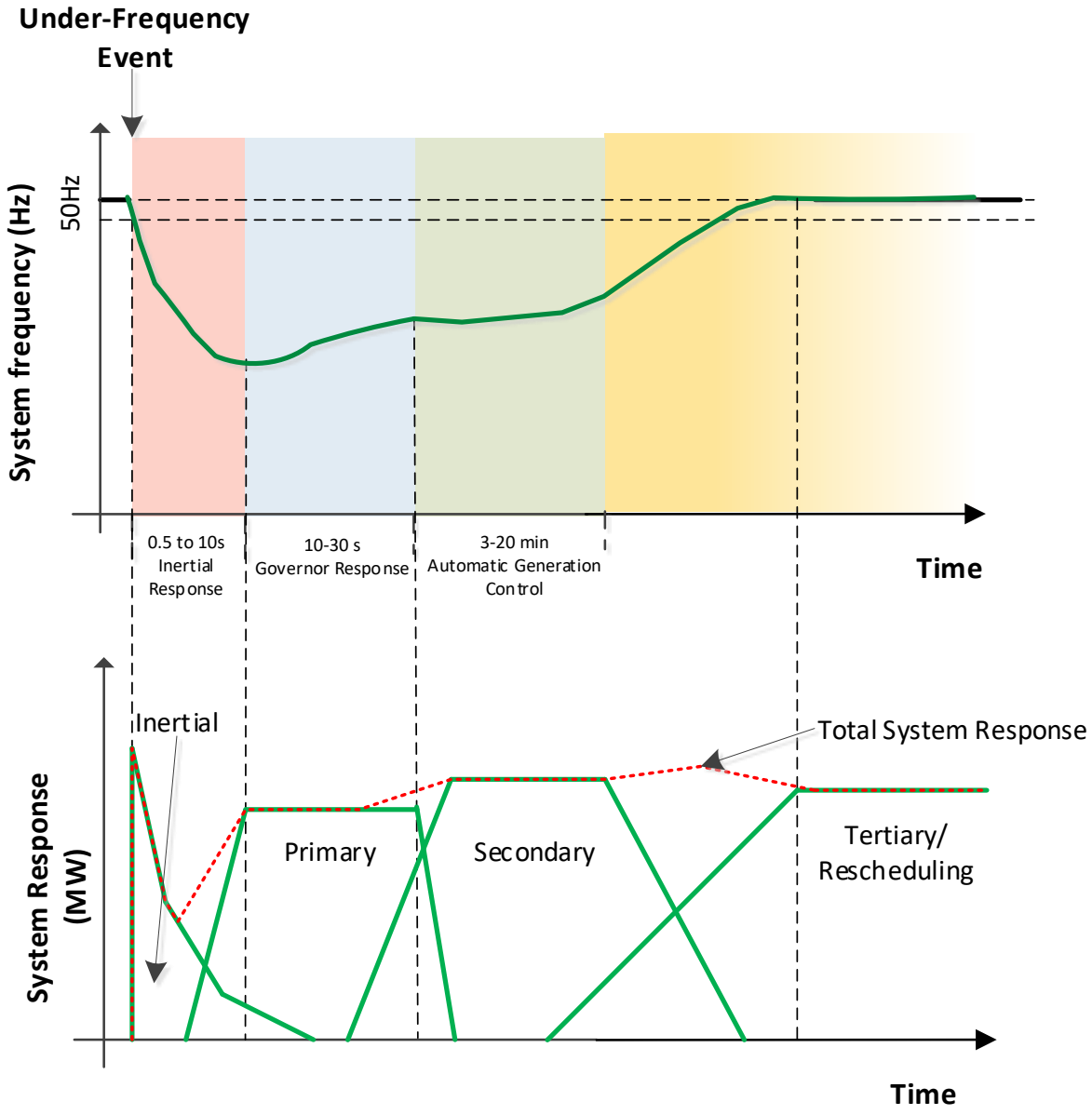

Figure 2.3: Representation of system frequency response and active Power Response from Synchronous generators

Speed) terms are in direct relation i.e. if the value of H is large (for example in a steam generator) then the $\frac{d\omega}{dt}$ alias $\frac{d\Delta f}{dt}$ that is imposed is small and vice versa.

$$\frac{2H}{\omega_s}\frac{d\omega}{dt} = P_g - P_l \tag{2.3}$$

$$\frac{2H}{\omega_s}\frac{d\Delta f}{dt} = P_g - P_l \tag{2.4}$$

On a system level this equation can be written in a more general form as shown in equation 2.5:

$$\frac{dE_{kin}}{dt} \approx J.f_o\frac{df}{dt} \approx P_g - P_l \tag{2.5}$$

Where :

ω_s : Rated Angular Frequency
S_b : Base Rated Power considered in the power grid.
E_{kin} : Kinetic Energy stored in the generators and motors shaft
f : system frequency
$\frac{df}{dt}$: Rate of Change of Frequency.
J : Total System Inertia

Since the active power of generators (P_{gen}) cannot be changed instantly. The kinetic energy released by synchronous generators will be used initially to curb the variation of frequency, this inertial response is an inherent feature of synchronous generators and is available immediately when there is a disturbance at the grid. Figure 2.3 depicts the inertial system response available naturally for the first few seconds of the disturbance. After 5 to 6 seconds, the primary frequency control, which is explained in the following section, is activated in order to eliminate the remnant frequency deviation.

2.8. Primary Frequency Control

In a traditional synchronous generators, primary frequency response will be provided by hydraulic valve management by automatic speed governors. The governors are responsible for regulating the speed of the rotor shaft according to the change in frequency and power. The operation of governor is autonomous but , by agreement, they accept instructions from secondary controls and tertiary controls responsible for system balancing. But ultimately, turbine governors have complete authority within their sphere of control and their time scale. Primary frequency control usually actuates within 4 to 5 seconds after the disturbance has occurred and will be active for 10 to 30 seconds, before secondary frequency controllers kick in.

In Power Electronics interfaced especially wind turbine generators, primary frequency can be related to blades pitch angle, but here, the response is much slower compared to synchronous generators.

2.9. Secondary and Tertiary Frequency Control

Secondary and Tertiary frequency control, consider system-wise rescheduling of dispatch which takes place for several minutes (3 to 20 minutes). Though governors are responsible for this change along with other reserves, the entity that is considered for monitoring is only frequency with a prime motive to bring back it to nominal 50Hz. These sections are not discussed in depth in this thesis since they are not an immediate concern and alternatives like Battery Storage Power Stations have already entered the renewable market providing secondary and tertiary supports.

2.10. Natural reserves of inertia in Renewable Sources.

Since most of the established renewable sources are Power Electronic Interfaced components, the frequency is determined by Voltage Source Converters (VSC) interfacing the renewable source and the grid. Hence there is no mechanical power backing up the frequency, except in Hydro Energy. Solar Photo-Voltaic is a classic example where the priority is to generate the most active power possible based on MPPT[23] and since it does not involve any rotating part and the power generated is primarily DC, and inertia emulation is impossible. Wind Energy has evolved over the years and now Type-4 Wind Turbines are the most common and established in the market which involves a complete back-to-back converter which isolates the generator and turbine from the rest of the grid, in order to protect the wind turbine setup from grid-related faults and to eliminate gear-box. The disadvantage with this is that the natural inertia that could have been extracted from the Wind Turbine Setup (Blades and Generator) is now lost. Flywheel technology in conjecture with tidal and bio-gas is still an emerging technology which can provide natural inertia support [24],[25] but it is not an immediate solution. To summarize, only the major sources of renewable energy like in its purest form cannot provide inertia support without modifications. In further chapters, discussions regarding how renewable energy sources can be modified to support inertia synthetically shall be briefed.

2.11. Virtual Inertia, Synthetic Inertia and Fast Frequency Response

From the previous section, it was seen that solar and wind are predicted to be more dominant renewable energy sources of the future. Also, bare solar technology with no ancillary support controls involved cannot provide any inertia back up, while wind can support only to an extent if they are directly coupled. Most of the Wind manufacturing industries prefer Type-4 Wind Generators. Though Type 4 wind turbines are equipped with inertia constants of up to 6-7 s, they will not be able to contribute inertia support to the grid frequency variations without suitable control modifications. The control modifications over the literature are available under various names like virtual inertia/synthetic inertia and fast frequency response/fast active power injection.

Most of the review papers [5], [21], [26] which intend to define Synthetic Inertia, Fast Frequency Response (FFR) underpin the reader to clearly understand the conceptual difference between them. Although Synthetic Inertia and FAPI/FFR work on variations of active power, they are delivered via different physical mechanisms and play roles that are not directly interchangeable. The definitions below provide a clear difference between terms.

2.11.1. Synthetic Inertia/Virtual Inertia

Definition 1*: synthetic inertia is defined as the controlled contribution of electrical torque from a unit that is proportional to the RoCoF at the terminals of the unit.*[19]

Definition 2*: Synthetic inertia is a response of a generating unit to frequency changes, in particular, a power exchange which is proportional to RoCoF.*

In literature, many papers claim to have proven that this control has been achieved, which is true but most of these papers assume the grid is already safely operating with enough inertia constant since enough synchronous generators are operating providing inertial response[20]. But in future when the grid is completely maintained by Power Electronics based Renewable sources, the H factor of the grid will be very low and with these conditions, synthetic inertial response is highly unlike to achieve.

2.11.2. Fast Frequency Response

FFR is based upon a control system that can be tuned to operate as desired and can inject active power to correct the imbalance, and restore power system frequency.

Definition 1*:[21] FR generally refers to the delivery of a rapid active power increase or decrease by generation or load in a time-frame of few seconds or less, to correct a supply-demand imbalance and assist in managing power system frequency. Many inverter-connected technologies, such as wind,*

photovoltaics (PV), batteries and other types of storage have the capability to deliver FFR, as well as by demand-side resources.

Given FFR can act quicker than current frequency control services, they may also assist in managing challenges related to high rates of change of frequency (RoCoF).

***Definition 2**: [20] Fast frequency response is the controlled contribution of electrical torque from a unit which responds quickly to changes in frequency in order to counteract the effect of a reduced inertial response.*

Fast frequency response based on frequency deviation can significantly improve the minimum instantaneous frequency after disturbance. (NADIR). The term synthetic inertial response must, therefore, correspond to the controlled response from a generating unit to mimic the exchange of rotational energy from a synchronous machine with the power system. Any other form of fast controlled response can then be termed as fast frequency response. To clarify, synthetic inertial response is a subset of fast frequency response which contains different responses based on frequency and RoCoF.

The definitions presented in the literature are very specific to wind turbines and are not sufficient to be applied to all the renewable resources. Hence there is a need for a unified general definition which encompasses all the essence of the above definitions.

2.12. Frequency related Grid Code requirements as per year 2020

Most of the countries in the world have transmission system that are designed to operate at 50Hz. As discussed before, in practice, the system frequency varies second by second as the balance between system demand and total generation changes[27]. Since each country has their own generation and demand levels, they have defined their own grid codes to ensure stable operation[28],[29]. Table 2.2 represents the normal and critical frequency variations for some countries which adapts 50Hz nominal frequency.

Country	**Normal Frequency Variation Interval**	**Critical Frequency variation interval**
Netherlands[30],[31]	49.9-50.1 Hz	47.5–51.0 Hz
India[32]	49.5-50.2 Hz	48.5 - 51.5 Hz
Denmark[33]	49.9–50.1 Hz	47.5–51.0 Hz
Germany[28]	49.5–50.5 Hz	47.0–52.0 Hz
Great Britain[34]	49.5–50.5 Hz	47.0–52.0 Hz
Ireland[35]	49.8–50.2 Hz	47.0–52.0 Hz
France[28]	49.5–50.5 Hz	47.0–52.0 Hz
Belgium[36]	49.5–50.5 Hz	47.0–52.0 Hz
Austria[37]	49.5–50.5 Hz	47.5–51.5 Hz
Poland[29]	49.5–50.5 Hz	47.0–52.0 Hz
Italy[29]	49.9–50.1 Hz	47.5–51.5 Hz
Romania[38]	49.5–50.5 Hz	47.0–52.0 Hz
Australia[21]	49.75–50.25 Hz	47.0–52.0/55.0 Hz
China[39]	49.8–50.2 Hz	48.0–51.0 Hz

Table 2.2: System frequency variation acceptable limits under Normal and Critical conditions based on Grid Codes

3

FAPR Definition and Control Strategies

Frequency Stability studies in EMT based software of the Fast Active Power Regulation (FAPR) Controllers are developed in this section. FAPR controller is a combination of 3 different controllers namely,

- Droop based FAPR controller
- Combined Droop and Derivative based FAPR controller
- Virtual Synchronous Power based FAPR controller

The droop and the combined droop-derivative controller topology can be applied to RES which has a rotating mass that can expend some kinetic energy (ex. wind turbines) when needed, but VSP based topology is suitable for any device which uses a full converter and has a stable DC link. Each of these approaches are analyzed and discussed in order to increase the share of power electronic interfaced generation of the grid without jeopardizing the security of supply in the power system. These controls are explained in detail in the following sub-sections.

3.1. Proposed Generic Definition

As mentioned in the previous chapter, literature had many definitions on frequency regulation from renewable generation sources but there was no generic unified definition which is applicable for all the power electronic interfaced devices. Hence the definition FAPR.

"Fast Active Power Regulation (FAPR) is a control action applied to power electronic converters used to interface renewable generation, storage, or responsive demand. It involves continuous measurement of grid frequency and/or active power deviation within very small time frames, followed by an action of a given controller scheme to regulate the injection/absorption of instantaneous active power to mitigate the frequency deviation caused by an imbalance. FAPR considers technical limitations or boundaries determining the capability of the controller to provide Fast Frequency Response.

FAPR is essentially a mechanism to quickly regulate the active power injection/absorbtion to mitigate frequency variations in low inertia systems. Since it may overlap with the time window of the inertial response of conventional synchronous generators (0.5 s from occurrence of active power imbalance), some authors use the alternative term 'inertia emulation' (IE) [26]. The actual source of energy for emulating inertia is stored in systems behind power electronic interfaces, such as batteries and rotating masses in wind turbines. A supplementary control loop for inertia emulation enables the wind turbine, or storage element, to release the stored kinetic energy up-to 10s to arrest the frequency deviation [19]-[40]. In the derivative based control, a derivative term of frequency is used to emulate inertia like

in conventional power plants. Several studies have shown that this type of control greatly improves the frequency Nadir as well as the frequency recovery process following an active power imbalance [4]–[14]. The application of derivative control alone provide a satisfactory response upto the point of Nadir but once the frequency reaches a settling point, the output of derivative tends to 0(derivative of a constant is 0) and hence the addition of droop-based control can be considered as a complementary control action to produce an additional change in the active power reference of the wind generator in proportion to the system frequency deviation for better recovery and enhancement of Nadir [41]–[15]. Most existing research works on FAPR are devoted to controller design considering a single wind turbine or a small set of wind turbines, which is usually connected to a small-size system. Nevertheless, a detailed analysis on the impacts of a given FAPR controller, its parameters, and the combination of wind generators equipped with FAPR controller is needed to determine the maximum share of power electronics interfaced generators (PEIG) that does not entail a risk of frequency instability. This section addresses this gap by performing sensitivity analysis, based on time-domain simulations, to assess the influence of FAPR control parameters on the system frequency performance in the frequency containment period. By evaluating individual and collective behaviour of PEIGs, an effective combination of wind generators with a FAPR controller and suitable settings for this controller will be pursued.

Since in both derivative and droop-based approaches, the input signal is the frequency error, therefore, the confident measurement of frequency in those methods is very important, and the application of different techniques for frequency measurements like (Phase-Locked Loop) PLL, Phasor Measurement Unit (PMU) may have some limitations. Moreover, an alternative FAPR controller, which is based on Virtual Synchronous Power (VSP) strategy is also proposed. In this approach, the input signal of the FAPR controller is the power deviation instead of frequency in previous methods. The active power loop control on VSP has a second-order characteristic, which makes a simultaneous influence of damping and inertia emulation into the system.

3.2. Droop Based FAPR Controller

Frequency droop control is a control strategy where active power is injected/extracted based on the droop of frequency from nominal frequency (50Hz / 60Hz) under the condition of dynamically changing loads/generations.

Figure 3.1 illustrates the droop control based FAPR controller. Here F_{meas} represents the system frequency is measured. But note, if the grid is large, the system frequency will be slightly different at different areas and hence inter-area oscillations exists, hence frequency at the most critical bus has to be considered. The most critical bus is where the highest load frequency variation can be observed. Another input f_o equal to 50 Hz (in case of 50 Hz grid). The error between the two input signals is passed through a dead band. From the grid codes[29], it was concluded that the frequency regulation controllers should be activated when frequency deviation is anywhere between 0.06% to 0.1% of its nominal value. Based on this, the dead band can be between 0.03 to 0.05. In this case, dead-band was chosen to be 0.03 for the high sensitivity of the controller. This signal is further normalized using parameters based on IEC 61400-27 standards. The resulting signal is multiplied with a proportional or droop gain K_p. The value of K_p is purely system dependent and is tuned son as to have a linear dependency with respect to the total power output extracted from the PEIG due to droop based FAPR controller. Further details on the selection of K_p will be described in section 4.4.1 . This resulting signal $P_{elecref}$ from droop based FAPR controller is now added as an additional signal to the electrical power reference signal which is quintessentially responsible for setting the electrical power demand required from PEIG.

So, with an additional reference from the droop controller, the electrical power reference $P_{elec-ref}$ could be altered proportional to the frequency deviation from 50Hz. Lastly, the findings from this method were that there was an improvement in the point of Nadir but this method was not supportive to improve the dynamic frequency response before Nadir or in other terms inital RoCoF after the disturbance.

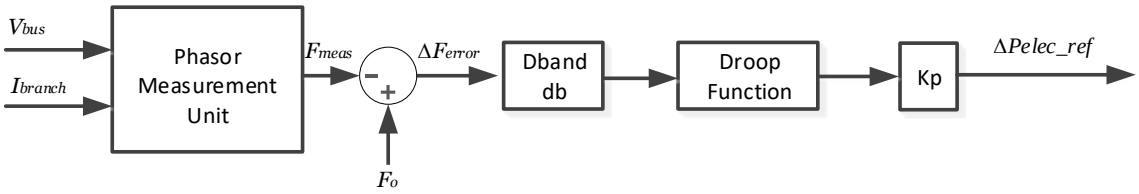

Figure 3.1: Block diagram of the droop based FAPR controller

3.3. Combined Droop and Derivative based FAPR Controller

Frequency based derivative approach is a control strategy where active power is injected/extracted based on the derivative of frequency from nominal frequency (50Hz / 60Hz) under the condition of dynamically changing loads/generations.

Figure 3.2 below illustrates the combined droop and derivative control based FAPR.

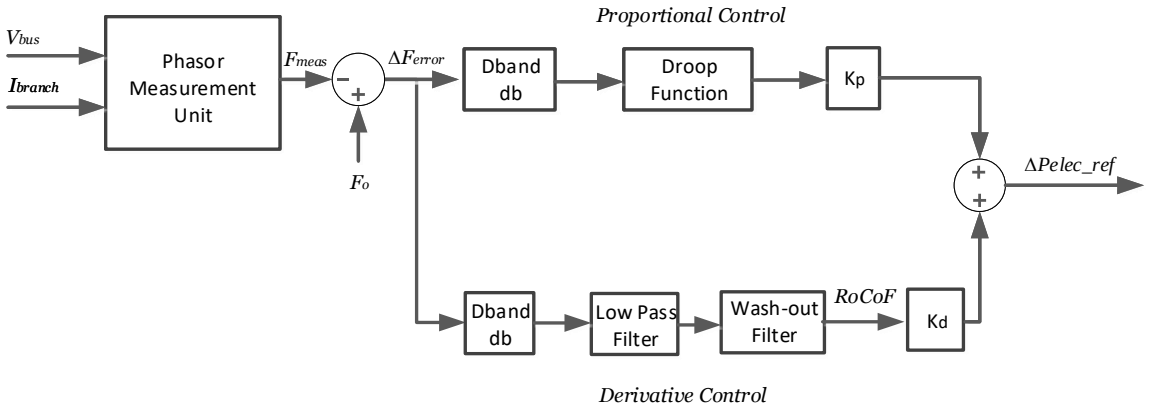

Figure 3.2: Combined block diagram of droop and derivative based FAPR

In this method, as the name suggests there are 2 controllers, namely droop controller and derivative controller. The droop controller remains the same as implemented in the previous Section 3.2. Now as an addition, the derivative control block was introduced. The derivative-based controller is required mainly to provide a faster response of controller during the initial few seconds right after the fault when the RoCoF is highest. Further, please note this section is explained considering the controller is applicable to wind turbine.

The derivative controller takes the frequency error as input, which is passed through the dead-band, here the dead-band is of negligible value because the immediate response of the controller is a priority during the containment period. Further, the error signal is passed through a combination of low pass and derivative function block in order to achieve the derivative of a frequency error signal. The characteristics of this resulting signal shall be as follows. For any constant frequency error signal, the resulting signal shall be 0 and for any varying error signal, the combined low pass and derivative function block reflects a value which is the derivative or slope of the input error signal (basically higher the frequency change, larger is the RoCoF value). The parameters for the low pass and the derivative block are selected accordingly to achieve this response. Further, this signal is multiplied with a user-defined gain called derivative gain K_d which shall define the response sensitivity of the derivative block. But the derivative control block alone cannot mitigate the frequency discrepancy, because derivative block output will only be active during a large dynamic frequency deviation and for the rest of the time (i.e. for example, when the frequency is settled at 49.6 Hz due to the load imbalance after the point of Nadir) the result of derivative block shall be zero. So, a cascaded droop and derivative block need to be active for improvement in both Nadir and RoCoF.

In summary, the derivative block's objective is to operate instantly to give maximum control response output based on RoCoF variation. So that, due to instant active power injection from the wind turbines the grid experiences an improvement in dynamic frequency response before Nadir, further, once the frequency curve reaches the point of Nadir, the slope of frequency is low and the control output from the derivative block is accordingly low. But, by this time, the error in frequency deviation is highest and the droop control block would be contributing the highest. Hence, by simultaneously operating both droop and a derivative control block, both the issues pertaining to high slope before Nadir and low Nadir point can be improved respectively. As explained in the previous sections of both droop and derivative based FAPR, the controller's output $P_{elecref}$ will be added as an additional signal to the $P_{elecref}$ block. This can be evident from figure 3.3 which is a modification of figure C.7 of Appendix C.1 presenting the outer loop controller generating Iq_ref from the electrical active power output of the wind generator (PM). So, further with modifications to the $P_{elecref}$ being established, it is important to explore how this shall reflect as higher power output from the wind generator. So, by setting a higher $P_{elecref}$, it is possible to increase actual electrical power output from the Wind generators, but since the wind speed is kept constant and no changes are made in the pitch angle controller, mechanical power governed by wind speed is unaltered. This difference in electrical Power and Mechanical Power will result in a decrease in speed and increase in torque at the wind turbine. Thus, depicting the extraction of kinetic energy from the wind turbine to emulate inertia. Also, it is observed that, bigger the wind turbines, higher will be the power rating, larger will be the inertia constant H of the wind turbine and thus more power extraction is possible.

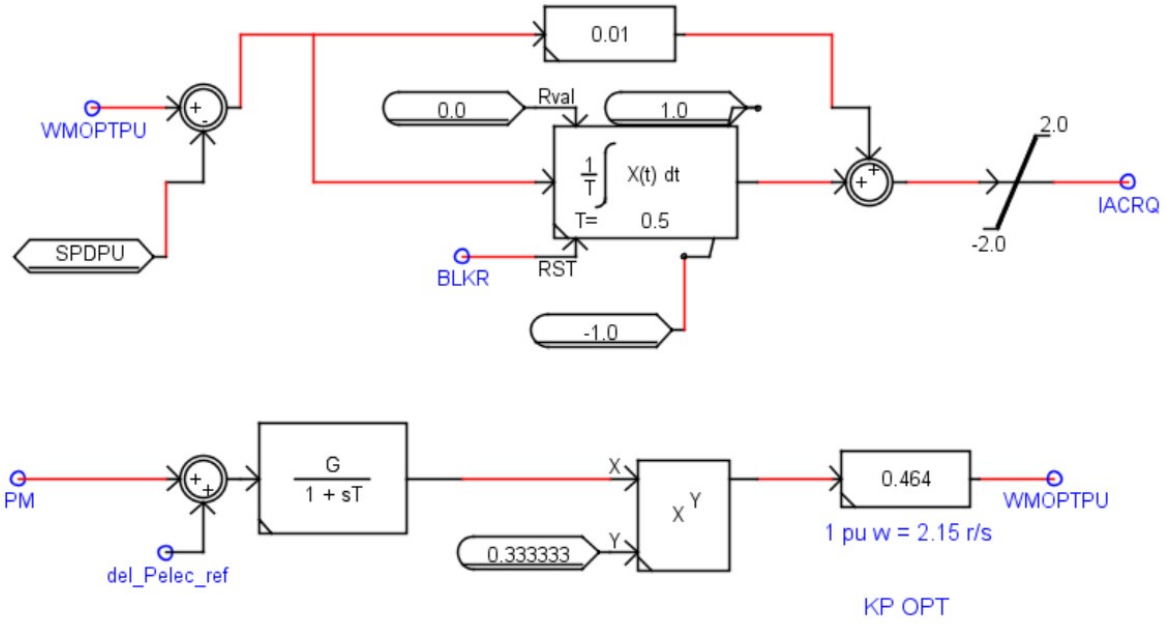

Figure 3.3: Snapshot of RSCAD implemented Iq_{ref} control block (outer loop controller)

3.4. Virtual Synchronous Power (VSP) based FAPR controller

In this section, the discussion is about how to improve the dynamics frequency response better compared to previous FAPR methods (Droop and combined droop and Derivative methods). The primary advantage of this method is that the frequency measurement ambiguities can be completely eliminated as it operates based on the measurement of power required at the bus with respect to the reference power available at the bus connected to the wind generator, and this difference during a load frequency variation will result as an error which will be satisfied by Energy Management Systems (EMS) (Battery, super capacitor depending on feasibility) by instant discharge into the grid.

The overall VSP setup has 2 parts namely battery power management system (BPMS) and VSP controller which is a signal generator.

3.4.1. Battery Power Management System

Figure 3.4 describes the block diagram of a BPMS which consists of a BESS (Battery Energy Storage System), Bidirectional DC-DC converter (Buck-Boost Converter) at last the DC link of any VSC converter based RES. A bidirectional DC-DC converter (shown in the Figure 3.4) is used to interface BESS to the DC link. The main function is to appropriately discharge the battery as per the pulse generated from the VSP control block. VSP based FAPR control block is explained in detail in the next section. And depending on the power flow the bidirectional converter allows operation as a buck or a boost converter. They are individually controlled by 2 different signals. Each of the converters consists of a Gate Turn off Transistor with an anti-parallel diode which is driven by a pulse width modulated (PWM) signals. The control action of the converter is made in such a way that it allows controlled power flow in both directions.

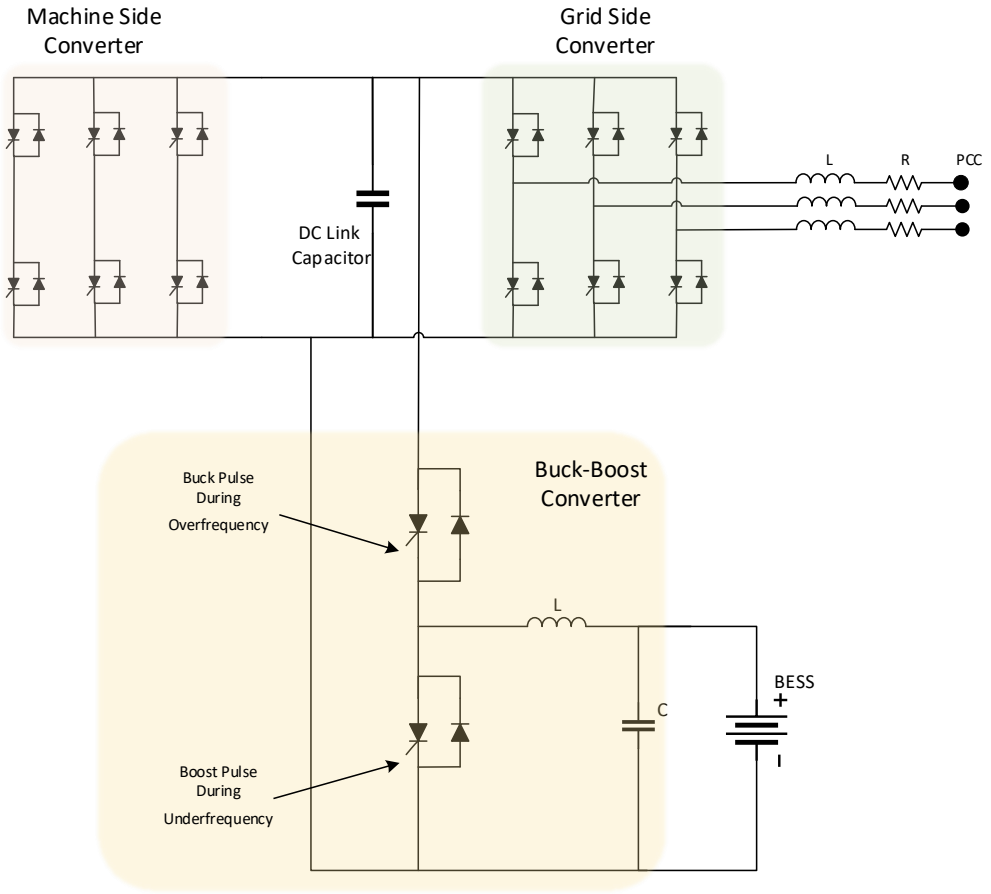

Figure 3.4: Block diagram of a VSP based battery power injection system. The active device is based on the Gate Turn-off Transistor and anti-parallel diode semiconductor technologies

The specialty of any full converter based RES like Solar Farm, Type - 4 wind turbine or an electrolyser is that it can provide power in isolation without responding to the dynamics of the grid, this is due to the presence of DC link and full Back to Back converter. This feature has been utilized for an advantage in the VSP based input measurement.

3.4.2. VSP based Signal Generator

Figure 3.5 depicts the VSP controller, which measures the power required at the bus at the PCC to the reference power available at the bus. Usually both these values will be equal during steady state condition, but during a load-frequency variation event, the measured power on the grid side deviates while the reference power that the RES delivers will remain same. This difference in power will result in error. Fpr example, as shown in figure 3.6, P_{bus} (Power going out from the Node bus) reacts to the grid when there is a load disturbance whereas P_{res} will not. This difference will be taken as P_{error}

in the VSP control block which is further passed through a dead-band and later through a 2^{nd} order transfer function mimicking a VSP topology. The details of the topology will be explained in the following section. The output of this block will be setting the duty cycle of a PWM controller. Hence the limits of this block shall be between 0 and 0.9. Based on the signal being sent to buck or boost converter, the switches are operated, and power will be withdrawn or injected into the DC link of RES respectively.

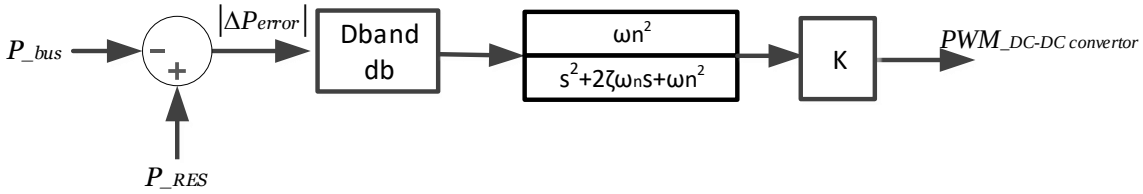

Figure 3.5: Block diagram of a VSP based FAPR controller

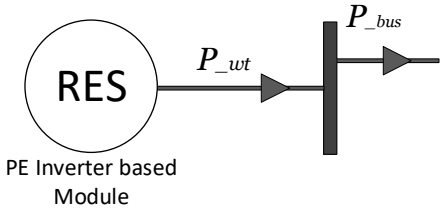

Figure 3.6: Connection diagram of a Wind Turbine to the Power grid to indicate the inputs for VSP based FAPR controller

3.4.3. Virtual Synchronous Power Strategy

In this section, the concept of VSP which is inspired on synchronous power control approach for voltage source converter stations. The general structure of a synchronous power control is presented in Figure 3.7. This control structure stems from the analogy of electrical performance expected from a Synchronous Generators (SG) in a digital framework, which is responsible for controlling the VSC-converter. But instead of an electro-mechanical model, a more dynamically faster BPMS is used. By modifying the swing equation of conventional synchronous generator, the general electro-mechanical control loop for VSP application in dynamic studies can be presented based on the diagram of Figure 3.8. This diagram represents a control, in which any variation between the delivered power by the converter (P_o) and the input power, (P_{in}) is processed by a Power Loop Controller (PWRLC) to set a relative frequency that should be added to the synchronous frequency of the grid, for generating the rotating frequency of a virtual rotor. The integral of such frequency gives the angular position of the virtual rotor leading to the power delivered by the power converter.

The representation of the PWRLC in the VSP controller has a second-order characteristic, which enables simultaneous emulation of damping (k) and inertia (J) into the system. Thus, dynamic relationships between input and output power of the VSP is as follows:

$$\frac{P_o}{P_{in}} = \frac{\omega_n^2}{s^2 + 2\zeta\omega_n s + \omega_n^2} = \frac{\frac{P_{max}}{J\omega_s}}{s^2 + \frac{k}{J\omega_s}s + \frac{P_{max}}{J\omega_s}} \tag{3.1}$$

Where ζ is the damping factor, ω_n is the natural frequency and P_{max} is the maximum delivered power gain. For implementing this second-order function in RSCAD the following equation is used:

$$\frac{P_o}{P_{in}} = \frac{1}{1 + T_z s + T_w s^2} = \frac{\frac{1}{T_w}}{s^2 + \frac{T_z}{T_w}s + \frac{1}{T_w}} \tag{3.2}$$

where $\frac{1}{T_w} = \omega_n^2$ and $\frac{T_z}{T_w} = 2\zeta\omega_n$

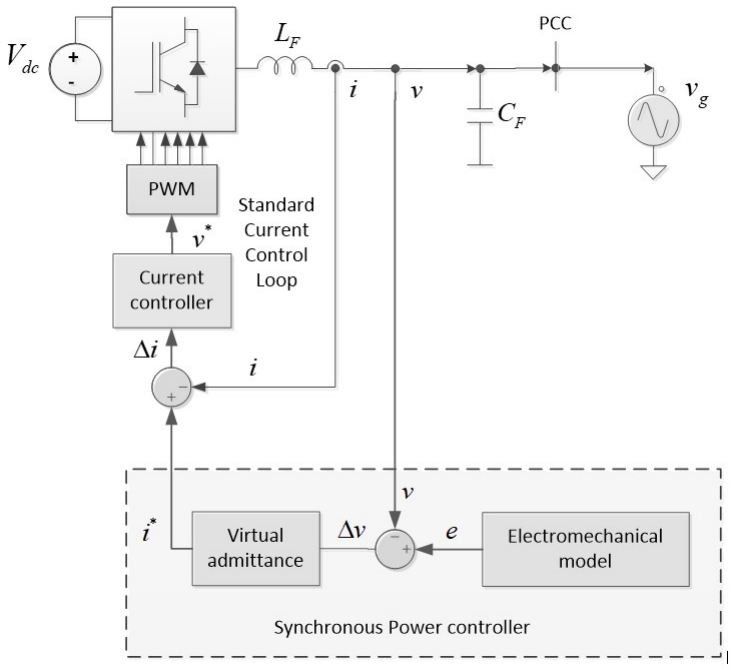

Figure 3.7: General structure of virtual synchronous power based control applied to a HVDC VSC converter

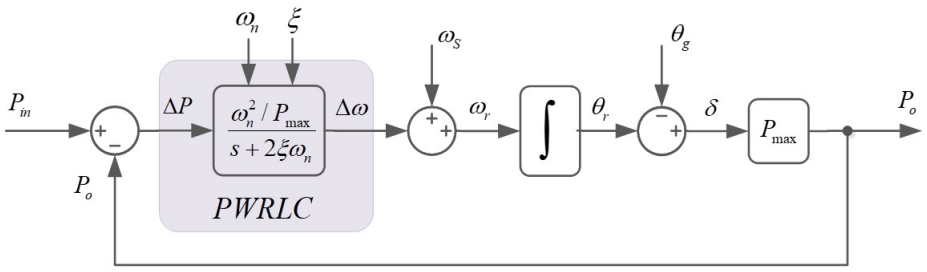

Figure 3.8: Electro-mechanical representation of synchronous power controller

3.5. Flowchart representation for implementation of FAPR Controllers

Flowcharts 3.9 and 3.10 represents the step by step instructions that should be followed for implementing FAPR controllers in a full converter based RES. Further, the basic requites needed to start frequency regulation strategies in RES have been explained, like for combined droop-derivative based controllers, RES that can provide inertial support and which can vary its active power conveniently has to be chosen while for VSP, a full converter model with a stable DC link has to be selected. Further boundaries of operation possible from an RES has to be determined. Along with this, various signal sensitivities that can actuate FAPR and trigger injection or absorption of Active power has to be tuned. With this information, FAPR controllers can be implemented and further tuning to inject/extract substantial amount of active power from RES proportional to generator-load mismatch event completes the procedural flowchart.

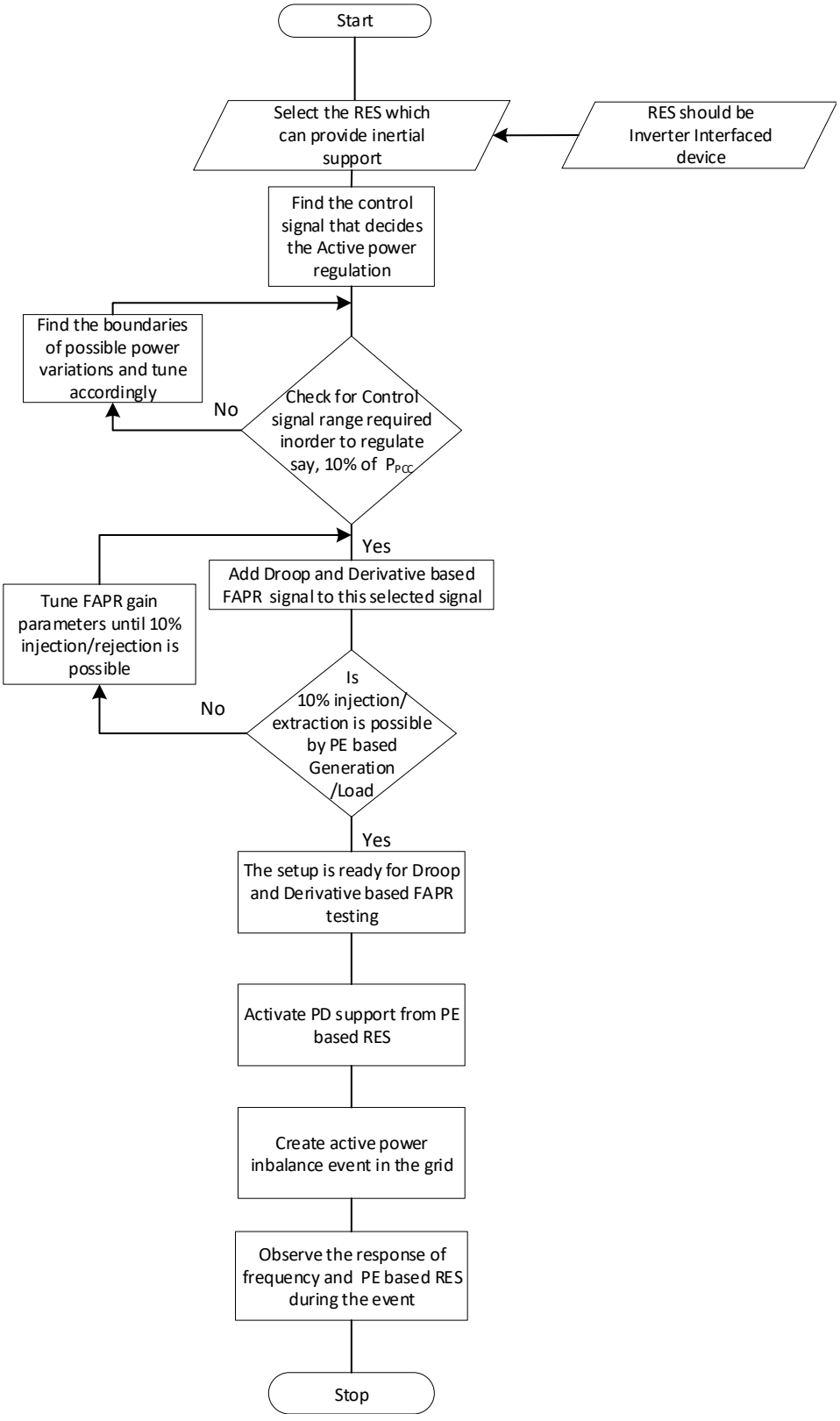

Figure 3.9: Procedure for implementation of combined droop and derivative controllers in a full converter based renewable devices for dynamic studies

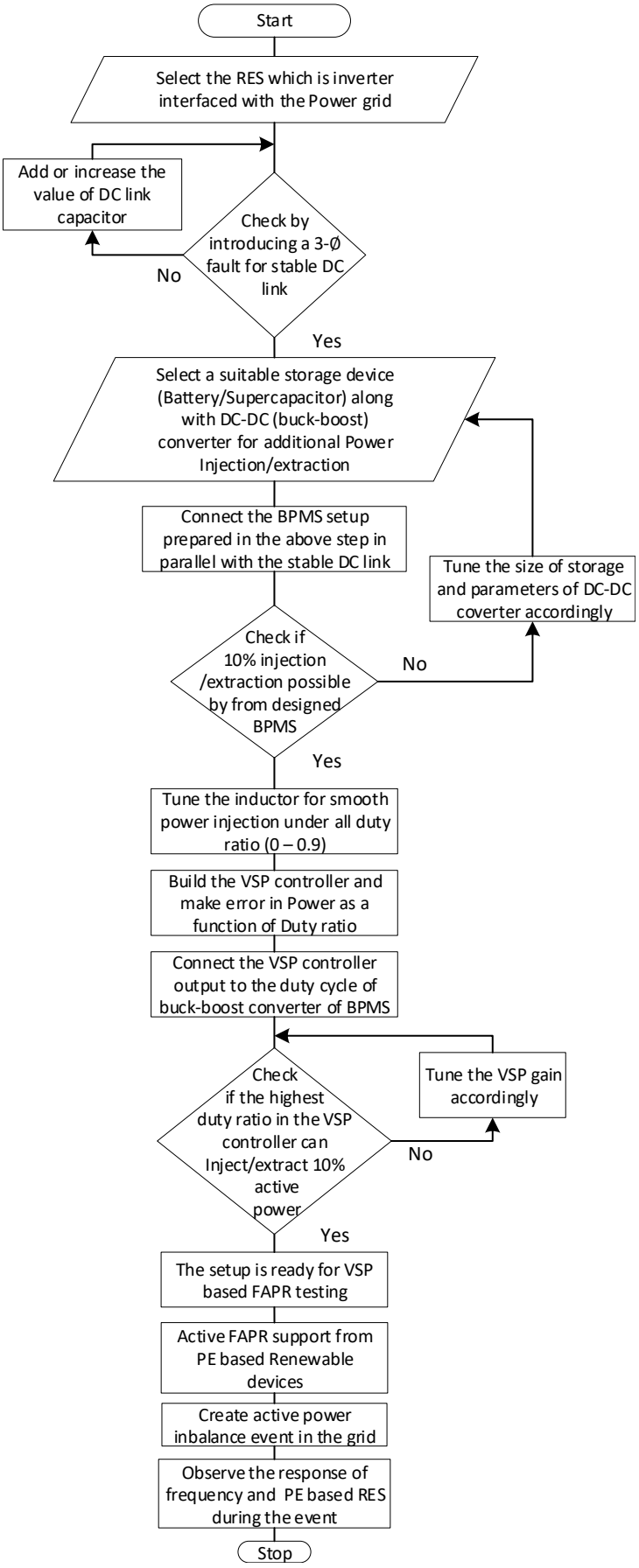

Figure 3.10: Procedure for implementation of VSP based FAPR in a full converter based renewable devices for dynamic studies

4

Application of FAPR to Type 4 Wind Generators

This section deals with the implementation of Fast Active Power Regulation (FAPR) control strategies in a Type-4 Wind Generators connected to modified IEEE 9-Bus system with 52% wind share. The purpose of this section is to verify the performance of FAPR control strategies in a full converter based Type-4 Wind turbine.A detailed description of the architecture of Type-4 wind generators have been explained in Appendix C.1. Also, since the analysis is performed in real-time EMT based software (RSCAD), this can be later implemented in an mockup grid emualator (HIL) and validate against the results obtained in RSCAD. The model will be tested in a Real-Time Digital Simulation (RTDS) platform using RSCAD software.

4.1. Modifications done in a Type-4 Wind Turbine to include FAPR controllers

:

It is worth mentioning that, the droop and combined droop-derivative controller is designed to extract inertia from the blades of the wind turbine, however the VSP based controller has a BPMS from which provide support during load frequency imbalance event. Hence based on this, we can club implementation of VSP controller from the other two as follows:

- Modifications to accommodate droop and combined droop-derivative controller.
- Modifications to accommodate VSP Controller

As explained in the previous chapter and also summarized in the flowchart 1.3, in order to implement droop and combined droop - derivative controller, it is important to locate the signal which controls the active power response. In a Type-4 wind generator there are many signal which has an impact on the delivered Active power Response like active current loop I_{d_ref} on the Grid Side Converter (GSC), DC link Voltage V_{dc}, Torque reference from the wind turbine T_{mech}, Reactive Current Loop I_{q_ref} on the Machine side converter(MSC). But here, since the priority is also to extract Kinetic Energy from the wind turbine blades, it is necessary to select the control signal which immediately provides a signal for extraction of Kinetic Energy. So in a Type-4 wind turbine set, the MSC is responsible for interaction between Permanent Magnet Synchronous Machine (PMSM) and the grid side setting the reference for electrical power demand from the. More specifically, the inner control loop of I_{q_ref} sets the electrical response from Wind Turbine. I_{q_ref} is controlled by Active Power of the PMSM P_{ref}. Hence the output of the droop and combined droop-derivative controller will be connected an additional signal to the P_{ref} of the MSC.

The VSP based FAPR controller, as explained in the section 3.4, requires a stable DC link Voltage for its operation. But it is an inherent property of any Back to Back converter to keep the voltage as

stable as possible under all conditions, this feature of the DC link facilitates the necessary condition to connect the BPMS in parallel with the wind turbine. The model representing an actual implementation of VSP based FAPR controller in a Type-4 wind turbine in RSCAD simulation platform is as shown in Figure 4.1.

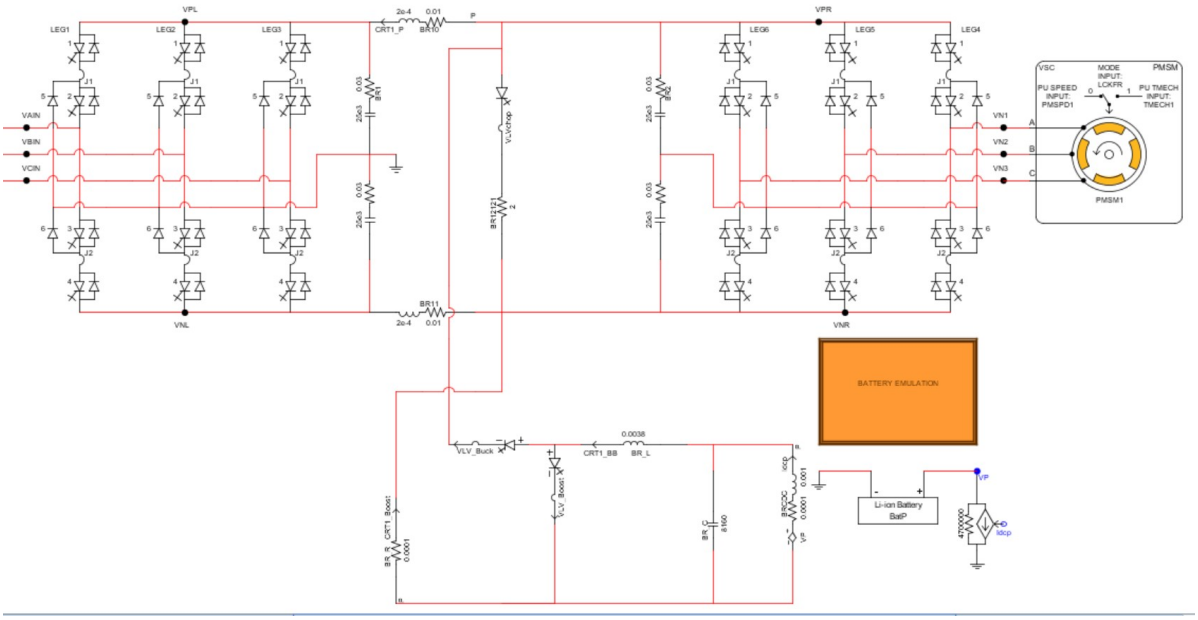

Figure 4.1: RSCAD representation of a VSP based battery power regulation system

4.2. Test Bench 1 - Description of Modified IEEE 9 bus system

With a successful implementation of FAPR control strategies in a Type-4 wind generator, it was now necessary to understand its interaction when wind turbines are connected to a model power system grid. Therefore, a modified IEEE network was developed as shown in Figure 4.2. This test bench developed consists of 2 wind turbines constituting a 52% wind share. It is noteworthy, that the wind turbine models used here are full scale not aggregate models. Table 4.1 describes the load flow results with test case working stable under normal operation.

Also, it is worth mentioning that the total generation and load balance has been maintained as same as a standard IEEE bus system. Penetration of renewables have not been increased just by increasing the active power from the wind turbines but rather replacing synchronous generators. At each generation and load bus the integrity of voltage and active power balance has been maintained similar to standard IEEE 9 bus system.

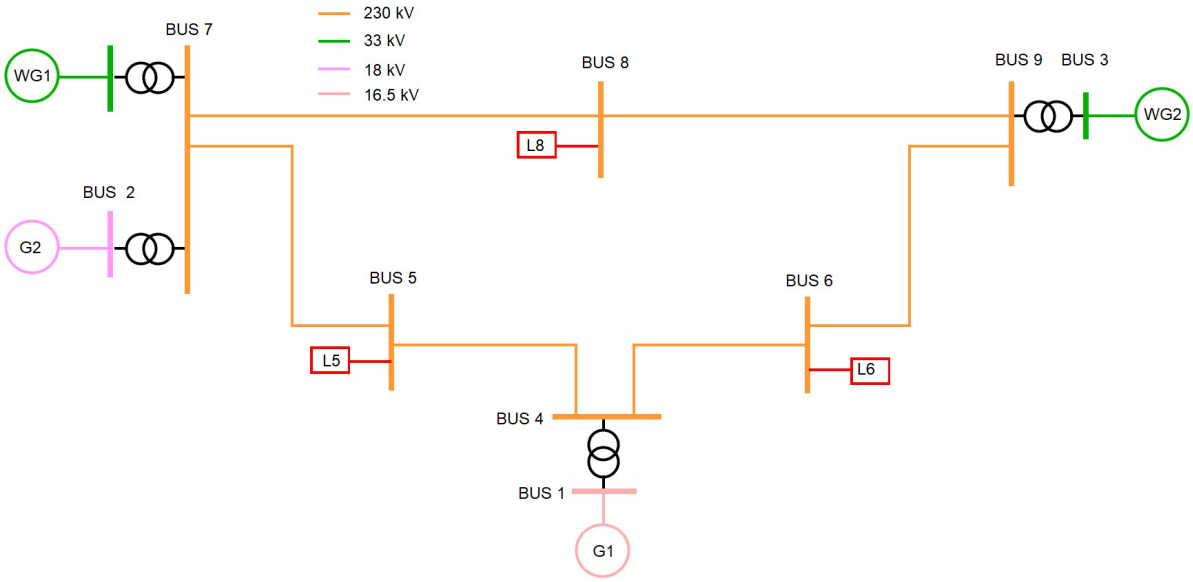

Figure 4.2: Modified IEEE 9 bus model with 52% Wind generator share

Table 4.1: Load flow results from the Modified IEEE 9 bus system with 52% wind share

Load Flow Results		P (MW)	Q (MVAR)
Generations	G1	73.4	33.8
	WG1	82.6	0
	G2	78.2	-1.8
	WG2	84	0
Loads	L5	125	50
	L6	90	30
	L8	100	35

Now to test the FAPR controller strategies, a generation load imbalance had to be created. More specifically an under-frequency event was created. This was possible in 2 ways, either by percentage generation outage or by load increase. From Modelling perspective in RSCAD, a load increase was more convenient, this is because to create a generator outage, the complication was that many parameters in the governor, excitation had to be tuned just to create an event, this was inefficient and cumbersome. However, load increase is convenient since the active power P and reactive power Q could be altered using a slider. Moreover, with load variation, bringing back the grid to a steady state condition after the disturbance was less cumbersome.

After testing the impact of load frequency variations at various busses. Bus 8 was selected to create an under-frequency event because the disturbance caused at this bus had the highest impact on Bus 3 and Bus 2 where the wind generators were connected. To create an under-frequency event the load at bus 8 had to be suddenly increased. From literature, it was found that any sudden load frequency variation of 3% to 5% was considered as a major under-frequency event [106]. Figure 4.3 depicts the response of frequency and power in pu delivered by synchronous generators and wind generators for 3% to 5% increase in load.

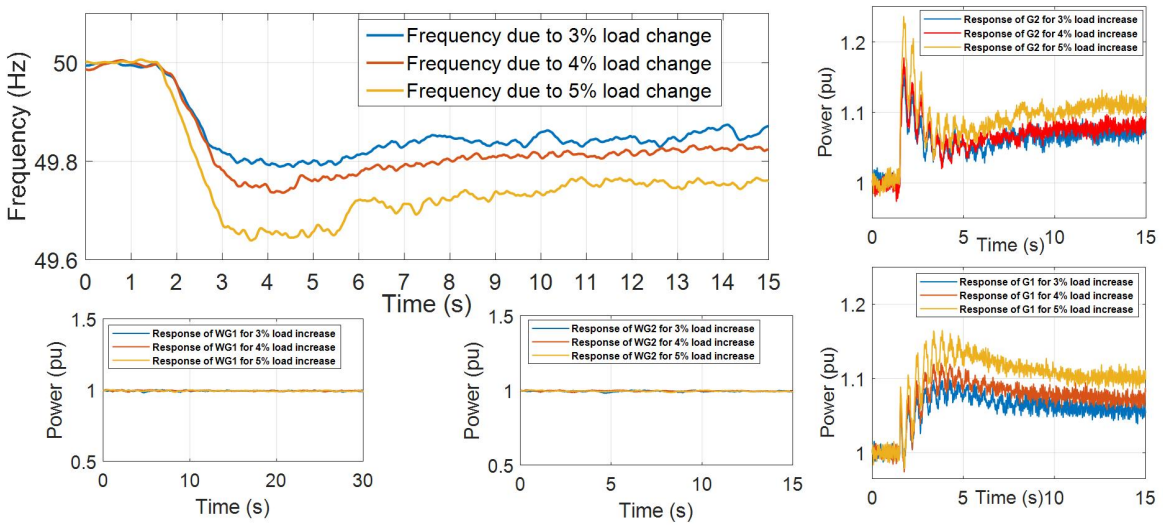

Figure 4.3: Frequency response due to load increase at bus 8 (main graph); Power response at various generator terminals due to load increase at bus 8

It can be observed that under normal operation without FAPR controllers active, the wind generators do not participate in the load frequency variation due to the presence of an AC-DC-AC full converter. Also, with higher imbalance, larger frequency deviation was observed. Please note that for all further analysis, a load disturbance of 5% shall be applied and frequency measurement which is required as an input to the FAPR controllers is measured at bus 8.

4.3. Comparative Assessment between EMT and RMS based simulation results

As described in Appendix A , simulation in RMS and EMT serves two different purposes. RMS simulations are mainly considered when the studies of large network load flows with high share of wind power generations must be performed. This is not a reliable simulation method to define the accuracy of results pertaining to the operation of a single system where dynamics response is a concern. Also, since RMS models are mostly average models and do not contain a full-scale representation of components (at least in a Type 4 wind turbine). Hence, the obtained results are mathematically simplified which capture only the trends caused by any disturbance event but not the entire dynamics of a disturbance that exists in a real model.

However, EMT model is more defined in terms of model complexity as it is a full-scale simulation model, which is a representation of control blocks built in a real apparatus considering the physical limitations of all the individual components forming a bigger control block. Hence from a control system's perspective, EMT models are best to define any controller performance compared to the RMS model.

Figure 4.4 represents the frequency plots extracted from EMT (RSCAD) and RMS (PowerFactory) models for a 5% load increase event at bus 8. Both the models were built on a similar scale as presented in section 4.2. Both graphs show similar frequency trends but EMT plot depicts a higher slope of frequency before Nadir compared to RMS plot. This is observable from the Figure 4.4 at time-period between 1.5 s and 4.5 seconds, which simply conveys that the model built in EMT model is more vulnerable to load frequency disturbance compared to RMS. Now, with the notion "EMT model is closer to real-time model" being established, it can be concluded that with 52% wind share EMT model shows a lower level of grid stability compared to RMS model, which is proved to be true most of the time in a real scenario. Also, observing the graphs between 5 to 10.5 s, it is noticed that the frequency curve in the EMT takes more time to settle to its final steady-state value while RMS frequency curve reaches this value faster, this depicts the additional time taken in the EMT model to mitigate load generation imbalance during containment period. At last, the steady-state values of frequency after disturbance

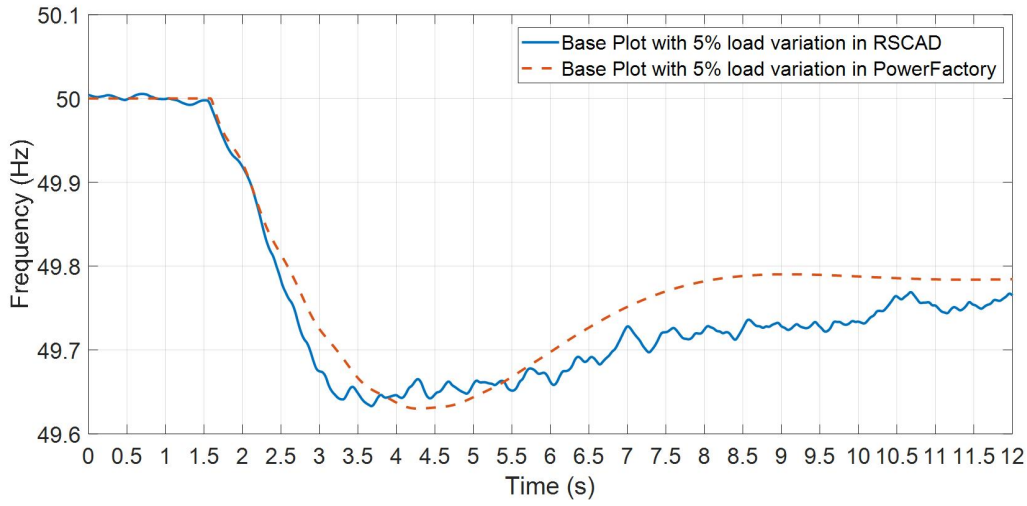

Figure 4.4: Frequency response due to load increase at bus 8 in RMS (PowerFactory) and EMT (RSCAD) workspace.

are different due to the difference in dispatch over the generator's rated value. This can be accounted for the difference in modeling architectures of Powerfactory and RSCAD.

So, with EMT model being more precise in simulation results, there raises a question of run time taken for simulation in EMT. In other words, if the considered grid becomes more complex, the simulation time may increase due to confined processing speed on the work station. Hence to mitigate such troubles in RSCAD simulations, it is focused to use external cores specifically designed for real-time operation of bigger grids which provides precise results though the grid size increases.

4.4. Simulation Results and Comparative assessment of FAPR in Modified IEEE 9 bus system

4.4.1. Droop based Controller Results

This section presents the results obtained for the droop based FAPR controller which was described in section 3.2. So, a 5% load increase at bus 8 created an under-frequency event. Figure 4.5 depicts the frequency plots obtained for various proportional gains in reference to droop controller. As noticed from the figure, when K_p =0 is the base plot where a droop controller is deactivated. As the value of K_p is increased, the influence of droop based FAPR controller in frequency regulation increases, and as a result, Nadir improvement is witnessed. This can be corroborated in the plots of K_p = 0.4, 0.5, 0.7.

But the further increase in K_p is leading to oscillations in frequency making the system behave as an under-damped system, causing a varying generation dispatch from wind generators. This is evident from the plots of K_p = 1 and 1.5.

Hence for K_p = 0.7, the best results were observed with a Nadir shift from 49.64 Hz (base case) to 49.78Hz which is an improvement of 38.88%. Hence, it can be concluded that the parametric sensitivity of droop controller depends on the load disturbance and other grid characteristics, like the share of Power Electronic based generation, the impedance of the grid, location of the disturbance.

In summary, for an under-frequency event caused by a 5% load increase in a modified IEEE 9 bus system, it can be concluded that with K_p = 0.7, Nadir improvement of 38.88% was observed. Further increase of K_p resulted in frequency oscillations. Figure 4.15 represents the power injected by the wind turbine with activated droop based FAPR controller with K_p set to 0.7.

A similar analysis was performed in RMS simulation on a generic test case 1 model. Here a 6.45% generation outage disturbance was introduced. Hence with droop-based controller tuned to its optimal K_p (Pm)= 1.5, a Nadir shift from 49.83Hz to 49.885Hz which accounted to 32.35% improvement was observed. Here, since it is a more stable grid with a large number of generators and loads acting, the Nadir in the base case is a higher value and hence less improvement is observed.

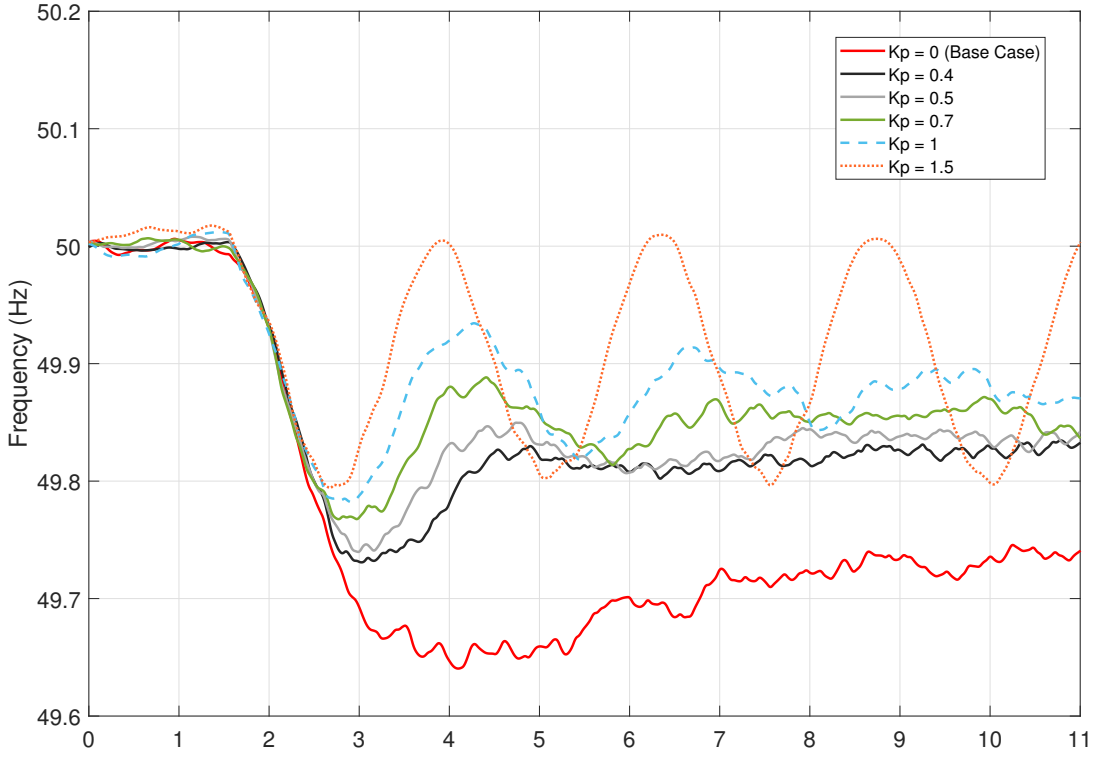

Figure 4.5: Frequency response due to load increase at bus 8 with proportional based FAPR controller at WG's

The optimal gains K_p in both RSCAD and Powerfactory are non-identical due to the difference in modeling architectures (RSCAD being a detailed model and Powerfactory an aggregate model), but in both case, K_p values were chosen so as to increase active power injection in steps by around 10% over the rated value during the containment period.

4.4.2. Combined Droop and Derivative Based Controller

This section presents the results obtained for the derivative based FAPR controller which was described in Section 3.3. One of the drawbacks observed in the droop controller was that it could improve the Nadir but due to its low response speed, it could not improve the RoCoF. As a solution, a faster control loop in terms of the derivative controller was added to droop controller. Figure 4.6 depicts the frequency plots obtained for various values of proportional (K_p) and derivative gains (K_d) in reference to the derivative-based FAPR controller. The values selected here are the possible combinations of K_p and K_d achieved by careful tuning. Here the optimal tuning of K_p and K_d by heuristic methods was beyond the scope of research, but can be referred as future work. Also, the values of K_p and K_d are not only system dependent but also dependent on the grid to which the wind generators are connected along with the disturbance to which they are exposed. Here the plot with K_p = 0 and K_d = 0, forms the base plot with no derivative controller action. With K_p = 0.4 and K_d = 0.6, it can be observed that since K_p value is less, Nadir improvement is a comparatively lower but considerable improvement in dynamic frequency response before Nadir can be observed.

A comparison between plots of K_p = 0.73, K_d = 0.65 and K_p = 0.73, K_d = 0.68 depicts how sensitive the controller's behavior is to the value of K_p and K_d and consequently, the latter case shows the issues with under-damping which brings the oscillatory effect. At last, the plot with K_p = 0.9 and K_d = 0.4 gave the best results with RoCoF improvement from 280mHz/sec (base case) to 139.7mHz/sec accounting to 52% increase in RoCoF and Nadir shift from 49.64 Hz (base case) to 49.845 Hz accounting to 58.3% increase in Nadir. RoCoF is calculated for a time window of 500ms from 1.905 secs to 2.405 secs after the time of dead-zone (around 405ms).

In summary, with the derivative based FAPR controller both Nadir and RoCoF could be improved by

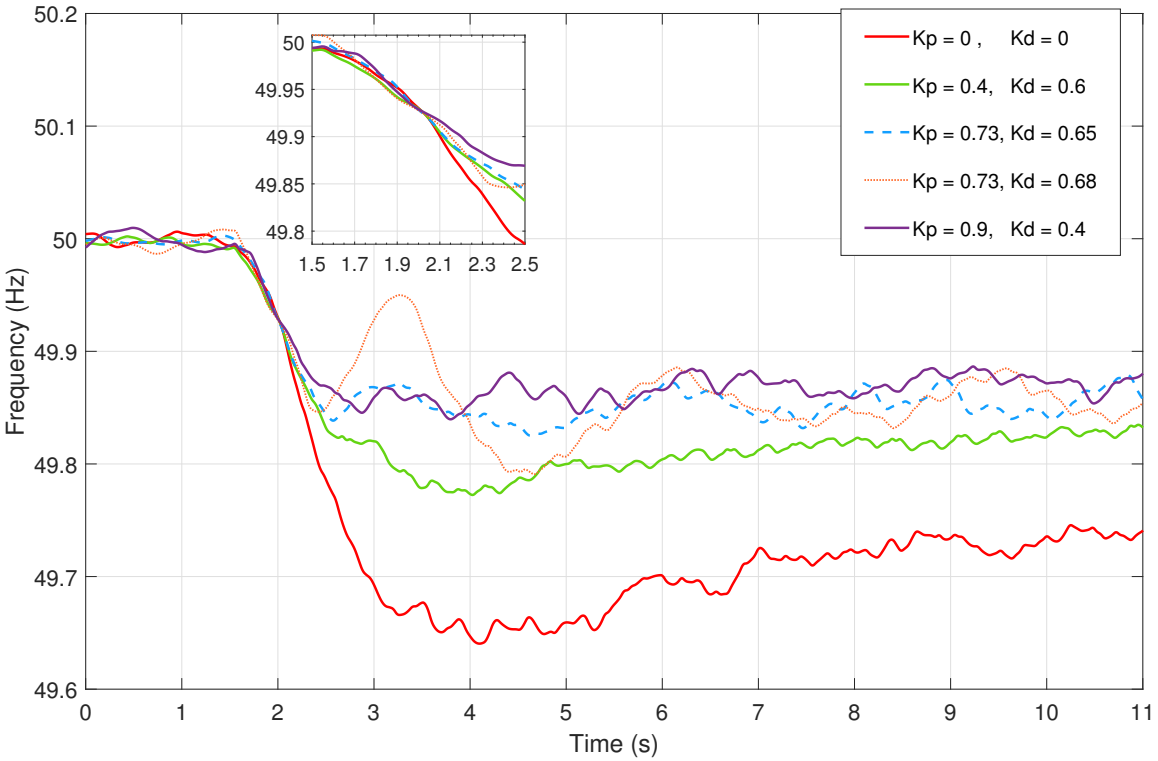

Figure 4.6: Frequency response due to load increase at bus 8 with Combined droop and combined droop-derivative based FAPR controller at WG's

careful tuning of controller gains.

4.4.3. VSP based FAPR Controller

This section presents the results obtained for the VSP based FAPR controller which was described in Section 3.4. The results obtained by this method is straight-forward since there is no involvement of wind turbine and kinetic energy interaction with the grid. Also, VSP block takes directly power as input and this eliminates frequency measurements through PLL or PMU and hence no controller measurement delays. As shown in the Figure 4.7 when K = 0 there is no response from BESS to the under-frequency event experienced in the grid. This can be considered as the base case. As K is increased in steps, the duty ratio for the DC-DC boost converter is increased based on the input provided by the VSP control block, hence more current is injected into the DC link and considerable improvement can be seen in RoCoF and Nadir measurements. So with K = 1, there is a shift in RoCoF from 280 mHz/sec (base case) to 40mHz/sec accounting to 85.68% improvement, and Nadir point shifted from 49.64Hz to 49.825Hz accounting to 52% improvement. Also, Figure 4.8 represents the DC link power increase due to the injection of Power from the BESS at DC bus. It was noticed that with K beyond 1, the frequency plots can be further increased, but there are other limitations to be considered like:

- The DC link Power cannot be increased beyond 10%, because of the limitation on VSC switches on the Grid side converter (inverter). With K =1, there is an increase of 8.2% on total DC link power.

- The Battery considered in RSCAD model is almost ideal since it does not take into consideration the electro-chemical behavior seen in the real system.

In the future, BESS can be replaced by a super-capacitor [13] and this will improve the frequency dynamics better, due to high power and energy density characteristics of a super-capacitor.

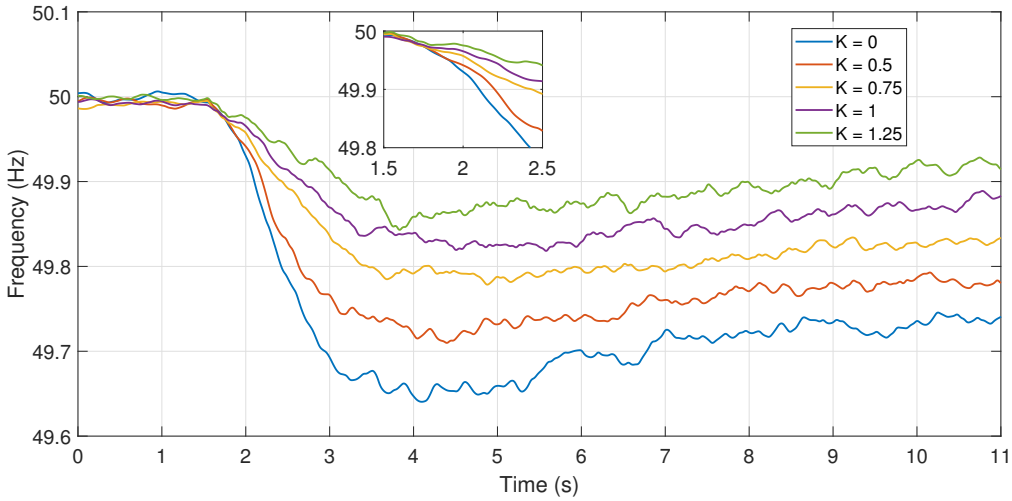

Figure 4.7: Frequency response due to load increase at bus 8 with VSP based FAPR controller at WG's

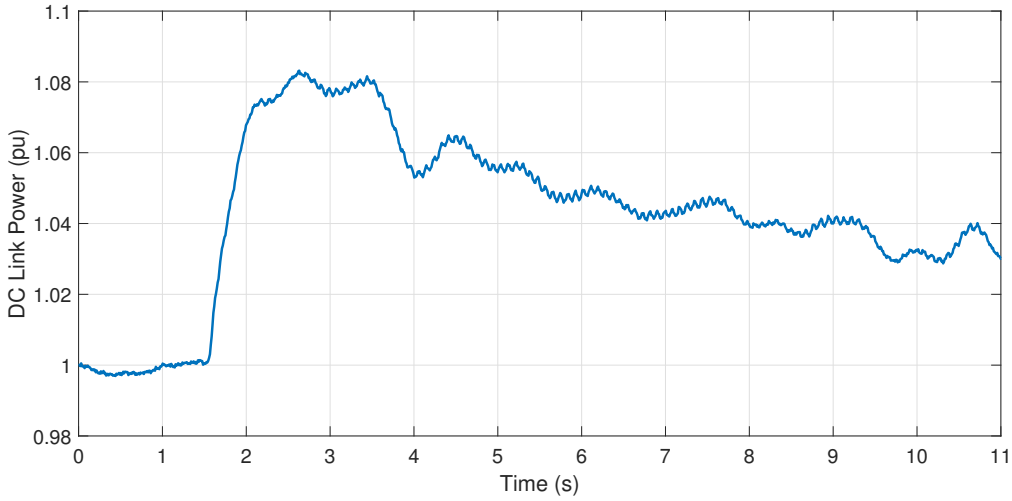

Figure 4.8: DC Power injected due to VSP based FAPR controller

4.4.4. Comparison between various FAPR controllers

Figure4.9 shows the comparison between the different FAPR control strategies that can be implemented in a Type-4 wind generator. The best plot from each of the controller is taken in order to compare. And it can be noticed that the best performance is from VSP based controller which improves both Nadir and RoCoF the highest, but this requires an extra BESS or super-capacitor for injection of additional power. An important observation to be noticed here is, both extraction of K.E (say by, proportional and derivative controller) and injection of additional power at the DC link through VSP based battery emulation is not possible at the same time as this action may cause over-voltage issues at the DC bus and trigger the DC link protection circuits (in RSCAD model, chopper circuit). Figure 4.10 shows the comparison of DC link Power of a Type-4 Wind generator due to different FAPR control strategies. Also table 4.2 provides an comparative assesment for FAOR controller. It is noticeable that, though triggering time is 1.5 s in all cases, VSP based controller has a response rate faster than other controllers due to 3 reasons, first being PLL less operation, second, ideal BESS operation and lastly the fast characteristics of 2^{nd} order transfer function used in VSP block.

FAPR Controllers	RoCoF (mHz/sec)	Nadir (Hz)
Base Case (Without FAPR Controller)	280 mHz/sec	49.64 Hz
Droop Controller	280mHz/sec	49.735 Hz (37.15% improve)
Combined Droop-Derivative Controller	139mHz/sec (50% improve)	49.79 Hz (41.6% improve)
VSP Controller	40mHz/sec (85.68% improve)	49.825 Hz (50% improve)

Table 4.2: Comparative Assessment for FAPR Controller

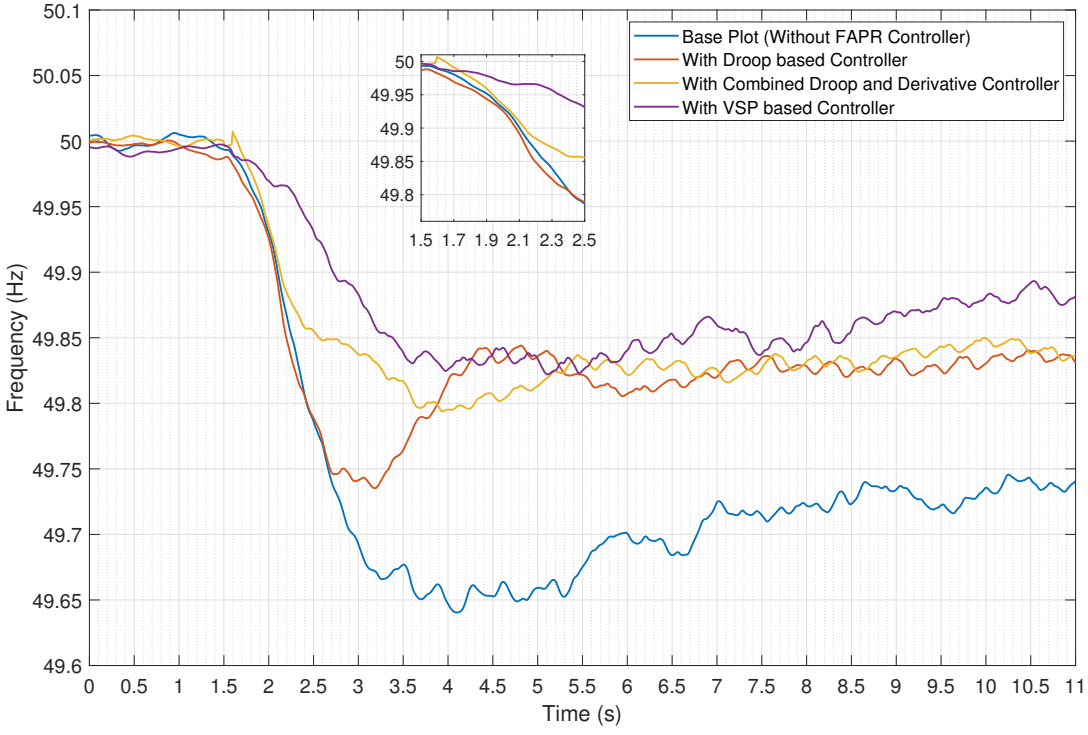

Figure 4.9: Frequency response due to load increase at bus 8 with VSP based FAPR controller at WG's

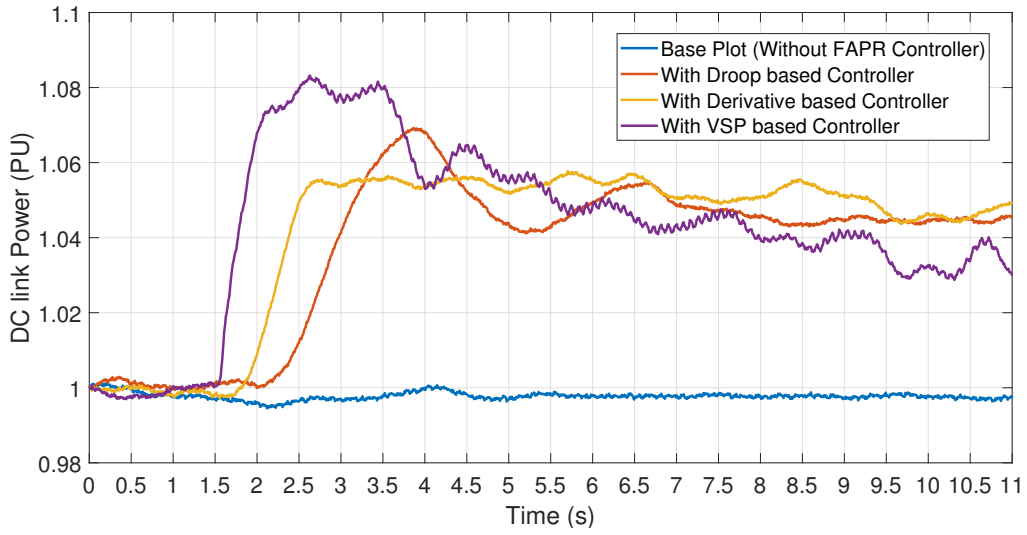

Figure 4.10: DC Link Power at the Type 4 wind generator due to FAPI controllers

5

Application of FAPR to a Multi-Energy System

As seen from the previous chapter 4, developed FAPR controllers were implemented in a Type-4 Wind Turbine and performance analysis was demonstrated in a Modified IEEE 9 Bus system. But one of the objectives of this thesis was to make FAPR control strategy more generic and implementable to all renewable energy sources with suitable modifications. Keeping this in mind, a Multi-Energy system has been created with Type-4 Wind Turbine setup, Solar Farm and an electrolyser. Later, FAPR control strategies were implemented and frequency responses were analyzed by creating a generation load miss-match event. The intention of this chapter is not only to show improvement in RoCoF and Nadir but to analyze the limitations, side-effects caused due to FAPR controllers and lastly to see till what threshold we can utilize these control scheme considering safety and security of both the RES and the power grid. So this chapter starts with the description of North of Netherlands Network (N3), followed by the modifications done in order to create a Multi-Energy system. Later a brief explanation of how the renewable energy sources have been modified to include FAPR shall be briefed and finally, the results of the simulations will be provided.

5.1. Test Case 2 - Description of North of Netherlands Network (N3)

The North of Netherlands Network N3 was developed in RSCAD under the guidelines of the ten-year development plan (2030) of the Dutch TSO TenneT B.V [3]. In this plan, the installation of a large-scale electrolyser plant is foreseen in the northern Netherlands. This part of the network includes a large-scale generation center, the connection of large-scale offshore wind and submarine interconnections with Norway (NorNed) and Denmark (COBRAcable) at Eemshaven and Eemshaven Oudeschip substations. Eemshaven Oudeschip is also a suitable location for a future 300 MW electrolyser plant, as abundant renewable energy generated by the offshore wind farm can be converted into hydrogen gas. The electrolyser plant can also support the power system stability by participating in ancillary services. The topology of the system, the power flow conditions, and the electricity demand were based on inputs received from the TSO. The modeled system covers the 380 kV and several key connections of the 220 kV EHV network of the year 2030. The system also features a generation capacity composed by two 2250 MVA thermal power plants equipped with two generation units each, 600 MW of offshore wind energy (Gemini wind park) and 3058 MW onshore wind energy distributed around the area and further aggregated into the corresponding 380 kV substations. Additional renewable energy is imported via the HVDC inter-connectors with Norway (NorNed) and Denmark (COBRAcable), both of them operated at the rated power transfer capacity of 700 MW.

The wind turbines and the synchronous generators were represented by generic models of each technology, which are available in the software. Generic steam turbine governors with droop control, exciter and power stabilizer are also implemented with the synchronous generators to enable dynamic control and the provision of ancillary services. For this particular study, it was assumed that the HVDC

Generator/HVDC Link	Year 2030 Scenario
GEMINI wind farm (EOS)	450 MW
GEN1 (EOS)	3 × 430 MW
GEN2 (EOS)	2 × 800 MW
GEN3 (DZW)	233 MW
NorNed import (EEM)	700 MW
COBRAcable import (EOS)	-700 MW
Total	**3490 MW**

Table 5.1: Generation sources and imported power sources in the N3 for 2030 scenario

inter-connectors did not participate in the regulation of the system. For such reason, the model of the HVDC links was simplified as a constant negative load. The connections to other parts of the network and the local demands were also modelled as constant loads. Figure 5.1 represents the load flow results of a N3 network of scenario 2030.

5.2. Modifications done in N3 Network to develop a Multi-Energy System

As explained in the previous section, N3 network for scenario 2030 had 300MW electrolyser model but it could not deliver frequency support. In this thesis, there are 3 main modifications done for frequency analysis. Firstly, an FAPR control strategy has been implemented in the electrolyser model in order to provide frequency ancillary support. Secondly, an 85MW full-scale Type-4 Wind Turbine has been implemented with integrated FAPR controllers. Thirdly, a solar farm of 300MW has been implemented with VSP based FAPR controller. The loads in the system have been adjusted accordingly. Here, the congestion in the grid has been increased mainly for 2 reasons. Firstly, to observe the effects due to the reduction in the total inertia of the system. Secondly to observe, if there are any other effects of congestion that could lead to system instability.

5.3. Frequency Regulation feasibility from a 300MW electrolyser model

Another component that was introduced in the N3 network was a 300MW Electrolyser as seen from the figure 5.1. Here the electrolysers are used as regulatory, responsive loads which can vary their basic functionality of Hydrogen production as per available energy. Due to the in-deterministic behavior of power production observed from Wind and Solar, this concept was earlier developed to maintain the security of supply in the power system by providing short-term balancing of renewable energy sources. Now the idea is to extend the concept to regulate active power more instantly so that frequency regulation is possible. Specifically, the stochastic variability of these sources could be controlled by adapting the consumption of nearby electrolysers to the variations of wind speed and solar irradiance.

5.4. Modified Electrolyser Model

In order to study the impact of a large-scale electrolyser in the Northern Netherlands Network, the 1 MW electrolyser model has been scaled up to a model of a 300 MW electrolyser plant. The model considered here is an aggregate model suitable for dynamic frequency analysis[42]. A detailed description of this control system can be found in Appendix C.3.

Although the electrolyser model shown in Figure 5.3 does not represent the real implementation of an electrolyser plant, this simplified model is sufficient for grid studies. Research is currently being continued to develop a model that accurately corresponds to the actual configuration of an electrolyser farm, which is a parallel connection of many smaller electrolyser stacks with each a capacity of several MWs. This model can provide more insight into the dynamics within an electrolyser plant. The main challenge of implementing this model in real-time simulations is, however, the limited capacity of the

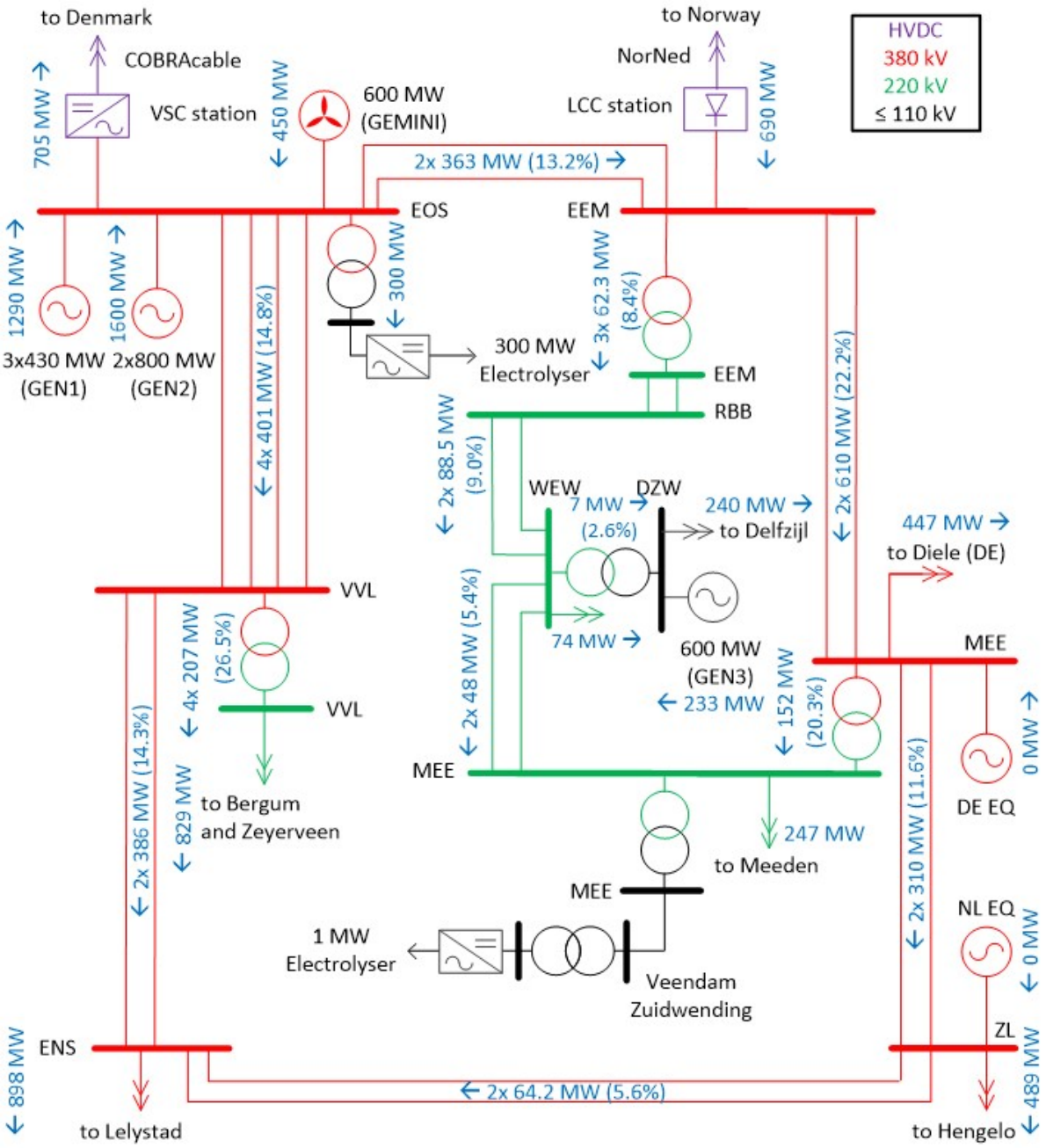

Figure 5.1: Power flow for year 2030 scenario 3

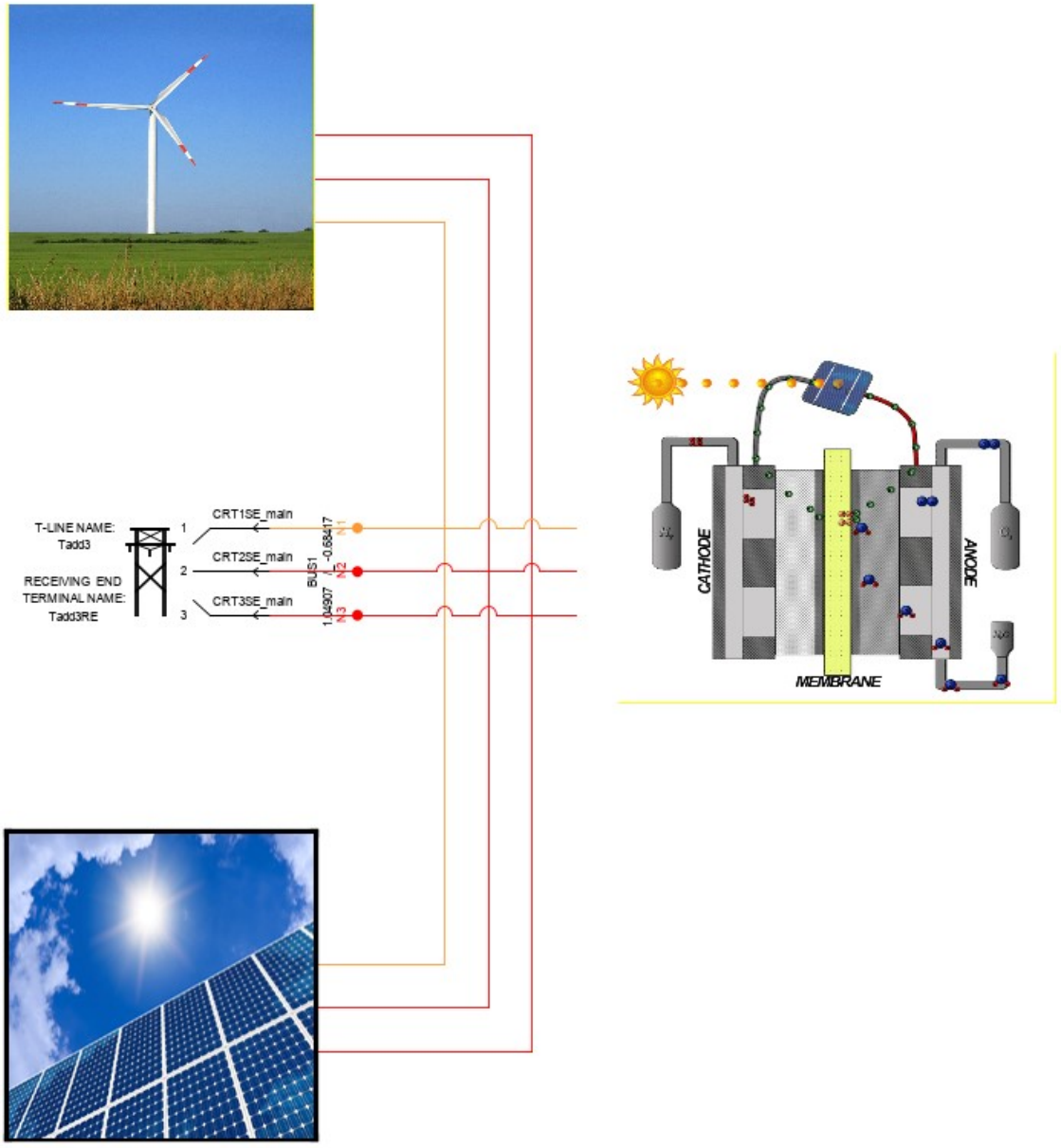

Figure 5.2: Screen-shot of RSCAD implementation of Solar Farm, Wind Turbine Setup and Electrolyser.

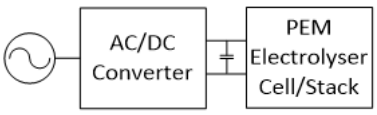

Figure 5.3: Block Diagram of the Inverter interfaced 300 MW electrolyser

Real-Time Digital Simulator (RTDS).

5.5. Modified Solar Wind Farm with VSP based FAPR strategy

It is a fact that, since the solar power plants do not have a rotating mass, they cannot provide inertial support. But it was seen in the previous chapter that, synthetically, inertia can be emulated from a battery source and can be connected to any stable DC link. Since the solar farm architecture provides a stable DC link and an inverter topology, VSP based FAPR controller could be implemented with suitable modifications. Figure 5.4 represents the connection diagram of a solar farm with VSP based FAPR controller.

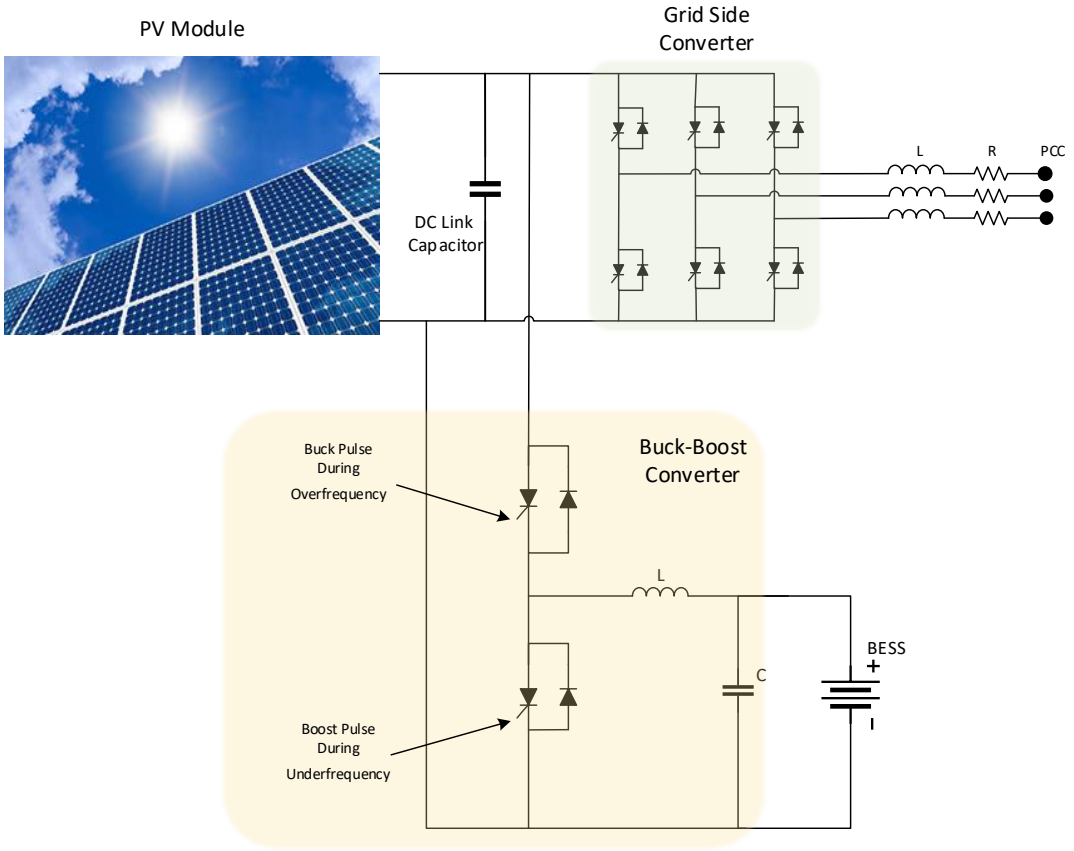

Figure 5.4: Architecture and connection diagram of a Solar Farm

The core idea of VSP controller remains the same where the difference in power demand due to load-frequency event seen at the PCC is measured and instant power is injected from the BESS. Due to this, the instant additional Power from the solar farm, the system RoCoF and Nadir will see an improvement. Figure 5.5 depicts the RSCAD implementation of the VSP based Solar Farm.

5.6. Type-4 Wind Turbine with FAPR controllers in an N3 Network

The last step of system integration done in this thesis was integrating the Type-4 wind turbine into an N3 system. It should be noted that the N3 network already had a Gemini Windfarm of 450MW. But this system was an average model which doesn't have a full-scale implementation and hence FAPR controllers couldn't be implemented. But in this case, full-scale type-4 wind turbine imposition served 2 purposes, mainly to display how the extraction of surplus inertial support can result in failure of Wind Turbines and another to prove the support of FAPR in a real N3 grid. Earlier, it was seen in chapter 4, that the wind turbine blades' speed always settled to a lower value but never destabilized due to excess inertia extraction. This was due to DC link chopper protection, which regulated DC link voltage such

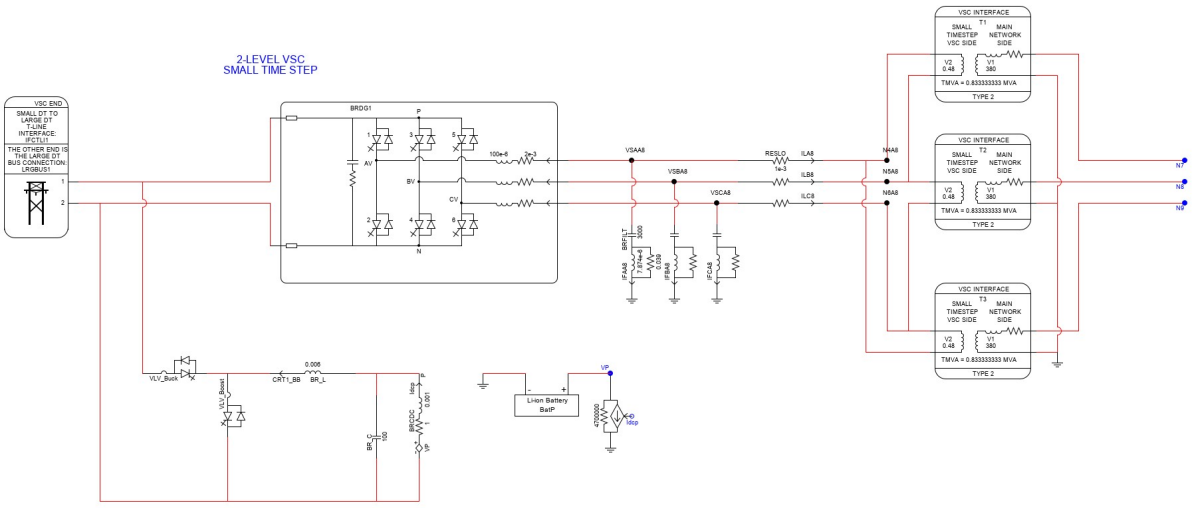

Figure 5.5: Screen shot of VSP based FAPR controller implemented in a Solar Farm

that the WT always operates around MPPT and hence will not lose synchronism due to high energy extraction. But in this model, in order to check the inertia extraction limits, DC chopper has been disabled.

$$P_{inertia} = \frac{KE_{rotor}}{\Delta t_{inertia}} = \frac{\frac{1}{2}J\left({\omega_{rotor}}^2 - {\omega_{rotor\_min}}^2\right)}{\Delta t_{inertia}}[W] \tag{5.1}$$

It should be noted that the upper limits are used on both droop and derivative controller based on wind speed. Also time of extraction has been regulated.

5.7. Simulation Results and Comparative assessment

5.7.1. Test Case setup for Generation Load imbalance event

The simulations tests are performed in the following order, where only support from the electrolyser is first explored. In this case, FAPR controllers are implemented and tested against a load frequency event. Next, a solar farm of 300MW is connected to the network, at last, a Type-4 Wind turbine of 80MW is connected. The loads are increased accordingly. As discussed before, the synchronous generators are not replaced in this case due to the increase in renewables, just to observe the effect of a decrease in total inertia due to the share of renewable sources.

further, to study the potential contribution of electrolysers to frequency stability a generation load imbalance event was created, that is, a 200MW sudden loss of Gemini wind generation capacity is simulated. Due to this sudden loss in generation, there was an under-frequency event. Hence, the test on how the renewable sources can support this event through dispatch of frequency ancillary services will be discussed in the further sections.

5.7.2. Frequency support through FAPR controllers implemented in Electrolysers

electrolyser models which were present in the N3 network has been modified with the inclusion of droop, combined droop-derivative and VSP based controller. So during a load frequency event, the generation reduces and since electrolyser is a load, the FAPR controllers reduce the active power absorption accordingly, which will improve the frequency. Figure 5.6 represents the active power variation of the electrolyser and figure 5.7 depicts the resulting frequency improvement due to each controller. As observed from the base plot, the electrolyser on its own does not regulate its power demand under load-frequency event, but with operational droop based FAPR controller, based on frequency deviation,

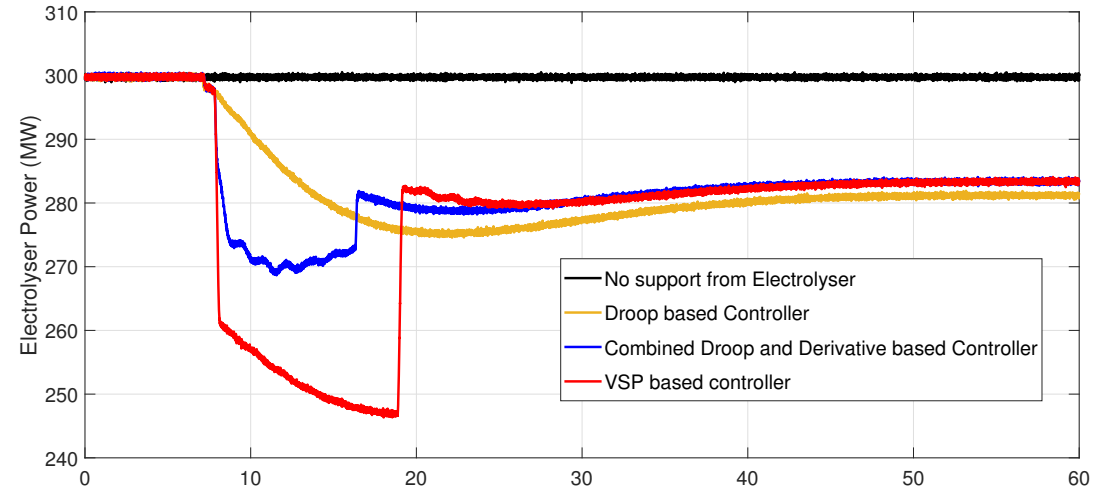

Figure 5.6: Power Response from Elelctrolyser due to FAPR controllers

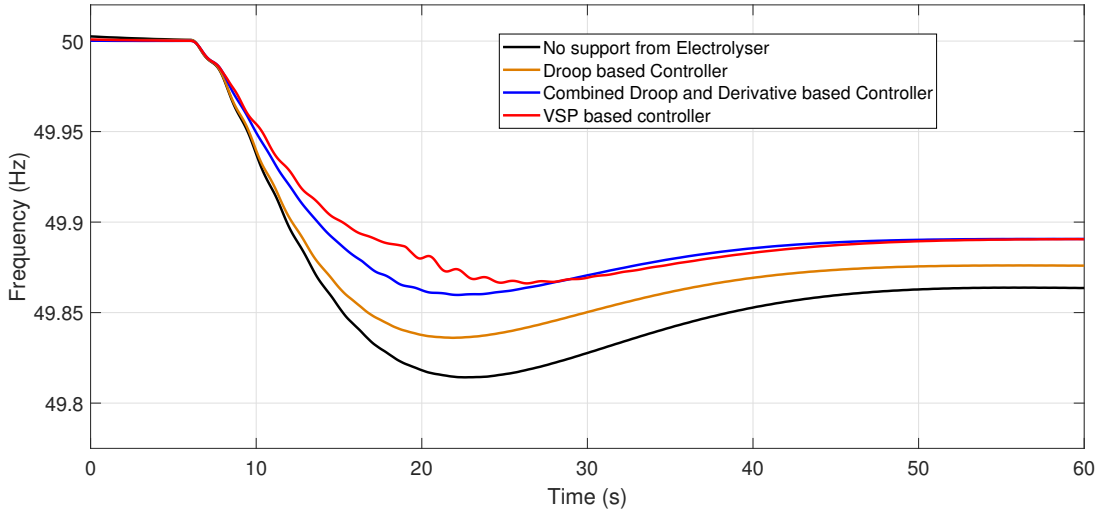

Figure 5.7: Frequency Response from Elelctrolyser due to FAPR controllers

the power demand of electrolyser was reduced which resulted in improvement in Nadir. With the combined droop-derivative controller in action, faster active power reduction could be created. this improved RoCoF significantly, and also, as a by-product, even Nadir improvement was observed. The last controller which was implemented was VSP based FAPR controller, Here, the VSP method is not integrated with BPMS, since electrolyser is a load and mostly the power regulation is by reducing the active power demand. The output of VSP is directly given to the active power reference input as in case of droop and combined droop-derivative controller. Also, please note that the droop controller is always active in combination with Derivative and VSP for the entire time. The time duration and active power reduction applied by derivative and VSP controller are different. VSP and derivative-based FAPR in application to Electrolyser is not different except how the inputs are measured and how the dynamics of error signal vary after the disturbance.

5.7.3. Frequency support through VSP based FAPR controller implemented in Solar Farm

As explained before in section 5.5, a 300MW solar farm integrated and VSP based FAPR with BPMS has been implemented. Now with a 200MW sudden loss of Gemini wind generation capacity, the generation load mismatch event is simulated and solar farm under this event detects the event and

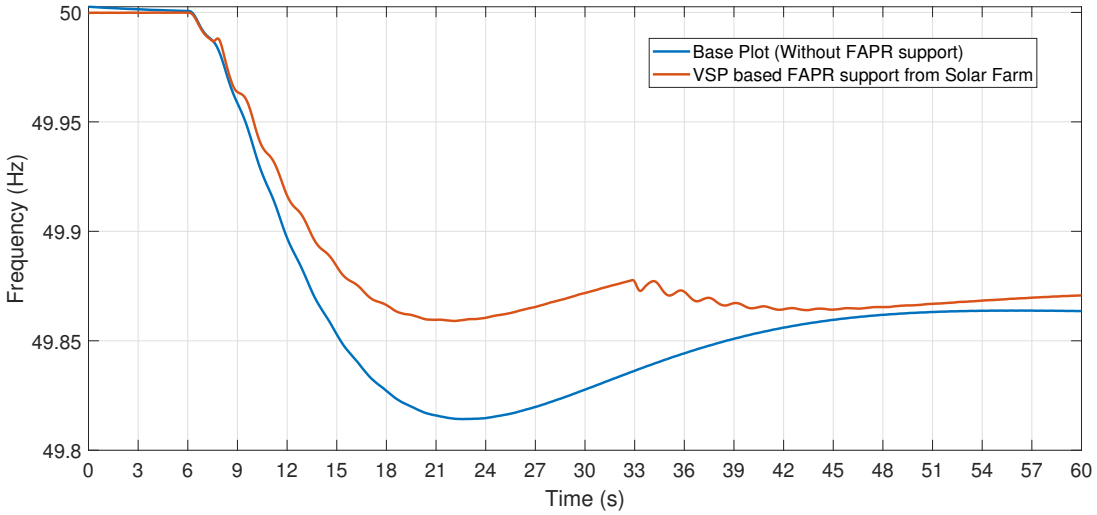

Figure 5.8: Frequency support from VSP based Solar Farm

provides support of 10% increase in active power i.e. 30MW for 10 seconds. As explained before more support in terms of higher active power injection and time of operation is limited by the size of BESS and grid side converter capabilities. Figure 5.8 depicts the improvement in frequency due to this inclusion. It should be noted that higher the support in active power during the frequency containment period, higher will be the frequency improvement. This is regardless of any inverter interfaced renewable source.

5.7.4. Comparative assessment of RES integrated FAPR controllers in a MultiEnergy system

From the previous sections, the frequency support through FAPR controllers in renewable sources like Solar, Wind and responsive loads like electrolysers was described. In this section, the cumulative effects of frequency support from all the devices acting simultaneously are explored. Figure 5.9 depicts frequency improvement with activation of frequency support from electrolyser and solar respectively. There are 3 phenomena that could be analyzed and discussed as follows.

Improvement in Frequency Nadir and RoCoF

It is now evident that, if more RES are able to respond positively towards variation in system active power, by balancing out the effect by quickly altering their active power respectively, the frequency dynamics such as RoCoF and Nadir will improve. But also the downside of sudden injection of active power in a low inertia system should be considered. To illustrate this effect, the VSP controller in the solar farm is suddenly activated sensing the frequency change, thereby giving 30MW of instant injection into the system. By comparing figure 5.8 and 5.9, it can be seen that the more RES sudden regulations, the more crooked the frequency curve. And this effect becomes cumulative if the system inertia is low and may possibly disrupt the expected frequency dynamics as seen in fig 5.9.

Non-uniform or crooked frequency waveform

A comparative assessment between the various plots in figure 5.9 shows that the un-evenness in the frequency waveform increases with increase in RES. This is because rotor swings of synchronous generators become predominant. Earlier the total system inertia was high since all the load demands were satisfied by purely synchronous generators but with the inclusion of RES and appropriate increase in loads, we see that the overall H/MW (inertia constant) in the system has reduced. This makes the synchronous generators more responsive if the disturbance event is close to them. A more detailed analysis has been shown in the next section.

Impact of Rotor Angle Swings and Inertia Response

In this section, the reason for the initial non-uniform frequency curve is analyzed more in detail. Also, with the load frequency variation concept understood, it is now possible to analyze the response of

power system to a power imbalance caused, here tripping of 200MW Windfarm. The response can be divided into 4 stages

Stage I	Generator Rotor Swings (first few seconds)
Stage II	Drop in Frequency (a few seconds to several seconds)
Stage III	Primary frequency control by the turbine governors (several seconds)
Stage IV	Secondary frequency control by the central regulators (several seconds to a minute).

Only the stages I and II are given importance in this thesis. As seen from the figure 5.1, the EOS bus is connected with 3x430MW and 2x800MW synchronous generators, a 300MW Electrolyser, a 700MW cobra cable load, 450MW Gemini Wind Farm. Now with a power imbalance of 200MW, there are 2 effects due to synchronous generators.

- The equivalent reactance of the system increases (generators are connected to each other in parallel), this helps in reducing the amplitude of power angle characteristics.

- Secondly, the mechanical power delivered to the generators from the turbine will be low compared to the electrical demand, this decelerates the rotor and consequently, loss in kinetic energy. Later they follow the dynamics of equal area criterion to settle to normalcy. From the equation 5.2 provided below, with a fixed transient reactance value for a particular generator (higher the better for stability), the power swing deviates due to disturbance each generators change its power angle and results in a swing before reaching steady-state.

$$P(\delta_0) = \frac{E'V_s}{x_d{}'} sin\delta' \tag{5.2}$$

δ_0 = Initial Rotor Angle $x_d{}'$ = Transient Reactance E' = Instantaneous generator voltage V_s = Voltage at the PCC

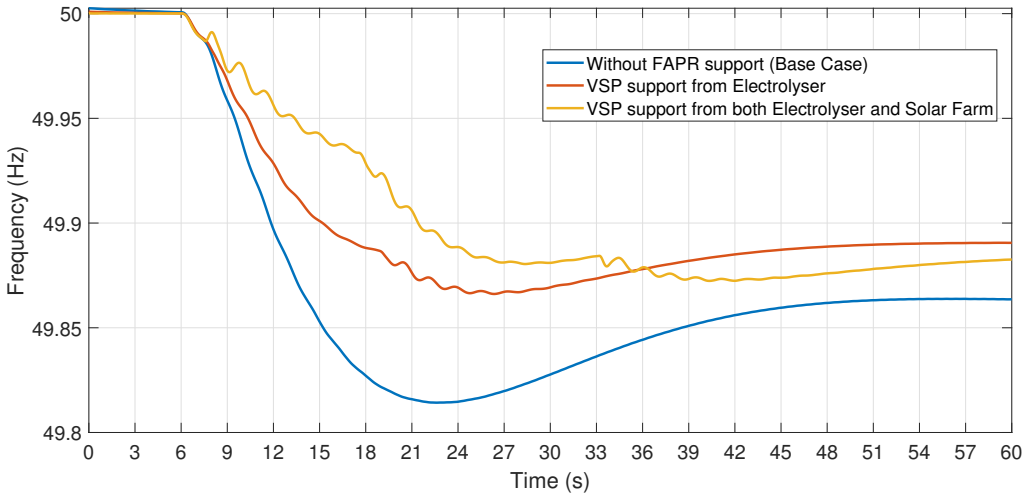

Figure 5.9: Frequency Comparison plots in a Multi-Energy System

5.7.5. Kinetic Energy extraction limitations of Inertial Support from Type-4 Wind Turbines

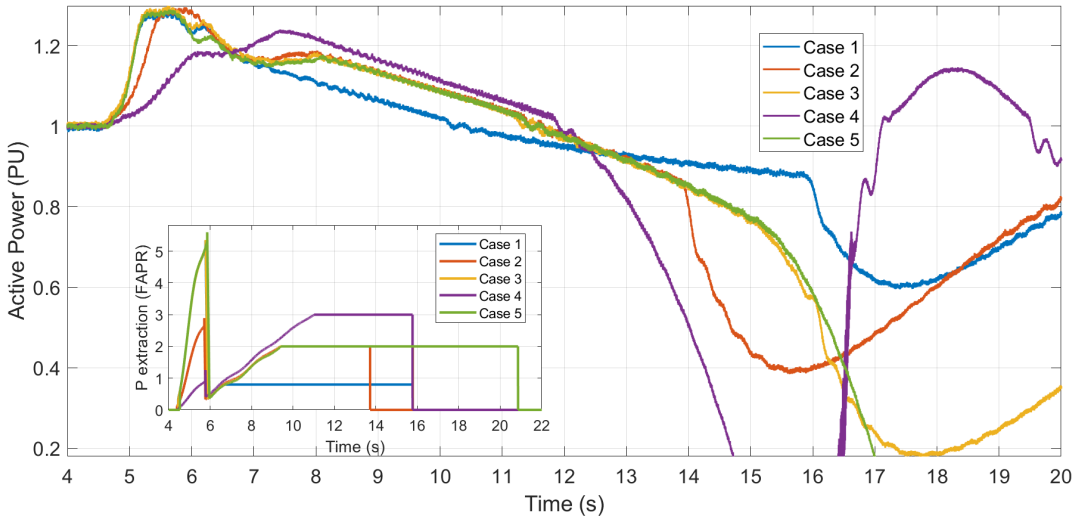

Figure 5.10: Inertial based Power Extraction from a Type-4 wind turbine

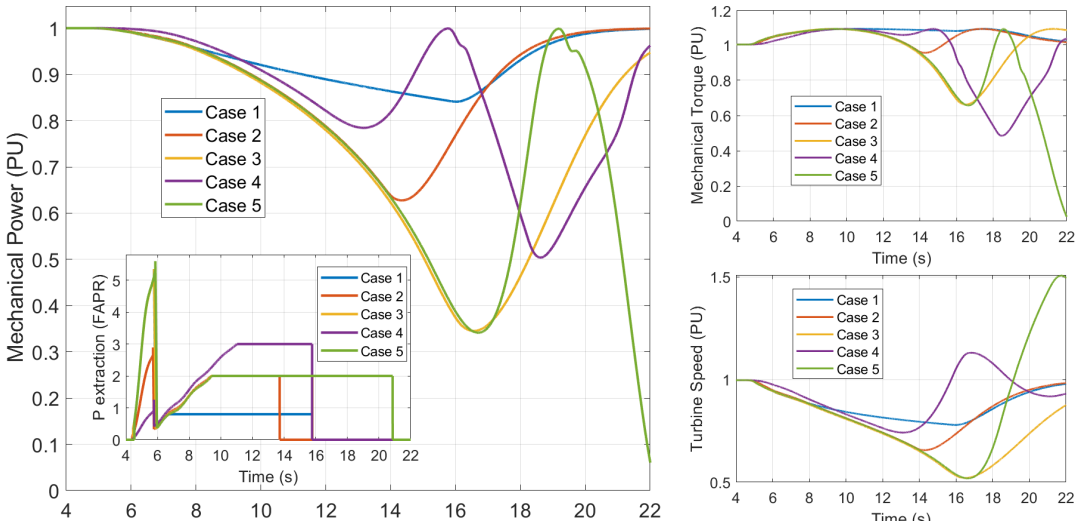

Figure 5.11: Behaviour of Mechanical Torques, drive train speed and Mechanical Power due to inertial based Power Extraction from a Type-4 Wind Turbine

This section deals with the discussion about the physical limitations of the wind turbine and how kinetic energy from the wind turbine can be extracted in the most efficient manner possible. For this, the wind turbines are tested at extreme conditions, both in amplitude and duration of energy extraction. In figure 5.10, the electrical response of wind turbine for various kinds of triggering FAPR signal $P_{trigger}$ from combined droop-derivative controller is explained. In figure 5.11 the mechanical power response is shown for the same signal. For a description of the plots 5 different cases have been considered, all these 5 cases exhibit different possible scenarios of power extraction. Also, a comparative analysis of the most efficient extraction which poses less threat of stalling of wind turbines shall be seen.

It should be noted that for the above cases the inertia constant H of the wind turbine has been fixed to 3.5MW/sec and rated wind speed is 12m/s. Inertia constant for a particular wind turbine will be a constant only when the wind turbine is operated at the rated conditions, but if the wind turbine is operated at a lower or higher speed, H varies proportionally. It is evident that if H is increased (in case

of larger wind turbines) more inertial support can be derived. The wind turbine output connected to the N3 grid is of 80MW (comparatively smaller to other sources in the grid, refer table 5.1). This is of purpose since higher active power from the wind turbine would alter the frequency response (input for FAPR controller) and thereby would hinder the following analysis. Also, The DC chopper circuit which was initially acting as protection for normal operation has been removed for testing extreme conditions.

case 1: In this case, the idea is to display the best possible inertia extraction from the wind turbine. As noticed the output of the FAPR signal ($P_{extraction}$ has high initial response due to which high active power response can be observed, but after about 1.4 seconds the output of the derivative controller is deselected and droop based FAPR measurement signal is applied for 10 seconds. The limitation of the droop signal is required because of critical operating limits of the wind turbine is being examined. Now due to this ($P_{extraction}$ signal, it can be seen that active power increases above the rated. Care should also be taken into how the turbine behaves after removing the FAPR signal. It can be seen that active power output reduces to 60% of the value before recovering. Further, from figure 5.11 it can be observed that the mechanical speed of the drive train starts gradually decreasing from the rated value, while mechanical torque increases. And $P_{mechanical}$ is a product of torque and speed. In this case, the extraction is optimal and this is because the mechanical torque is still above 1 p.u. and turbine speed recovery is uniform.

case 2: From the previous case, the operation of the wind turbine under threshold conditions was made clear. Also, due to the initial fast injection of active power, the droop effect had to be decreased. In this case, the idea is to see the response of the wind turbine, with slower derivative signal and larger (in magnitude) droop signal (limited to 2 instead of 1) operating for a shorter time (8s). As noticed, the active power injection rate has decreased initially, but due to higher droop signal, active power extraction is kept high for a longer time, but soon after FAPR signal is released. P_{wt} reduces to 40% before recovery. Also T_{mech} has reached below 1 PU and shaft speed has further reduced due to high extraction. Hence it can be inferred from case 1 and case 2, that if T_{mech} of wind turbines play a major role in deciding the healthiness of the wind turbine after kinetic energy extraction.

case 3: From the previous cases, it was understood the magnitude of droop controller beyond a certain value will be a threat for the healthiness of the wind turbine, but the threshold of total possible extraction was missing. Hence, in this case, the derivative signal is increased also the time of droop operation has been increased to 10 seconds to check the behavior of wind turbines. As expected the initial active power extraction was high and consequently P_{wt} reduces to 20% before recovery. Also T_{mech} reaches a very low value by the time FAPR signal is released. An important inference that can be derived by comparing cases 1, 2 and 3 is that the larger the positive energy extraction, larger will be the probability of WT's losing synchronism. But energy extraction depends on the size of the wind turbine or inertia constant of the wind turbine. Hence at least for an inertial response, having bigger wind turbines in the grid will be a great advantage in providing ancillary support during load frequency variations.

case 4: From the previous cases, it was clear that possible kinetic energy (power x time) extraction for each wind turbine has to be defined based on the H constant. But the question is whether this is the only value that can decide the possibility of wind energy extraction and also if the method of extraction has any influence on the amount of energy derived remains unanswered. So in this case, the $P_extract$ signal is shaped so that, the initial derivative signal is slow and of smaller magnitude, but droop signal has a larger magnitude so that, active power extraction increases uniformly and reaches a maximum value after 4 seconds and gradually decreases as T_{mech} reduces. In this case, once the FAPR signal is deactivated, it can be noticed that wind turbine loses its synchronism and wind generator starts to behave like a motor reacting to the grid variations. Hence the inference that can be drawn from comparing case 3 and care 4 is that the dynamics of energy extraction through a wind turbine also plays an important role, along with the amount of energy extraction.

case 5: As a learning from the previous case, the concept of high initial energy extraction followed by intermediate or lower energy extraction at later stages and possible energy extraction depending on the H of the wind turbine was established. Hence, in this case, the $P_{extraction}$ has been restored to back to normal (where it is limited to 1) but the duration of droop has been increased, just to see the

Test Case	Kinetic Energy in PU.sec	Status	Inference and learnings
Case 1	0.715	Operational Threshold	For KE extraction, both droop and derivative controllers have to be efficiently used.
Case 2	0.968	Highly Critical	For safe extraction, dynamics of Tmech plays an important role.
Case 3	0.997	Not Recommended	Larger the positive energy extaction, larger will be the probabliity of WT's losing synchronism
Case 4	0.9575	Lost Synchronism	Only magnitude of KE extraction will not provide a clear picture on safe operation of WT's.
Case5	0.954	Lost Synchronism	Both magnitude and dynamics of KE extraction play a pivotal role in healthiness of WT's

Table 5.2: Qualitative Comparison between different cases of kinetic energy extraction

after-effects due to large time energy extraction. But as predicted, the response is satisfactory until FAPR is active, but the wind turbine goes to unstable and starts reacting to grid changes once the input is removed

5.7.6. Comparison of cases with similar extracted energies following different envelopes

Table 5.2 represents a qualitative comparison summarizing the above cases from section 5.7.5. Figure 5.12 represents 2 different envelopes of energy extraction from the wind turbine. Here 2 cases with similar energy extraction values are taken, where case 2 has 0.968 p.u. sec and initially high active power is drawn due to high derivative signal, followed by droop signal. While case 4 has 0.9575 PU.sec, and initially a slow active power is drawn and gradually increases based on the high droop signal. Though case 2 had a higher energy extraction interestingly case 2 survived the extraction but in case 4 the wind turbine lost synchronism even though less energy was drawn compared to case 2. This pinpoints the importance of the dynamics of energy extraction. So in summary, it can be concluded that both magnitude and dynamics of extracted kinetic energy plays a pivotal role in maintaining the healthiness of the wind energy extraction.

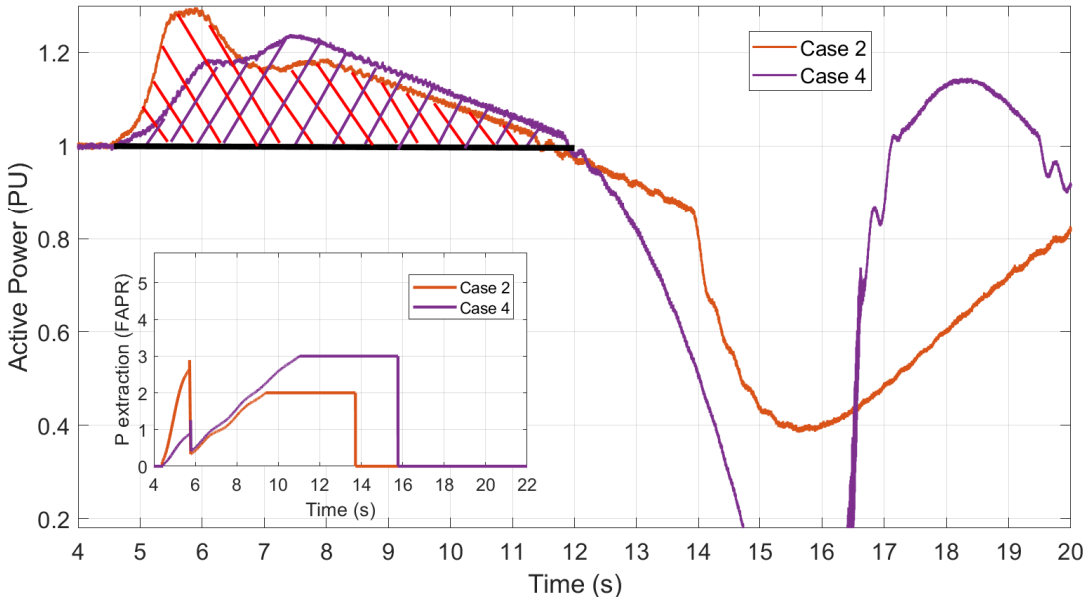

Figure 5.12: Comparison of Kinetic energy extraction envelope for case 2 and case 4

6

Hardware-in-the-Loop Validation and Testing

It was seen from the previous chapters 4 and 5 that, FAPR controllers developed that were developed in 3 were successfully implemented in a Type-4 Wind turbine, Solar farm and an Electrolyser load. Simulations were performed and improvement in frequency Nadir and RoCoF were observed.

This chapter deals with the validation of the proposed FAPR controller methodology on a mock-up Hardware in Loop (HIL) setup and verify the hardware results against the results obtained through RSCAD. Furthermore, based on the review of grid codes and advice received from industrial experts, a criteria for compliance testing of devices supporting frequency regulation has been put forward, which specifies the lengths and breaths of FAPR performance expected. Lastly, through an illustrative example, it has been proved that the controller designed is operating within boundaries of requirements.

This chapter can be seen as a continuation of chapter 4 since, Test case 1 has been used as a benchmark and Type-4 Wind turbine simulation results have been used for comparison.

6.1. General Description of a Hardware in Loop Setup

Hardware-in-the-Loop (HIL) simulations offer a cost-effective and safe method to test physical devices under real-time operating conditions. Real-time HIL simulation is the standard for developing and testing the most complex control, protection and monitoring systems. Real time HIL is classified as control hardware in the loop (CHIL) and power hardware in the loop (PHIL). Testing of control systems has traditionally been carried out directly on physical equipment (i.e. plant) in the field, on the full system or on a power test-bed in a lab. While offering testing fidelity, this practice can be very expensive, inefficient and potentially unsafe.

In this study, a HIL test set-up has been developed to validate the FAPR control strategies of inertia emulation and control strategies for mitigation of transient stability threats. Detailed description of the developed test set-up has been discussed in the following sections.

6.2. Implementation of FAPR in selected case studies

The FAPR controllers based on droop, derivative and virtual synchronous power (VSP) based control strategies have been discussed in detail in chapter 3. In section 4.4, FAPR controllers were implemented in EMT based RSCAD software to simulate in real time on RTDS. In order to validate these control strategies in HIL, a test set up has been prepared, as depicted in Figure 6.1.

6.3. Methodology for Compliance Testing:

The steps adopted for compliance testing of FAPR control methods, for instance attached to a grid side converter are as follows.

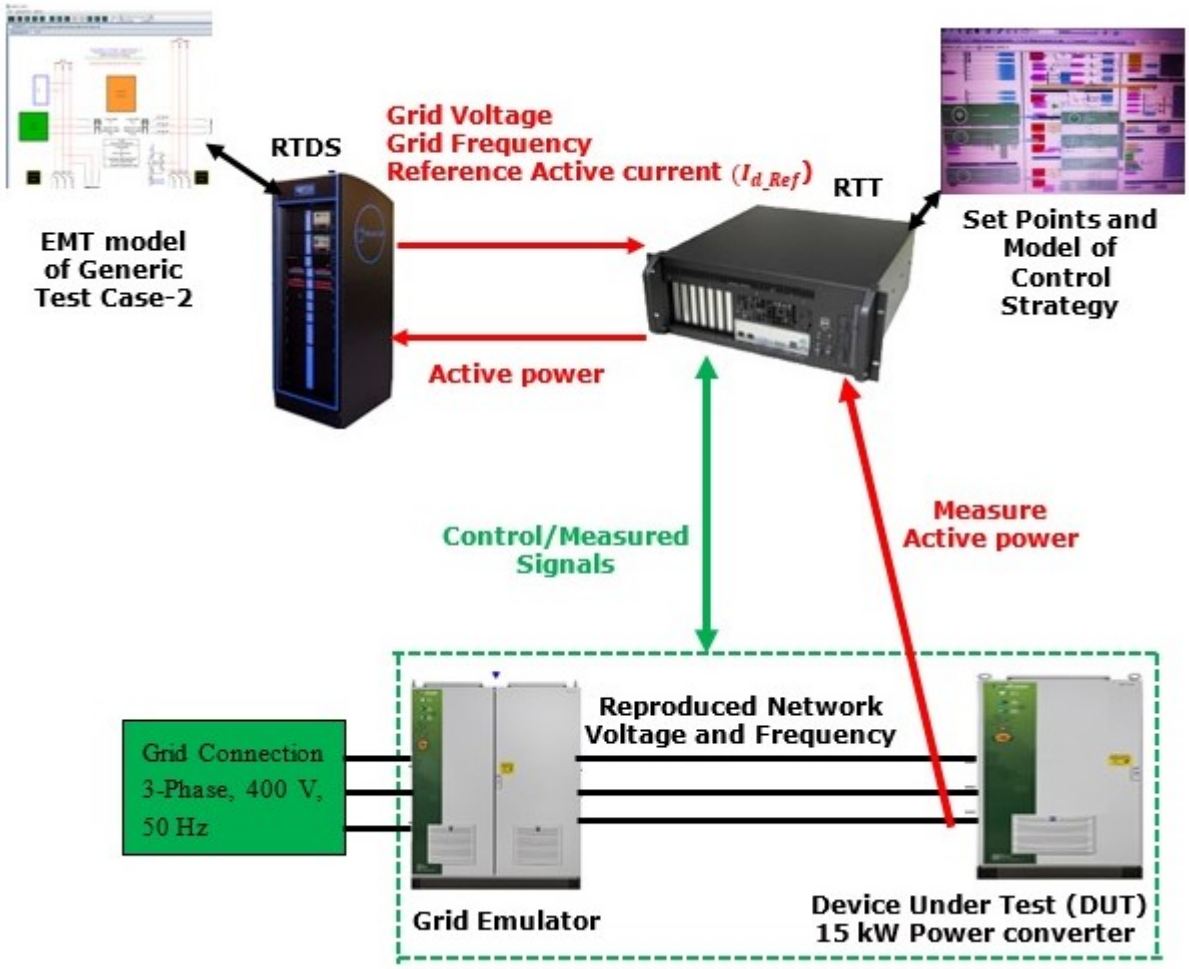

Figure 6.1: HIL test for FAPR control strategies

- The EMT model of interconnected power system is developed on RSCAD and running on RTDS NovaCor. RTDS allows external devices to be interfaced to the power system being simulated.
- The Software model for controlling of the grid emulator and DUT was developed by Triphase in Matlab/Simulink environment, which is running on a Real-Time Target (RTT) in real-time. RTT is a powerful, multi-core PC-based unit equipped with a real-time Linux/Xenomai-based operating system. A real-time inter-PC interface enables RTT to connect in real-time to the RTDS.
- User has access and control on set-points of voltage and frequency of grid emulator and current set-points of DUT. RTT receives these set-points from RTDS.
- The Aurora communication protocol is used to exchange information between RTDS simulations and the RTT. The RTT uses a circular inter-process communication (CIPC) buffer. CIPC is a shared memory strategy based on ring-buffers to allow Matlab/Simulink models to communicate with each other and other processors. Each buffer has one writer block that writes data into the buffer, from which multiple readers can read out the data. A standard Simulink model using buffers as communication infrastructure has a write functionality and/or a read functionality. To interpret the data in the buffers correctly, the read and write blocks in Simulink make use of bus definitions. The bus definitions contain the names and sizes of the signals in the buffer. The sizes of the signals entered in the write block need to cohere to these bus definitions and the signals extracted from the read block will have the names and sizes defined in the bus definitions. It should be ensured that same bus name previously defined as input/output bus name in the write/read blocks.
- The voltage and frequency of the simulation network are sent from RTDS to RTT to reproduce the desired voltage and frequency at the output terminals of DUT by grid emulator.
- As RTT and RTDS both are running in real time, control strategies of FAPR can be implemented either in RSCAD or Matlab software. The implemented FAPR Control strategies generate a current reference for active power generation. The DUT, which is a mock-up VSC, is virtually connected to the grid (which is running on RTDS), and injects active power towards the grid emulator depending on the applied FAPR control strategy.

6.4. Comparative assessment of HIL vs RSCAD.

The effectiveness of FAPR control strategies have been tested under the following conditions:

- (a) The developed modified IEEE 9 Bus system has 52% share of wind power generation of wind power as given in Figure 4.2
- (b) Device under test is emulated the grid side converter of the wind turbine connected at bus 7 (Figure 4.2),
- c) 5% sudden increase in Load at bus 8.
- (d) FAPR controllers are active for 10 Sec.

Figure 6.2 shows the active power injected into the grid by the FAPR controllers droop, derivative and VSP based respectively. It can be observed that the active output power of DUT or real converter is same as the RTDS simulation results in all three control strategies under study. HIL results validate the simulation results and RTDS model. The RTDS simulation results have completely mimicked the dynamics of the real converter. The dynamics of the active power injection by FAPR controllers and its counter effect on the frequency have been illustrated in Figure 6.3 and Figure 6.4 respectively. It can be seen that improvement in frequency dynamics depend on the rapidity and amount of power injected into the grid. Derivative-based FAPR controller power injection rise time is less than the only droop-based controller. Hence, the former is more effective in improving both Nadir and frequency slope before Nadir than the latter. Unlike droop and derivative based FAPR controllers, VSP based controller is independent of frequency measurement. Hence, its response is faster and exhibits lower rise time of active power injection as shown in Figure 4.2 As a result, its impact on frequency dynamics improvement is better than droop and derivative.

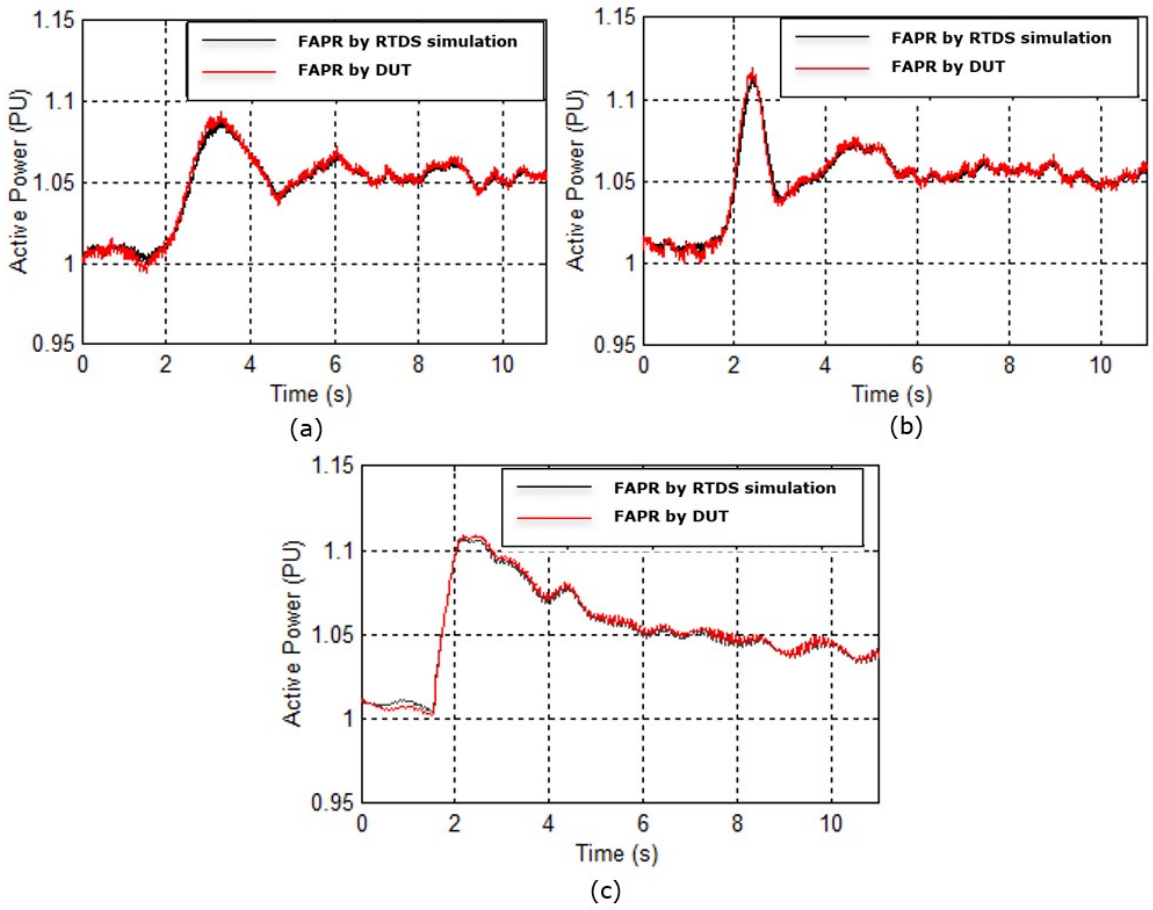

Figure 6.2: FAPR by simulated and DUT converters (a) with droop controller (b) with derivative based controller and (c) With VSP based controller

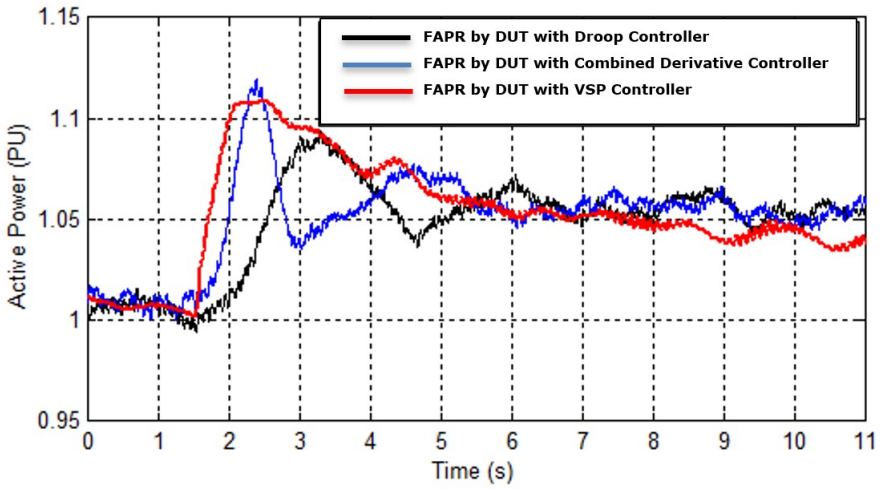

Figure 6.3: Comparison among FAPR controllers

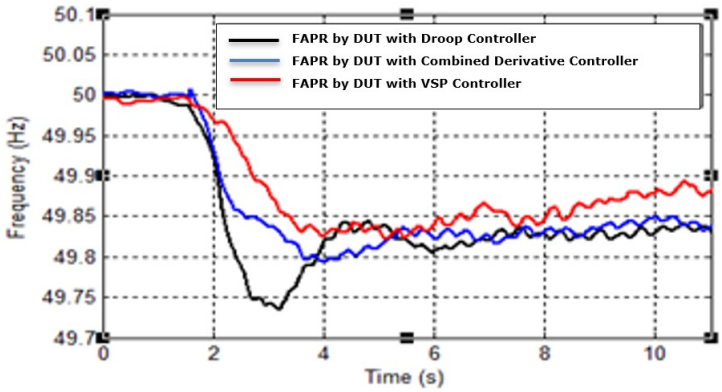

Figure 6.4: Dynamics of frequency due to FAPR controllers.

6.5. Criteria for Compliance Testing

The FAPR control methods should satisfy the following conditions, defined here based on requirements given in [41],[14],[43],[21]. These requirements can be adjusted depending on the type and size (e.g. kW or MW wind generator) of the source of active power, and the properties of the transmission grid to which it will be connected.

- Frequency RoCoF and Nadir should comply with grid code requirement (E.g. 0.5 Hz/s for RoCoF, 49.2 Hz for Nadir) for outage of the biggest generation unit.
- The FAPR control should respond according to the controller gain to inject the amount of power. The gain is tuned depending on the amount of available active power.
- At all times the control will be able to increase or decrease the active power injected into the network within a range of ΔPmax from the steady state active power output value prior to the disturbance. The value ΔPmax depends on the technology of a specific manufacturer. According to existing literature, as an indicative reference value, it may be considered that the value ΔPmax can be adjusted between 0 and 10% of the maximum capacity of the grid interfacing Power electronic converter.
- If FAPR controller is implemented separately with storage then, injected active power depends on the storage capacity and power requirements to grid.
- After triggering FAPR, the response speed should be 500 ms-700 ms (rise time of injected active power as shown in Figure 6.2). The installation can increase or decrease the active power in at least a value of 10% of the maximum capacity of the grid interfacing Power electronic converter (if module is operating at its rated and the same converter is used for power injection by FAPR).
- Must be able to supply an energy equivalent to 5-10% of the grid interfacing Power electronic converter's maximum capacity for 8-15s as shown in Figure 6.6. After this period, it is expected that primary frequency containment reserves operate and depending on the recovery strategy, the FAPR controller can be deactivated. The duration of FAPR can be adjusted for instance, by using a coordination strategy to achieve a trade-off between the maximum reserves provided and the duration of the response provided is seen [44].
- Controllers should have frequency insensitivity band between ± 10 mHz to ±50mHz (depending on the stiffness of grid) [45].
- This control should not contribute negatively to the damping of power oscillations of the electrical system.

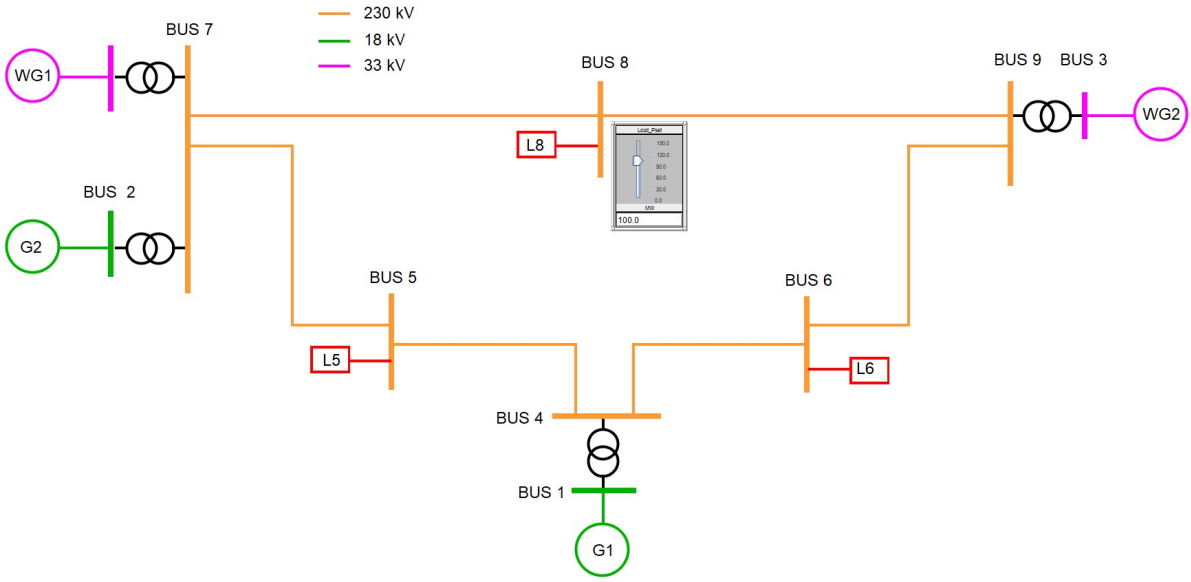

Figure 6.5: Modified IEEE 9 Bus system with 50% wind share for load frequency variations

6.6. Illustrative Example

For illustration purposes, VSP based FAPR control strategy has been tested under the following conditions: (a) The modified IEEE 9 bus system has 52% share of wind power generation of wind power as given in figure 6.5, (b) Device under test is emulated the grid side converter of the wind turbine connected at bus 7 6.5, (c) 5% sudden increase in Load at bus 8 6.5 and (d) FAPR controller is active for 10 s. Detailed overview of the modified IEEE test system and FAPR controller are presented in D1.5 [46]

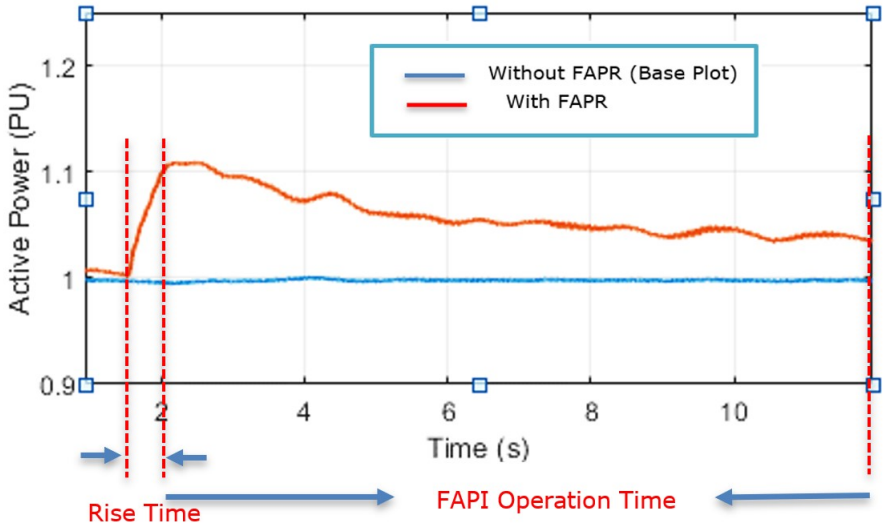

Figure 6.6: Active power output of VSP based FAPR controller

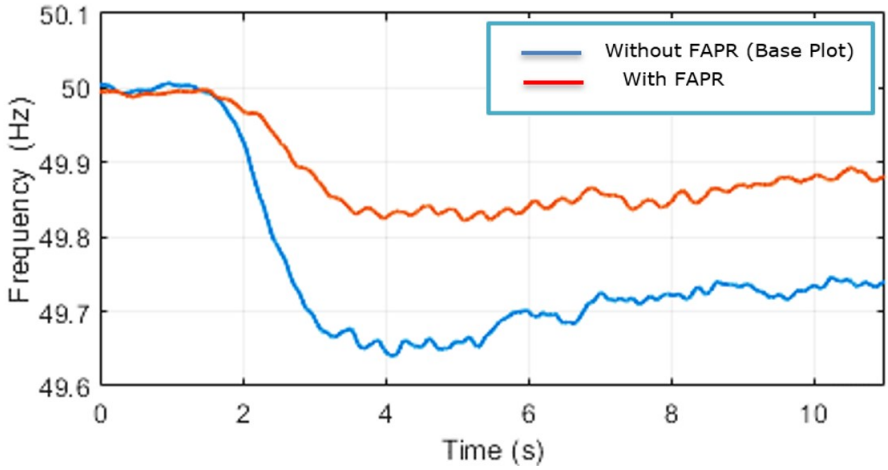

Figure 6.7: Dynamics of frequency due to VSP based FAPR controller

From Figures 3.6 and 6.7, it can be seen that active power injection and frequency curves are complying the above indicated compliance criteria for FAPR:

- The frequency Nadir and RoCoF are within the defined limit. Nadir is improved from 49.64Hz to 49.82 Hz. While RoCoF is improved from 0.28 Hz/s to 0.04 Hz/s.
- The gain of controller is tuned (K=1 pu) to inject 10% of the rated power.
- It is injecting 10% of rated power. After few second power injection decreases due to decrease in the requirement of power and improvement in the frequency.
- Rise time of active power is 510 ms which is within the specified limit.
- The FAPR controller is active for 10s.
- Frequency insensitivity band of ± 30 mHz has been considered.
- The power system is stable and implemented FAPR has not contributed negatively to the damping of power oscillations of the electrical system.

7

Conclusions and Future Work

In corroboration to the results obtained in Chapter 4, 5, 6. This chapter will draw conclusions that can be derived from the simulation results, the contribution of this thesis is going to be highlighted, and more detailed answers to the research questions of this project are briefly discussed and proposals for future research are going to be referred with references to the appropriate chapters that include a more detailed analysis and lastly proposals for future research are going to be suggested.

So this chapter has 4 sections, the first section draws chapter-wise conclusions and findings observed from chapter 4, 5, 6, the second section provide answers to the research questions formulated, the third section provides a summary of all the results, findings and contribution from this thesis and the last section provides a summary of future work that can be built on the present work.

7.1. Chapter-wise Conclusions

7.1.1. Summarizing conclusions based on chapter 4

For the studied system (Modified IEEE 9 Bus system), by performing EMT simulations, it was observed that fast active power regulation (lower rise/fall time) and the amount of available energy are the two key factors to influence the effectiveness of a FAPR controller. Combined Droop and Derivative-based FAPR controller in WTs inject power faster than the droop based FAPR controller due to early detection of the frequency change event. Hence, the former is more effective in improving both RoCoF and Nadir than the latter. Unlike droop and derivative based FAPR controller, VSP based controller is independent of frequency measurement. Hence, its response is faster and exhibits lower rise time of active power injection as shown in figure 4.9. As a result, its impact on frequency dynamics improvement is better than droop and combined droop-derivative. However, the performance of VSP controller is limited by the response speed of battery technology available in the market.

7.1.2. Summarizing conclusions based on chapter 5

Since this chapter aimed at proving FAPR controllers as a generic concept, they were implemented in Solar Farm and Electrolyser. So with inertial response not possible through Solar Farm, only VSP based FAPR has been implemented and mitigation of frequency discrepancies have been demonstrated in section 5.7.3. Also, in section 5.7.2 a responsive load (electrolyser) is modified to support under-frequency event by quickly lowering is active power absorption, so that generation-load imbalance is reduced and frequency Nadir and RoCoF improved has been demonstrated. Here an important observation is that since electrolyser works on reducing its power output, it can support for all 3 stages (inertial, primary and secondary) of frequency regulation. Lastly, unlike Powerfactory, simulations in RSCAD also provide insights into the mechanical power extraction of the wind turbines since a detailed wind turbine model is available for analysis. This helped to conclude the physical limitations of wind turbine based on inertial extraction through combined droop and derivative based FAPR controller

7.2. Summarizing conclusions based on chapter 6

In this chapter 6, EMT simulations and a HIL test set-up (grid side converter of wind generator Type-4 used as device under test – DUT) based testing of mitigation measures for frequency stability is presented and discussed. Both approaches were conducted by considering the EMT model of the modified IEEE 9 bus system, implemented in RTDS, with 52% share of wind power generation. It was observed and concluded that, the active power responses obtained from RSCAD and HIL setup at PCC were identical and no trips or islanding were observed from PHIL based Mock up converter due to FAPR controller operation.

7.3. Answers to Research Questions

Research Question 1: What is the added value of using Real Time Digital simulation instead of offline RMS simulations to model and evaluate the performance of FAPR?

The added value of using dynamic simulations using RTDS over RMS simulations using PowerFactory are listed below:

- In RSCAD, the RES models used contain full models, which considers the switching operations of the converters (Grid Side Converters and Machine Side Converters). This helps in the analysis of the FAPR controller's performance with respect to the overall system performance in terms of reaction rate observed at the PCC of any RES.
- Pertaining to Wind Turbines, another advantage of using the full model of Type-4 Wind turbine setup is that, the performance of Wind turbines due to additional power extraction during frequency curtailment period based on the inputs of FAPR controller can be investigated. The similar performance analysis on energy extraction from rotating mass of wind turbines is not possible from PowerFactory models because Powerfactory model does not consider the intermittent nature of available inertia based on wind speed, in other words, in PowerFactory,the available inertia is fixed for all wind speeds based on inertia constant set at rated speed, which is not true, since inertia constant varies proportional to the wind speed. These limitations are considered in RSCAD which makes the analysis closer to real-life situation.
- Fundamental difference between RSCAD and Powerfactory is that the former considers electro-magnetic transient behaviour of components but the latter just considers Electro-mechanical transients, since all the electrical equipments connected to the grid follow B-H curve, consideration of electro-magnetic transients for equipment and system analysis is most important.
- EMT modeling in RSCAD with support of RTDS hardware creates a platform to perform Hardware-in-the-Loop test using real converters. This helps in validation of the developed FAPR controllers.
- Last but not the least, RTDS involves "Real Time data computation" which has dedicated servers for complex power system computation. This reduces computational time drastically compared to offline EMT based PSCAD software.

And below are the sections which support the above conclusions.

A detailed overview of various RMS simulations, offline EMT simulations and online (Real-Time) EMT simulations used in Power systems are briefed. Also, clarity has been provided in section A regarding, which software application has to be selected for a particular simulation study. Further, in section 4.3, a similar test bench of a modified IEEE 9 bus with 52% wind share was developed in both PowerFactory (RMS) and RSCAD (EMT). With this, a qualitative performance comparison between results obtained in PowerFactory and RSCAD was performed and importance of EMT studies in future with large share of renewable resources was stressed. Some of the

Research Question 2 : Is it possible to propose a generic definition of FAPR, considering the existing propositions in the current state of the art?

In section 2.11, various propositions available in existing state of the art for frequency regulation strategies have been presented and later a plausible generic definition has been proposed in section 3.1 based on the feedback received from industrial experts. With this definition as baseline, controllers of FAPR were designed in RES to mitigate frequency related discrepancies.

Research Question 3 : Is it necessary to modify existing compliance requirement on FAPR?

In section 3.1, a list presenting criteria for compliance testing on FAPR is presented. This confined and revised list was outlined based on the feedback received from industrial experts.

Research Question 4 : What is the most effective FAPR strategies that can help to elevate frequency Nadir and decrease RoCoF when applied to different sources of Fast Frequency Reserve?

As discussed in Chapter 3, FAPR control strategies comprises of 3 controllers namely

- Droop based FAPR Controller
- Combined Droop and Derivative based FAPR Controller
- Virtual Synchronous Power based FAPR Controller

The first two controllers operate based on extraction of additional active power based on the inherent inertia that the wind turbine posses in real time. Here the inertial support is highly dependent on the wind speed and the rating of the turbine. The third controller (VSP) has a separate Battery Power Management System connected to a stable DC link which acts as a source of Fast Frequency Reserve which injects power during frequency curtailment period. Due to different built set up, a qualitative comparison between controllers was performed and based on the this, the following conclusions could be summarized.

- Frequency is a global variable and is dependent on inertia constant, Short Circuit Ratio etc. So since the first 2 controllers take frequency as input, the more deviation in frequency, the more is the controller output. But the limiting factor here will be the thermal and mechanical capabilities of wind turbine.
- Droop and Combined Droop-Derivative controller response highly depends on initial MPPT operation point based on wind speed, size of the wind turbine, location of the wind turbine.
- Battery Power Management system working based on VSP controller have the best performance based on its response to frequency discrepancies due to the following reasons.
  - Presence of External Energy source which assumes Battery almost ideal and hence is not designed by considering electro-chemical properties.
  - The injection of power is direct to DC link and Machine side controller propagation delays are absent.
  - 2^{nd} order transfer function which when tuned can provide the optimum solution for overshoot and rise time better than derivative block.

Research Question 5 : Does HIL testing provides similar findings as observed with only RSCAD based analysis?

As observed from Chapter 6, the responses observed from RSCAD and HIL setup were similar. Hence validation of the FAPR controllers.

7.4. Overall Conclusions

This thesis presents the details and findings derived from the analysis and development of frequency discrepancies mitigation measures through Fast Active Power Regulation controllers. The developed frequency stability phenomena were tested and validated at laboratory scale Mock-up Grid Side Converter.

So, with this background, the overall conclusions drawn can be summarized as follows:

- Three variants of fast active power regulation (FAPR) controllers were implemented initially on a wind generator Type-4 with grid following control: droop based FAPR (a state-of-the-art control method), modified derivative based FAPR (new proposal for combining methods of droop control and frequency derivative-based control), and virtual synchronous power (VSP) based FAPR

(new proposal for implementation in the form of a mathematically simple second-order transfer function, unlike complex high order models for virtual synchronous machine reported in existing literature). The structure of the proposed methods are attractive for practical implementations.

- Based on EMT simulations performed in section 4, and hardware in-the-loop testing done in section 6, it was found that the modified derivative based FAPR and VSP based FAPR constitute effective solutions for mitigation of frequency Nadir and RoCoF (computed in the time window of 0.5-2 s from the time of occurrence of an active power imbalance).

- The boundaries for effectiveness and flexibility of these methods are defined by the source of energy used to support fast active power regulation and the technical limit of the power electronic converter used to interconnect with the power system. Current technologies and inner control methods of power electronic converters allow around 10% overload during 10 s[41]. This enables to provide inertial support from wind and additional active power support through the hybrid system attached to inverter interfaced solar device.

- VSP based FAPR constitutes the most attractive option for application in different types of PEIG, as well as for power electronic interfaced storage and responsive demand. VSP based FAPR can provide damping and inertia support simultaneously, without limitations from frequency measuring devices for providing input signals to the FAPR controller. Since they operate on difference in power demand to the power supply. Also, VSP implemented on Electrolysers show that FAPR implemented in large size flexible demand (e.g. electrolysers) is highly effective in quickly mitigating frequency excursions during the frequency containment period as seen from the section 5.7.2. Therefore, to tackle limited headroom for FAPR, and to avoid exhausting operational limits, or increasing the cost of PEIG due to over-dimensioning (e.g. wind and solar PV generation), smart algorithms that can manage power supply and still provide frequency ancillary services have been suggested below.

7.5. Suggestions for Future Works

Based on the confidence gained by performing dynamic studies on frequency regulation strategies developed in RES, extendable topic of research have been suggested as future works and below is a concept that the author would like to see in reality. The suggested concept is practical and can be achieved from the available setup present at TU Delft.

Imagine in future the offshore wind energy technology has evolved substantially and there is a high share of Type-4 full converter based Wind turbines each rated around 20MW. Now FAPR controllers have been implemented and VSP based FAPR also has been integrated, but here instead of Battery Power Management system connecting to DC link, two new devices are connected in parallel with redundant operational qualities namely, Super-Capacitor based power management system which has characteristics of practical fast power injection for inertial responses and another component is an Electrolyser acting in parallel. One more mechanical modification required is ***the elimination of pitch angle concept for over-speed conditions*** but however pitch angle and braking can be used for extreme speed conditions and stalling. These are the modifications that can be done at wind turbine side. Now 4 operations scenarios can be imagined to check the feasibility of concept.

- **High Wind condition:** As a priority, lets say the active power support from the wind turbine is fixed at rated 20MW. Now with turbines rotating at more than rated speed, additional power shall be generated and this additional power shall be directed to electrolyser to produce Hydrogen which will be later explained how it has to be utilized.

- **High Wind condition and occurrence of load frequency imbalance event:** During this condition, when the event occurs, initially power from the super-capacitor shall be released based on frequency or power imbalance measurements and later after a few seconds of support from super-capacitor, due to high wind speed and high rotational inertia available, inertial energy is drawn until the turbine torque reaches threshold extraction limitation. During this time, electolyser can be made to draw less power.

- **Low wind speed condition :** Electrolyser and hydrogen production can be stopped. Also based on wind speed prediction data, super-capacitors should be charged and kept ready for any unpredicted load frequency events.

- **Low wind speed condition and occurrence of load frequency imbalance event:-** The initial response from super-capacitors should not a problem to improve RoCoF and Nadir during imbalance event the but a higher inertial response cannot be extracted due to lower wind speed, hence the following controller is shown in figure 7.1 may decide the extraction possible based on wind speed. The non-linear functional block outputs are purely dependent on the wind generator and its ancillary support capabilities. Manufacturers of WT are responsible to provide this data based on experience and calculations. Hence once this data is known based on wind speed, duration and possible limits on power extraction with respect to the wind speed can be calculated.

Further, the hydrogen generated by electrolyser can be sent in pipelines to a nearby storage area, in the next stage this hydrogen is utilized in *"**Controlled hydrogen-based power plants to run high inertial synchronous generators and flywheels**"*.

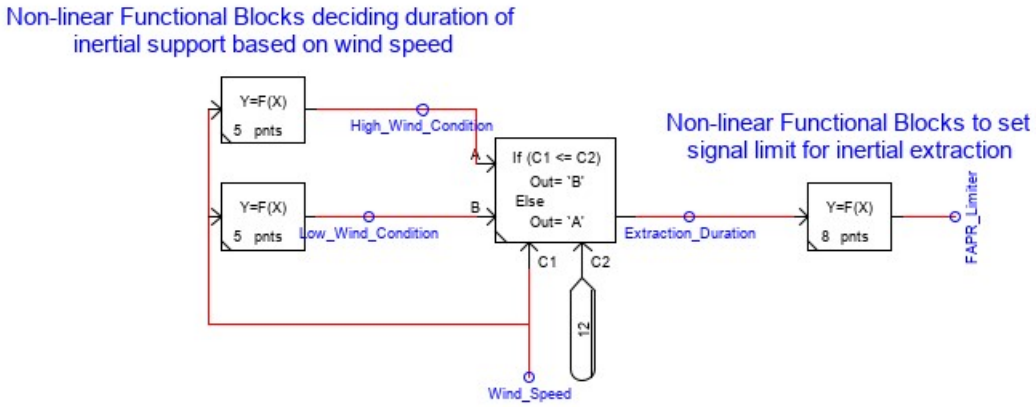

Figure 7.1: Inertia extraction limiter based on Wind speed

From this futuristic concept the following advantages can be seen:

- Security of supply can be promised due to Multi-Energy system.
- Hydrogen based power production has a very low carbon footprint and can provide huge inertial support which will be much in need.
- Higher wind speeds up to a certain degree can be utilized efficiently.
- Presence of Super-Capacitors based FAPR controller can provide inertial support better than synchronous generators.
- Investments done in the past on conventional power plants can still be modified and utilized.

Appendices

A

RMS vs EMT simulations

A.1. Qualitative comparison between EMT and RMS simulation platforms

Simulations are being performed on the power systems for almost decades now and integration of renewable energy systems, switching power electronics, smart control systems are adding complexity to simulation tools. So, the depiction of a modern power grids on simulation tools are pushing for more accuracy since the dynamics of various systems needs to be captured and observed. The disturbances in power systems are based on transients that vary in time, which leads for time-domain simulations necessary to be carried out in analysis of stability and control actions. These simulations are characterized by their different operating time frames depending on the sensitivity of the control action which can also be related to frequency ranges of the phenomena and disturbances studies.

In a broader sense, the transients captured by the simulation tools can be broadly classified into 2 categories namely Electro-Magnetic Transients Electromechanical Transients. Electromagnetic transients (EMT) are very fast phenomena occurring in the microseconds to milliseconds range; they are triggered by sudden changes in the power grid configuration, that may be caused by closing or opening action of circuit breakers, or power electronic switches, by faults or equipment failures.

The study of these EMTs requires accurate simulation of the network components such as transmission lines, transformers, protection devices, and power converters. On other hand, for the power plant equipment like governors, synchronous generators), the time constants are comparatively large. Hence, EMT simulation often use simplified model of these equipments since the effect of slow fundamental frequency is not relevant to the analysis.

Some of the EMT software's available are :

- Offline: PSCAD, EMTP, EMTP-RV.
- Real Time: eMEGAsim, HYPERSIM, RSCAD and others

Electromechanical transients are slower transients than Electromagnetic transients occurring in the range of milliseconds to seconds. They are often caused by a mismatch between power production and consumption. The analysis of this kind of transients is known as stability simulations. In stability simulation, the electromagnetic transients are filtered out and the mathematical models of electromechanical transients are therefore simplified or averaged from electromagnetic transient models. And this is achieved by using the quasi-steady-state approach, where the network is modelled using the conventional phasor technique while, contrary to this technique, the phasors are allowed to change in time, thus accounting for the dynamic response associated with the rotary and other mechanical equipment.

Some of the commercial software for electro-mechanical transient simulation are:

- Offline: EUROSTAG, PSS/E, CYME, ETAP.
- Real-Time: ePHASORsim

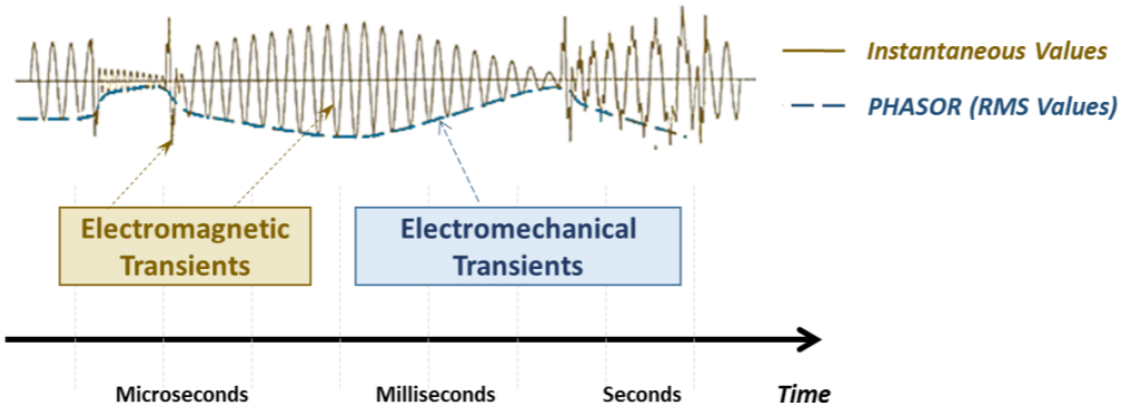

Figure A.1: The two types of transients in Power Systems tion

Figure A.1 describes how the disturbances captured in phasor values by RMS based softwares with disturbances included in various time ranges. Usually RMS based simulations are very accurate in capturing Electro-mechanical transients due to the smooth behaviour of devices producing it. But in power systems world, no devices are completely electro-mechanical. All the devices are electromagnetic ranging from relays to synchronous generators. Hence, all the devices have materials that follow hysteresis curves for their behaviour and they react based on these magnetic properties. Hence to capture the entire dynamics of instantaneous values, only RMS based simulations proves to be less significant. However, several power system analysis and simulations need not required EMT studies and maybe electromechanical transients or fundamental frequency transients is quite sufficient, here there is no need for calculation of all the state variables of complete system at a very small-time step. Hence simulations are carried out at 10 to 20 milliseconds. The advantage of using such large time steps is the possibility of simulating large power grids with many generators and thousands of busses using a single standard processor at high speed. But the compromise is, the results obtained are not any more detailed waveforms but sufficient for stability analysis. Lately, most the simulation platforms have introduced Electro-Magnetic Transient (EMT) studies and are able to simulate electro-mechanical transients if adequate dynamic models of machines and load are used. So the results of such simulations looks something like in figure A.1 where both slow and fast phenomena are captured in real time. But such simulations are carried out in the time step of 10 to 100 µs. And as the number of busses and components increases, the network complexity increases, and it will be inevitable to use a higher core processor in order to process such a large data. And if such simulations are run on a normal PC, the software would take large computational time to provide results. Hence the requirement of parallel simulators which are specialized and expensive becomes inevitable. On discussion with Original Equipment Manufacturers (OEM), the feedback regarding model accuracy (wind and solar PV generators) was that an EMT model provides the most accurate representation of the generating system when compared with the recorded meter data. However, it wasn't clear when EMT models should be used and when RMS models should be used.

B

Working principle in RSCAD

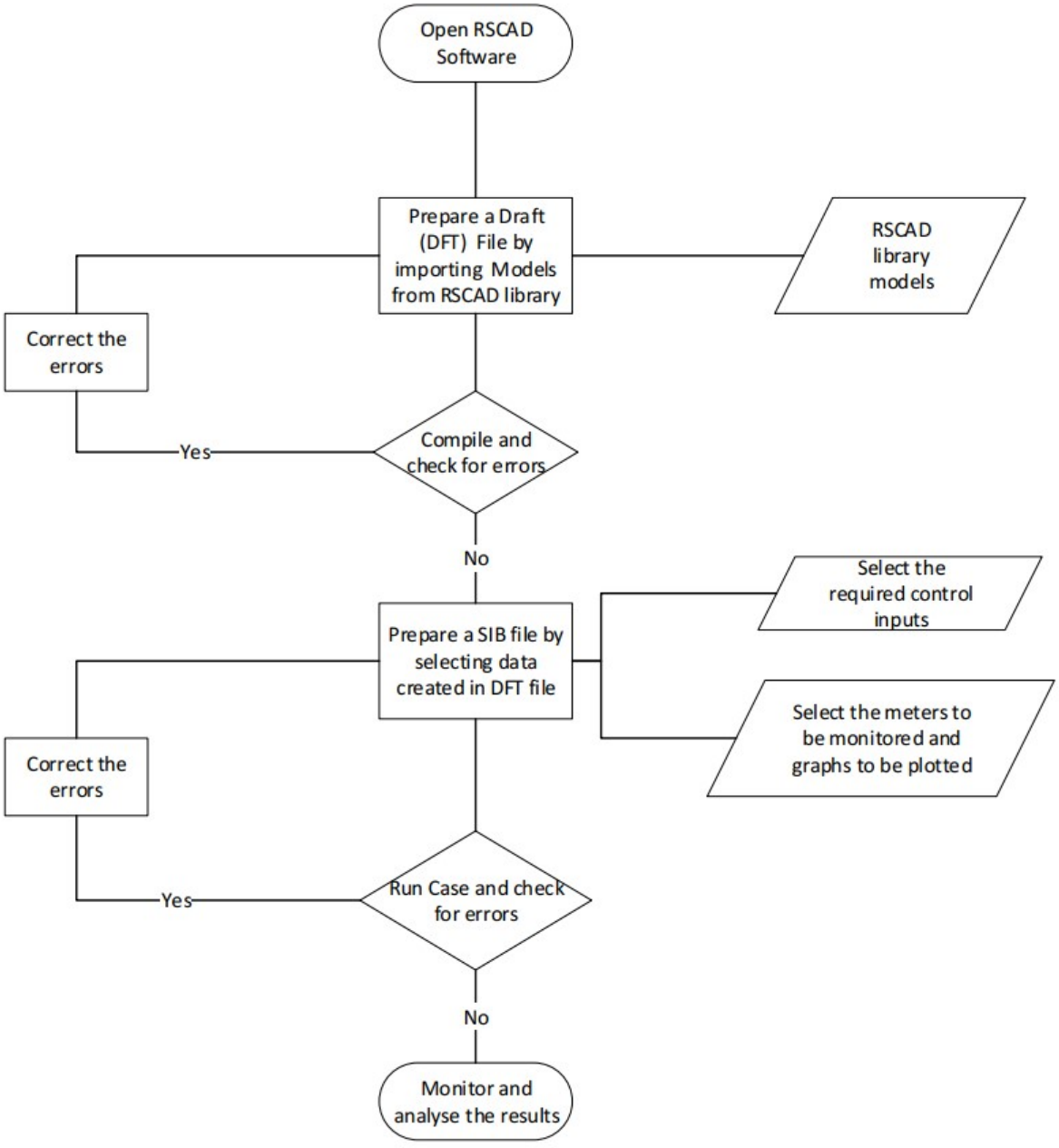

Figure B.1: Working Principle in RSCAD

C

Renewable Energy Models used

C.1. Type-4 Wind Generator Model

The popularity of Type 4 wind generators has led to a search for reliable models to evaluate the impacts of integrating these generators into the existing grid. This was the most convincing technology which could not only represent large scale Power electronic devices in the grid but also seemed practical for upscaling it to higher MW's. On this front, a model which was generic, modular and parametric enough to produce full scale, real-time, manufacturer-independent wind generator has been proposed in this section. Figure B.1 represents the model implemented in RSCAD for RTDS studies. The models are adequate to be used for frequency stability, rotor angle stability (large and small signal), sub-synchronous converter interactions (SSCI) and harmonic stability studies. In this section an overview of the main control blocks type-4 (full converter wind turbine models) generic Electro-Magnetic Transients (EMT) models developed in RSCAD for real-time power system stability simulation shall be studied. Typical grid code compliance strategies have been applied. Also, note that in the figures below from C.1 to B.5, the signal notations are non-standard and has not been changed, because the model is generic and will be used by many parties, and changing nomenclatures may affect the similarity between files. The converter topology of the model consists of a PMSM (permanent magnet synchronous machine) which is interfaced to the grid through an AC-DC-AC conversion system. On this front, the controls section of a typical Type 4 wind generator can be divided into 3 parts, namely

- Aerodynamic Block
- Grid Side converter Block
- Rotor side converter block

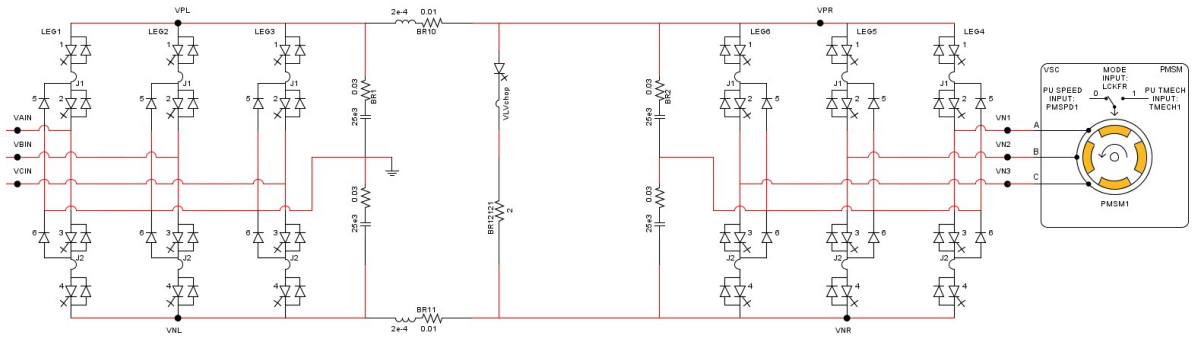

Figure C.1: Type 4 wind generator with bidirectional controllers model in RSCAD

rtds_sharc_ctl_WINDT

CONFIGURATION | TURBINE DATA | COEFFICIENT TYPE 1 | AIR DENSITY

Name	Description	Value	Unit	Min	Max
GR	Rated Generator Power	6	MVA	0.1	1000.0
TR	Rated Turbine Power	6	MW	0.1	1000.0
WR	PU Gen Speed @ Rated Turbine Speed	1.0	pu	0.1	10.0
WSR	Rated Wind Speed	12.0	m/s	1.0	100
WSCI	Cut-in Wind Speed	6.0	m/s	1.0	100.0

Figure C.2: Turbine Data of a 6 MVA wind turbine

rtds_sharc_ctl_WINDT

CONFIGURATION | TURBINE DATA | COEFFICIENT TYPE 1 | AIR DENSITY

Name	Description	Value	Unit	Min	Max
c1	Cp(lmda,Beta) =	0.5176		0.0	1.0
c2	c1(c2 * lmdai - c3 * Beta - c4) *	116		0.0	1000.0
c3	exp(-c5 * lmdai) + c6 * lmda	0.4		0.0	1.0
c4		5		0.0	20
c5	lmdai = (1 / (lmda + 0.08 * Beta)) -	21		0.0	50
c6	(0.035 / (Beta**3 + 1)	0.0068		0.0	1.0

Figure C.3: Cp-lambda curve parameters

C.1.1. Aero-dynamic Block

The aerodynamic block can be further divided into 3 parts: tip-speed ratio calculation block, aerodynamic torque calculation block, and pitch angle calculation block. In this section, only aerodynamic torque block has been given importance, since the other blocks are not altered and are less significant for the current studies. Figure C.2 represents the block diagram of the aerodynamic torque calculation block, figure C.3 captures the turbine data used, and figure B.2 (c) captures the parameters Cp versus lambda and beta values used, where Cp (λ, β) is the performance coefficient of the turbine which is a function of λ, the tip speed ratio and β, the blade pitch angle which is the output of pitch controller. The aerodynamic block designed in B.2(a) takes wind speed and pitch angle as inputs. Along with this, it can be observed that the speed reference is set by the PMSM instead of the wind turbine. But in a real wind turbine set up, gearbox (usually planetary gearbox) will be present to regulate the speed of the drivetrain. But the considered RSCAD model doesn't have a gearbox. Hence speed reference is taken directly from the PMSM. With these defined inputs the turbine provides torque mechanical as output. Further, the product of speed and torque constitutes mechanical power.

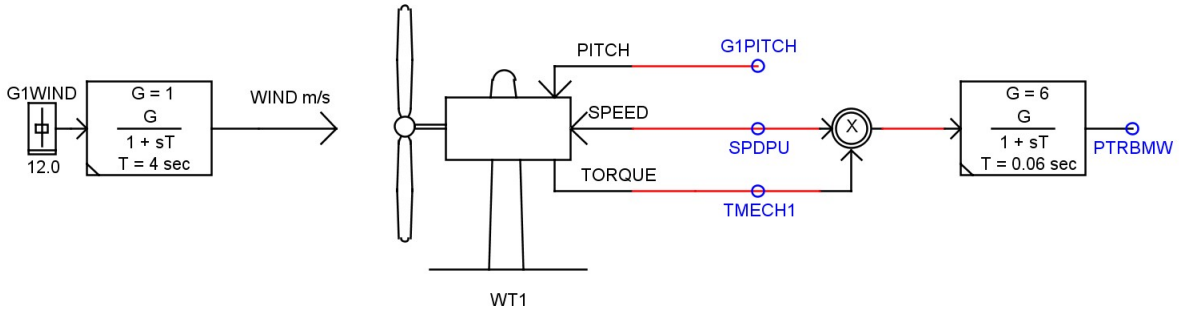

Figure C.4: Aerodynamic model of wind turbine with fixed wind speed

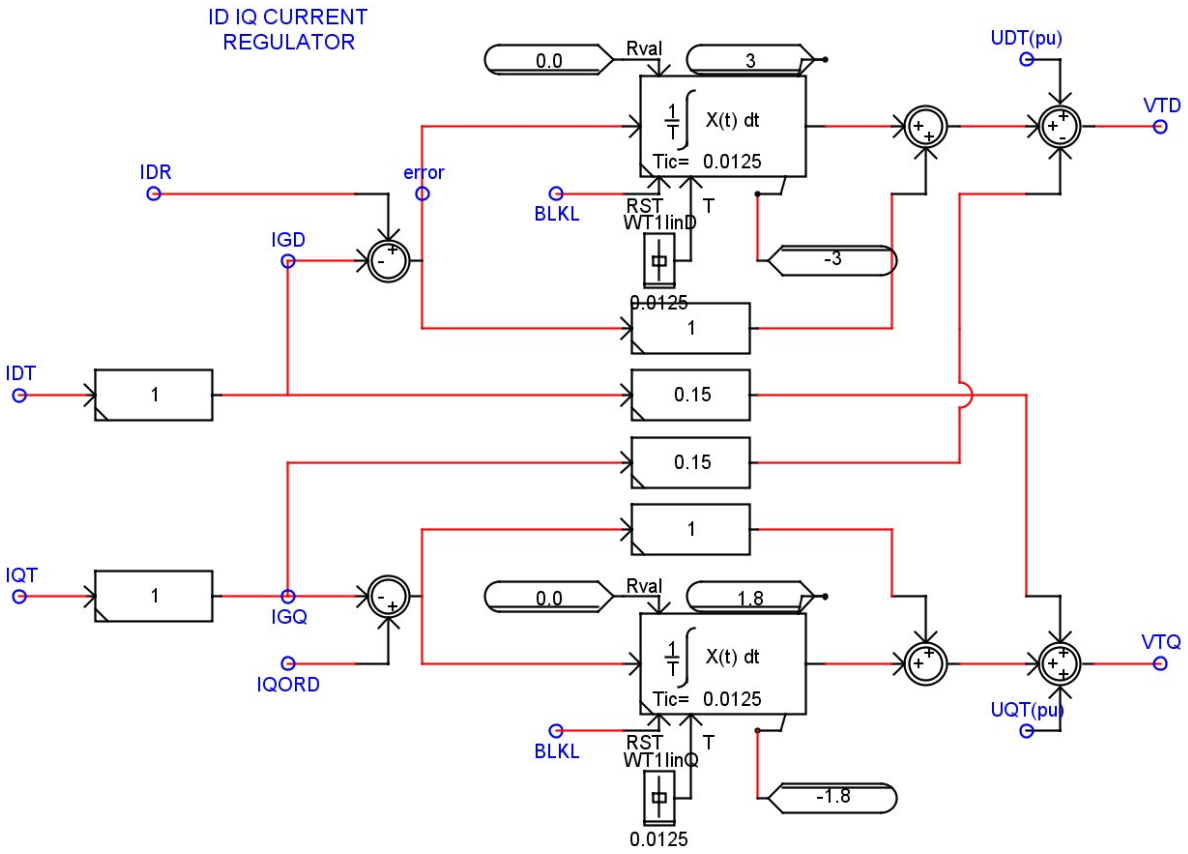

Figure C.5: Inner current control loop of the grid side converter

C.1.2. Grid Side Converter (GSC)

This section discusses the main control blocks constituting the grid side converter. Under normal operation, GSC functions as a three-phase inverter which converts the DC power from the DC link to 3 phase AC power which will be further injected into the grid. During a grid fault, the variations in current and voltage response (grid dynamics) affect the complete dynamic behavior of the grid side converter of the type-4 wind turbine. Here, the stiffness of the DC link Voltage plays an important role to provide constant power to the grid even under these conditions. The DC link voltage is governed by GSC and hence it is very important to have an accurate representation of GSC control blocks in both generic and modular form. The model is built in the per-unit system, using the base-values required for a 6MVA generator.

The main component of the grid side converter is the inner current control loop as shown in figure C.5. The current control scheme is developed in the synchronous direct-quadrature (DQ)-reference frame since active power and reactive power can be individually controlled through the modulation signals for the grid side VSC converter during steady and transient conditions. The inner loop provides voltages in DQ frame which will be further converted into modulation index for the gird side VSC converter switches. The inner loop controller works by taking inputs from the outer loop control blocks. Typically, the d-axis component is associated with the control of the active power (since the q-axis voltage is controlled to be zero). The d-axis current reference is dynamically given by the DC bus voltage regulator as shown in figure C.6. which is nothing more than a PI-regulator which controls the DC link voltage by controlling the power balance in the DC link. The DC voltage is active only during normal grid conditions when the AC grid voltage is not disturbed. During grid faults, since the AC voltage is at very low values, the DC voltage regulator is set to freeze state. The same applies also during the post-fault ramping upstate, where the active current is ramped linearly. Both during the fault and post-fault period, the DC link voltage is controlled by the DC chopper.

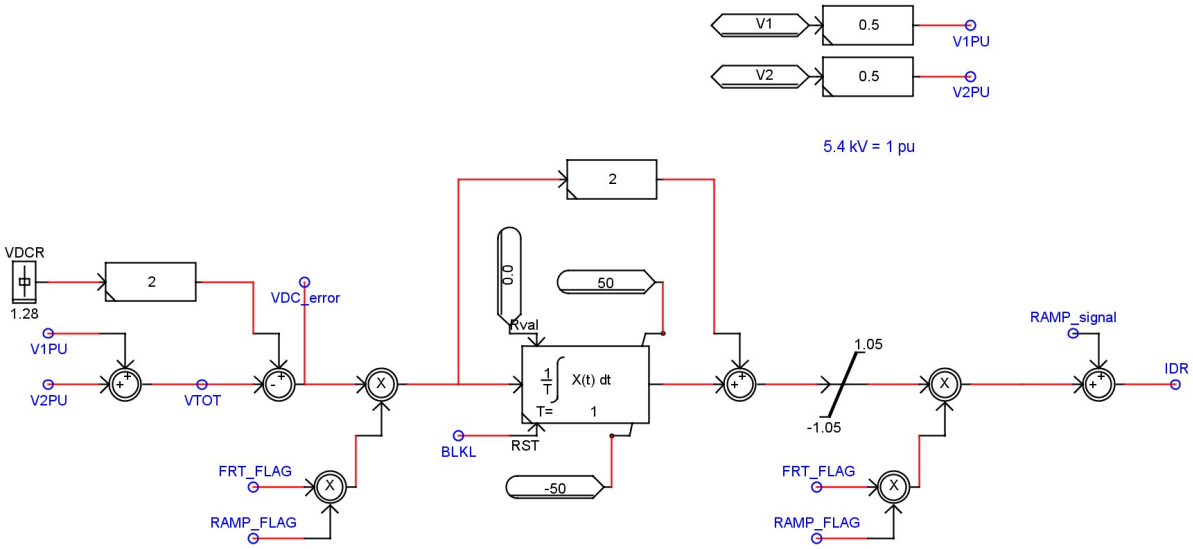

Figure C.6: DC bus voltage regulator

C.1.3. Rotor Side Converter (RSC)

This converter under normal operation functions as a three-phase rectifier which converts the AC power from the PMSM to DC power which will be injected into the DC link. The VSC switches are controlled by the modulation index further defined by inner loop and outer loop parameters. This section discusses the main control blocks at the rotor side converter. Similar to GSC, the rotor side converter is developed in the per-unit system using the base. Compared to the grid side converter, where the DQ reference frame is aligned with the grid voltage vector, the rotor-side converter uses a different DQ frame orientation. The aim here is to align the DQ-frame with the machine flux, enabling the use of q-axis current to control the machine's torque. Hence q-axis current (Iq_{ref}) will define the electrical power requirement from the wind turbine. Based on this value the P_{mech} will be derived from the Wind turbine. Figure B.5 depicts the generation of Iq_{ref} from the electrical output of PMSM (PM). Here PM is the active power generated from the PMSM. The (Iq_{ref}) or torque reference can then be created from the measured power by regulating the rotor speed.

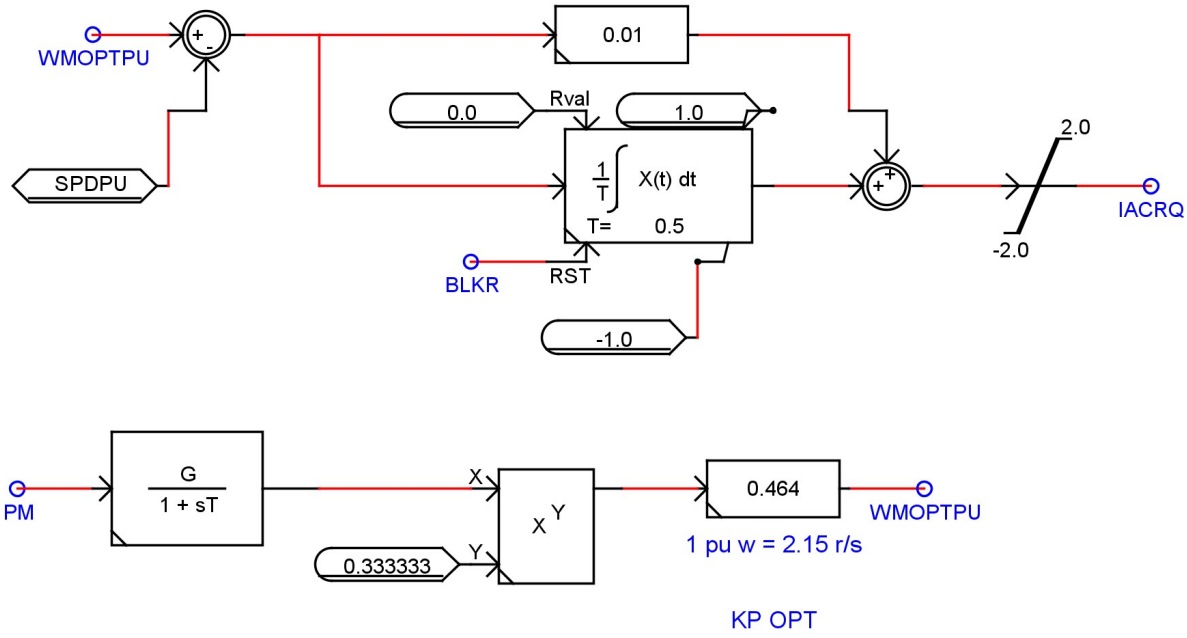

Figure C.7: Outer loop controller generating Iq ref from the electrical active power output of the wind generator (PM)

C.2. Solar Farm Model

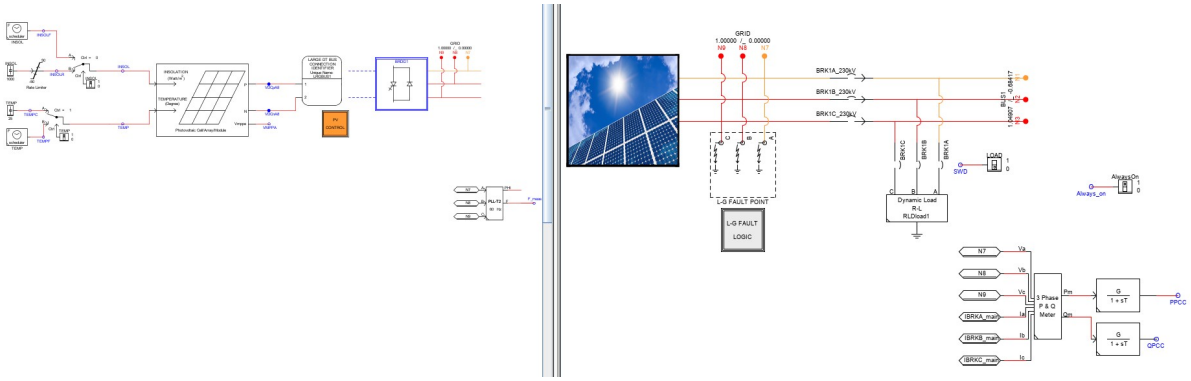

Figure C.8: Integration of 300 MW Solar farm in N3 Network

C.3. Electrolyser Model

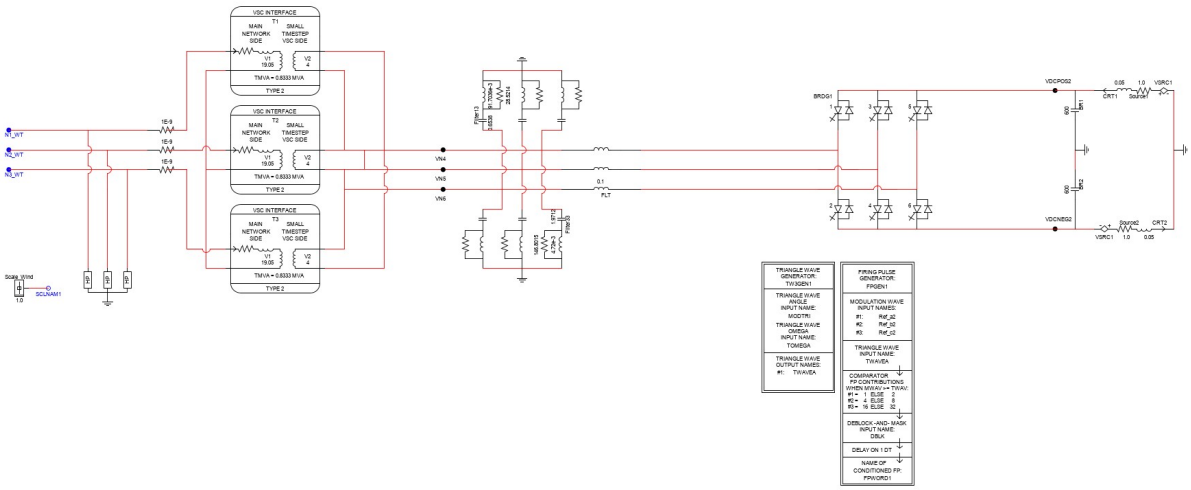

Figure C.9: RSCAD implementation of Electroyser Model used as a responsive Load

D

HMI screen (.SIB) implementation of FAPR controllers

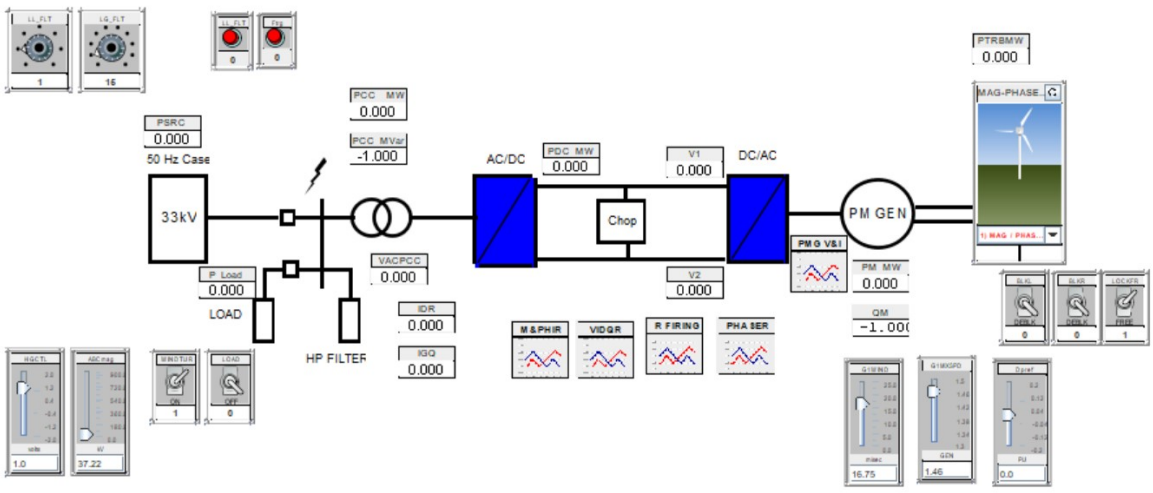

Figure D.1: SIB screen of a Type-4 Wind Generator

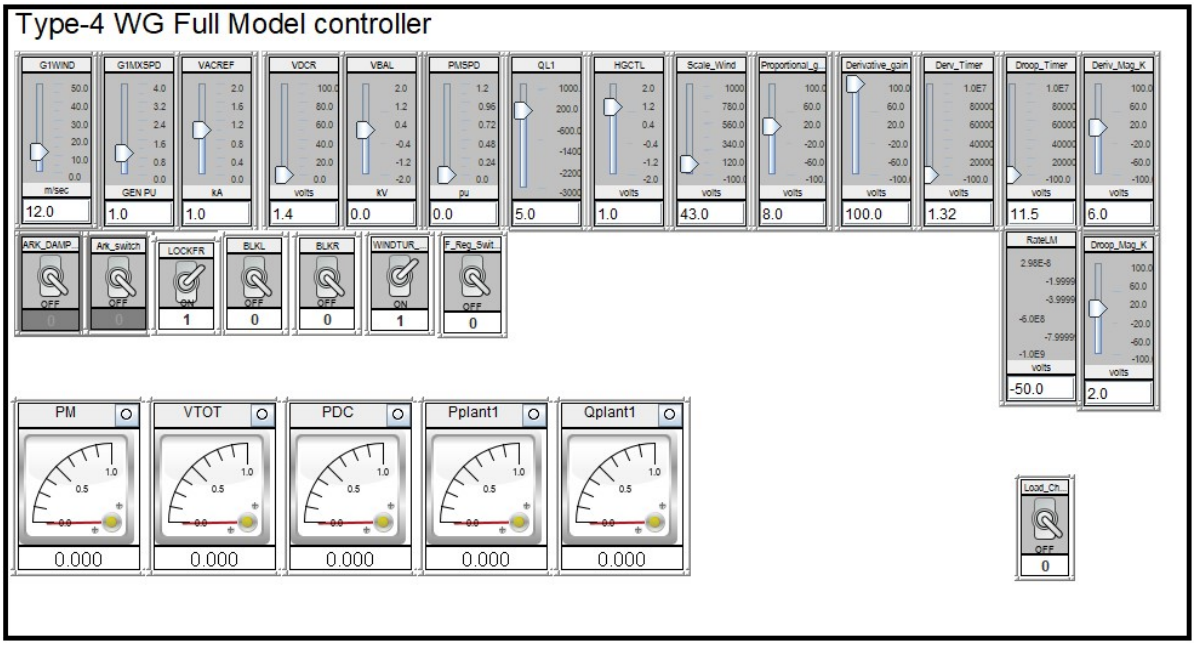

Figure D.2: Controls of Type-4 Wind Generator

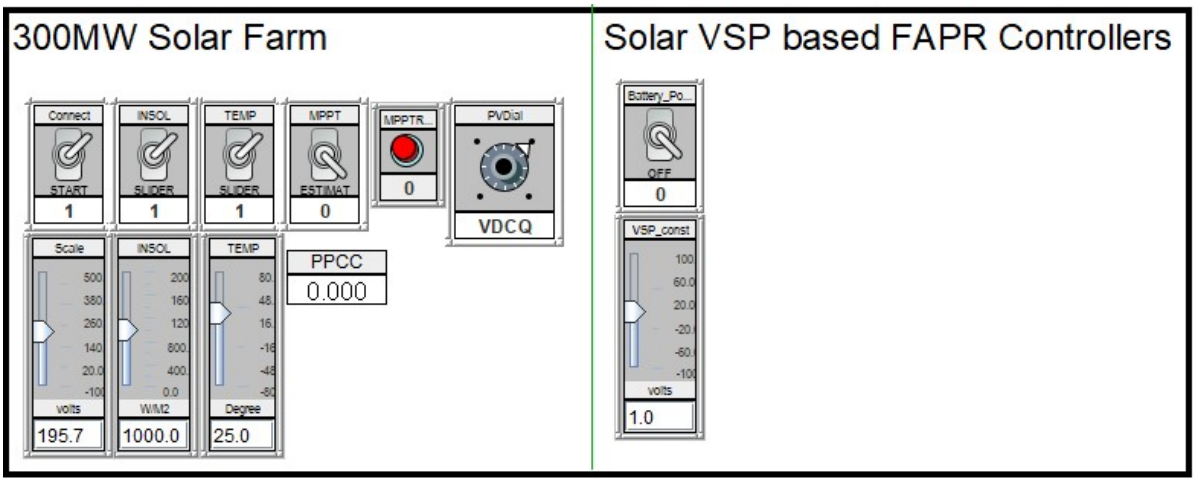

Figure D.3: Controls for a 300MW wind farm

Bibliography

[1] *What happened to our electricity system on Friday August 9th 2019?* .

[2] L. D. Kirsch and H. Singh, *Pricing ancillary electric power services,* The Electricity Journal **8**, 28 (1995).

[3] *Voor u ligt de Visie2030, een langetermijnvisie van TenneT op het 380 kV en 220kV deel van het landelijke elektriciteitstransportnet.* (2017).

[4] P. Tielens and D. V. Hertem, *The relevance of inertia in power systems,* Renewable and Sustainable Energy Reviews **55**, 999 (2020).

[5] R. Eriksson, N. Modig, and K. Elkington, *Synthetic inertia versus fast frequency response: A definition,* in *IET Renewable Power Generation* (2018).

[6] J. Morren, S. Member, S. W. H. D. Haan, W. L. Kling, and J. A. Ferreira, *Wind Turbines Emulating Inertia and Supporting Primary Frequency Control,* **21**, 2005 (2006).

[7] M. Dreidy, H. Mokhlis, and S. Mekhilef, *Inertia response and frequency control techniques for renewable energy sources : A review,* Renewable and Sustainable Energy Reviews **69**, 144 (2017).

[8] F. Ha and A. Abdennour, *Optimal use of kinetic energy for the inertial support from variable speed wind turbines,* **80** (2015), 10.1016/j.renene.2015.02.051.

[9] O. Mo, S. D'Arco, and J. A. Suul, *Evaluation of Virtual Synchronous Machines With Dynamic or Quasi-Stationary Machine Models,* IEEE Transactions on Industrial Electronics **64**, 5952 (2017).

[10] R. Kotti and W. Shireen, *Maximum power point tracking of a variable speed PMSG wind power system with DC link reduction technique,* in *2014 IEEE PES General Meeting | Conference & Exposition* (IEEE, 2014) pp. 1–5.

[11] A. Cultura and Z. M. Salameh, *Modeling, Evaluation and Simulation of a Supercapacitor Module for Energy Storage Application,* (2015) pp. 876–882.

[12] J. Zhu, J. Hu, S. Member, W. Hung, C. Wang, S. Member, X. Zhang, S. Bu, S. Member, Q. Li, H. Urdal, and C. D. Booth, *Induction Generator Wind Turbine Generators Using Lithium-Ion Supercapacitors,* **33**, 773 (2018).

[13] L. Qu and W. Qiao, *Constant Power Control of DFIG Wind Turbines With Supercapacitor Energy Storage,* **47**, 359 (2011).

[14] E. Rakhshani and P. Rodriguez, *Inertia emulation in ac/dc interconnected power systems using derivative technique considering frequency measurement effects,* IEEE Transactions on Power Systems **32**, 3338 (2016).

[15] C. Paper, E. Rodrigues, and R. Godina, *Influence of Large Renewable Energy Integration on Insular Grid Code Compliance Influence of Large Renewable Energy,* , 295 (2015).

[16] F. Mahr, J. Jaeger, and F.-a.-u. O. F. E.-n. Fau, *Frequency-Adaptive MPC of Grid-Forming VSC-HVDC Systems with Optimal Voltage Reference Tracking during Grid Restoration Keywords Restoration area VSC-HVDC Healthy grid State space modeling Equivalent circuit of the grid-forming MMC,* 2018 20th European Conference on Power Electronics and Applications (EPE'18 ECCE Europe) , P.1.

[17] A. Merabet, K. T. Ahmed, R. Beguenane, and H. Ibrahim, *Feedback linearization control with sliding mode disturbance compensator for PMSG based wind energy conversion system,* in *2015 IEEE 28th Canadian Conference on Electrical and Computer Engineering (CCECE)* (IEEE, 2015) pp. 943–947.

[18] X. Hao, T. Zhou, J. Wang, and X. Yang, *A hybrid adaptive fuzzy control strategy for DFIG-based wind turbines with super-capacitor energy storage to realize short-term grid frequency support,* in *2015 IEEE Energy Conversion Congress and Exposition (ECCE)* (IEEE, 2015) pp. 1914–1918.

[19] H. Dharmawardena, S. Member, K. Uhlen, and S. S. Gjerde, *Modelling Wind Farm with Synthetic Inertia for Power System Dynamic Studies,* 2016 IEEE International Energy Conference (ENERGYCON) , 1.

[20] D. Ochoa and S. Martinez, *Fast-Frequency Response Provided by DFIG-Wind Turbines and its Impact on the Grid,* **32**, 4002 (2017).

[21] AEMO, *Fast Frequency Response in the NEM,* (2017).

[22] *Renewables 2014. Global status report 2014*, Tech. Rep. (RES21, 2018).

[23] F. Low, I. Power, S. Using, and C. Technique, *Primary Frequency Response Enhancement for Future Low Inertia Power Systems Using Hybrid Control Technique,* (2018), 10.3390/en11040699.

[24] J. I. Itoh, D. Sato, T. Nagano, K. Tanaka, N. Yamada, and K. Kato, *Development of high efficiency flywheel energy storage system for power load-leveling,* in *INTELEC, International Telecommunications Energy Conference (Proceedings)* (2014).

[25] D. Curtiss, P. Mongeau, and R. Puterbaugh, *Advanced composite flywheel structural design for a pulsed disk alternator,* IEEE Transactions on Magnetics **31**, 26 (1995).

[26] H. Bevrani and J. Raisch, *ScienceDirect ScienceDirect ScienceDirect On Virtual inertia Application in Power Grid Frequency Control Assessing the feasibility of using the Raisch heat demand-outdoor temperature function for a long-term district heat demand forecast,* Energy Procedia **141**, 681 (2017).

[27] M. Draganescu, Y. Li, and S. Miao, *Review of Voltage and Frequency Grid Storage Applications,* (2018), 10.3390/en11051070.

[28] *E.ON Netz GmbH, Annexe EON HV Grid Connection Requirements.* (2006).

[29] E. Analysis, E. I. Division, and L. Berkeley, *Review of International Grid Codes,* (2018).

[30] *Nordic Grid Code 2007 (Nordic collection of rules)*, Tech. Rep.

[31] A. Q. Al-Shetwi, M. Z. Sujod, and N. L. Ramli, *A review of the fault ride through requirements in different grid codes concerning penetration of PV system to the electric power network,* ARPN Journal of Engineering and Applied Sciences **10**, 9906 (2015).

[32] *INDIAN ELECTRICITY GRID CODE THE CENTRAL TRANSMISSION UTILITY*, Tech. Rep. (2002).

[33] F. Møller, A. Stine, G. Jensen, H. V. Larsen, P. Meibom, H. Ravn, K. Skytte, and M. Togeby, *Analyses of Demand Response in Denmark*, Tech. Rep. (2006).

[34] R. Llewellyn, *Chapter 5 Electricity transmission 2009*, Tech. Rep. (2009).

[35] *Grid Code v6 EirGrid Grid Code*, Tech. Rep. (2015).

[36] M. Jimeno, *Renewable energy policy database and support – RES-LEGAL EUROPE National profile : Profile,* , 1 (2015).

[37] *Austrian Power Grid, Transmission System Operator for Austria,* .

[38] *Rate of Change of Frequency (RoCoF) withstand capability,* (2018).

[39] *Rated Voltage Levels of China National Grid, EEPW Website,* .

[40] A. T. C. Jecu, D. R. S. Bacha, and R. Belhomme, *Contribution to frequency control through wind turbine inertial energy storage,* **3**, 358 (2009).

[41] J. Fang, S. Member, H. Li, Y. Tang, and S. Member, *On the Inertia of Future More-Electronics Power Systems,* **6777**, 160 (2018).

[42] V. Ruuskanen, J. Koponen, K. Huoman, A. Kosonen, M. Niemelä, and J. Ahola, *PEM water electrolyzer model for a power-hardware-in-loop simulator,* International Journal of Hydrogen Energy (2017), 10.1016/j.ijhydene.2017.03.046.

[43] F. M. Gonzalez-Longatt, A. Bonfiglio, R. Procopio, and B. Verduci, *Evaluation of inertial response controllers for full-rated power converter wind turbine (Type 4),* in *IEEE Power and Energy Society General Meeting* (2016).

[44] A. Nikolopoulou, *Wind Turbine Contribution to Ancillary Services under Increased Renewable Penetration levels*, Ph.D. thesis (2017).

[45] B. J. Kirby, J. Dyer, C. Martinez, R. A. Shoureshi, R. Guttromson, and J. Dagle, *Frequency Control Concerns In The North American Electric Power System*, Tech. Rep. (2002).

[46] Migrate Work Package 1, *MIGRATE Deliverable D1.5: Power system risk analysis and mitigation measures,* (2019).